Available online at www.sciencedirect.com
SCIENCE DIRECT®
Earth-Science Reviews 66 (2004) 261–330
EARTH-SCIENCE REVIEWS
www.elsevier.com/locate/earscirev

Ground-penetrating radar and its use in sedimentology: principles, problems and progress

Adrian Neal*

School of Applied Sciences, University of Wolverhampton, Wulfruna Street, Wolverhampton WV1 1SB, UK

Received 22 April 2003; accepted 19 January 2004

Abstract

Ground-penetrating radar (GPR, also referred to as ground-probing radar, surface-penetrating radar, subsurface radar, georadar or impulse radar) is a noninvasive geophysical technique that detects electrical discontinuities in the shallow subsurface (< 50 m). It does this by generation, transmission, propagation, reflection and reception of discrete pulses of high-frequency (MHz) electromagnetic energy. During the 1980s radar systems became commercially available, but it was not until the mid-1990s that sedimentary geologists and others began to widely exploit the technique. During the last decade numerous sedimentological studies have used GPR to reconstruct past depositional environments and the nature of sedimentary processes in a variety of environmental settings; to aid hydrogeological investigations, including groundwater reservoir characterisation, and to assist in hydrocarbon reservoir analogue studies. This is because in correctly processed radar profiles, and at the resolution of a survey, primary reflections usually parallel primary depositional structure. Despite the wide use of GPR, a number of fundamental problems remain in its application to sedimentary research. In particular, there are a wide range of approaches to the processing of radar data and interpretation techniques used on the final subsurface images vary widely, with little consensus over a common methodology. This review attempts to illustrate that methods for the collection, processing and interpretation of radar data are intimately linked and that thorough understanding of the nature, limitations and implications of each step is required if realistic sedimentological data are to be generated. In order to extract the maximum amount of meaningful information, the user must understand the scientific principles that underlie the technique, the effects of the data collection regime employed, the implications of the technique's finite resolution and depth of penetration, the nature and causes of reflections unrelated to primary sedimentary structure, and the appropriateness of each processing step with respect to the overall aim of the study. Following suitable processing, a radar stratigraphy approach to reflection profile interpretation should be adopted. New or modified terminologies and techniques to define a radar stratigraphy are also recommended, in order to make the interpretation process more transparent and to avoid confusion with related methodologies such as seismic stratigraphy and sequence stratigraphy. The full potential of GPR in sedimentary research will only be realised if more thorough and systematic approaches to data collection, processing and interpretation are adopted.

Keywords: Geophysics; Electromagnetic; Stratigraphy; Sedimentary structure; Bounding surface; Facies

1. Introduction

For humans, the shallow subsurface is perhaps the most important geological layer in the earth. This

* Present address: Groom's Cottage, The Gardens, Penylan Lane, Oswestry, Shropshire SY10 9AA, UK.
E-mail address: A.Neal@wlv.ac.uk (A. Neal).

0012-8252/$ - see front matter © 2004 Elsevier B.V. All rights reserved.
doi:10.1016/j.earscirev.2004.01.004

layer contains many of the earth's natural resources (e.g. building aggregates/stone, placer deposits, drinking water aquifers, soils) and also acts as a sink for human waste (e.g. landfill sites). In addition, through the study of rocks and unconsolidated sediment accumulations at or near the surface we have discovered much about earth history and behaviour of its dynamic landforms. These insights have aided environmental management, such as prediction of natural disasters, helped exploration for more remote natural resources such as oil and gas, and increased understanding of the geological development of other planets in our solar system. Given the large rise in human population predicted for the 21st century, a more detailed understanding of the shallow subsurface will be required if humans are to sustainably manage many of the earth's finite resources.

As Grasmück and Green (1996) note, given the importance of the earth's upper layers to human development, it is surprising that during much of the 20th century techniques for exploring them did not change significantly. Analysis of field exposures linked via data from limited numbers of widely spaced boreholes, shallow excavations and geophysical surveys is still typical. Drilling and trial pits are time-consuming and expensive, often yielding only limited additional information that is difficult to correlate between distant sampling points. In some instances such invasive techniques cannot be implemented due to environmental or conservation considerations.

The most common geophysical techniques employed in shallow subsurface investigations are seismic reflection and seismic refraction, although these have a vertical resolution that does not normally meet the submetre resolution required in many practical situations. Consequently, during the 1970s attention increasingly turned to using other, higher resolution, geophysical techniques. One technique that has proved extremely useful is ground-penetrating radar (GPR or ground-probing radar, surface-penetrating radar, subsurface radar, georadar or impulse radar). GPR detects electrical discontinuities in the shallow subsurface (typically <50 m) by generation, transmission, propagation, reflection and reception of discrete pulses of high-frequency electromagnetic energy in the megahertz (MHz $=10^6$ Hz, 1 Hz $=1$ cycle/s) frequency range. GPR's origins lie in research carried out during the early 20th century by German scientists trying to patent techniques to investigate the nature of various buried features (Daniels, 1996; Reynolds, 1997). Pulsed electromagnetic waves were first used in the mid-1920s. Following these initial developments, much early work using radar was in glaciology (Plewes and Hubbard, 2001), with civil engineering, archaeological and geological applications becoming more frequent from the 1970s onwards (Daniels, 1996; Conyers and Goodman, 1997; Reynolds, 1997). However, it was not until the 1980s that GPR systems became commercially available and digital data acquisition was feasible (Annan and Davis, 1992). Since the mid-1990s there has been an explosion of interest in GPR, with an ever-increasing number of research articles published on the technique each year (Fig. 1). Many publications relate to geological applications of GPR, a significant subset of which have a strong sedimentological component (Fig. 1). GPR has been used by sedimentologists to reconstruct past depositional environments and the nature of sedimentary processes in a variety of environmental settings, aid hydrogeological investigations (including groundwater reservoir characterisation), and assist hydrocarbon reservoir analogue studies (Table 1). It is these applications in sedimentology that form the basis of this review

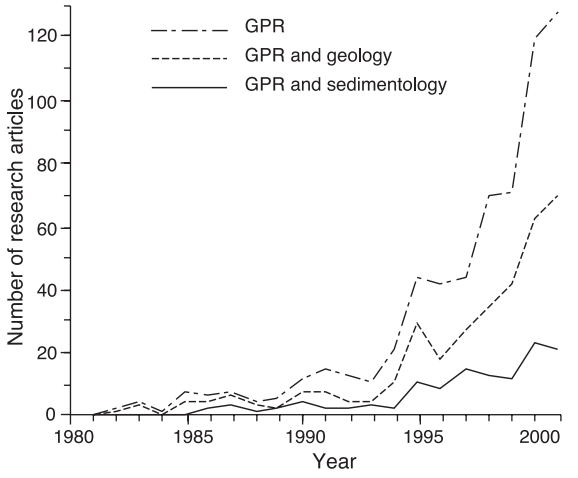

Fig. 1. Number of research articles produced each year between 1980 and 2001 on ground-penetrating radar (GPR) in general, geological applications of GPR (including sedimentology), and just the sedimentological applications of GPR, based on data extracted from Thomson ISI's Science Citation Index.

Table 1
Important sedimentological ground-penetrating radar studies, classified according to the main depositional setting investigated

Depositional setting	Relevant GPR Papers (most recent first)
Fluvial	Best et al. (2003), Cardenas and Zlotnik (2003); Skelly et al. (2003), Woodward et al. (2003), Corbeanu et al. (2001, 2002), Hammon et al. (2002), Hornung and Aigner (2002), Baker et al. (2001), Nobes et al. (2001), Szerbiak et al. (2001), Bristow et al. (1999, 2000b), Bridge et al. (1995, 1998), van Overmeeren (1998), Asprion and Aigner (1997), Leclerc and Hickin (1997), McMechan et al. (1997), Poole et al. (1997), Roberts et al. (1997), Taylor and Macklin (1997), Aigner et al. (1996), Birkhead et al. (1996), Naegeli et al. (1996), Wyatt and Temples (1996), Alexander et al. (1994), Stephens (1994), Gawthorpe et al. (1993), Jol and Smith (1991)
Fluvioglacial	Cassidy et al. (2003), Heinz and Aigner (2003), Jackobsen and Overgaard (2002), Regli et al. (2002), Tronicke et al. (2002a), Heinz (2001), Russell et al. (2001), Huisink (2000), Sénéchal et al. (2000), Asprion and Aigner (1999), Augustinus and Nichol (1999), Beres et al. (1995, 1999), Vandenberghe and van Overmeeren (1999), Greaves et al. (1996), Fisher et al. (1995), Olsen and Andreasen (1995), Huggenberger et al. (1994), Huggenberger (1993), Fisher et al. (1992b), Sutinen (1992)
Glacial	Bakker and van der Meer (2003), Jackobsen and Overgaard (2002), Lønne et al. (2001), Overgaard and Jakobsen (2001), Bano et al. (2000), Berthling et al. (2000), Dehls et al. (2000), Gilbert (2000), Goes (2000), Augustinus and Nichol (1999), Busby and Merritt (1999), Busby (1997), van Overmeeren (1994, 1997), Lønne and Lauritsen (1996), Maijala (1992), Sutinen (1992), Beres and Haeni (1991), Ulriksen (1982)
Coastal	Buynevich and FitzGerald (2003), Mäkinen and Räsänen (2003), Møller and Anthony (2003), Moore et al. (2003), Neal et al. (2001, 2002a,b, 2003), O'Neal and Dunn (2003), Smith et al. (2003), Daly et al. (2002), Jol et al. (2002), Nichol (2002), O'Neal and McGeary (2002), Clemmensen et al. (1996, 2001), Neal and Roberts (2000, 2001), Rossetti and Góes (2001), Anderson et al. (2000), Bailey and Bristow (2000), Bristow et al. (2000c), Jol et al. (1996a, 2000), Junck and Jol (2000), McGourty and Wilson (2000), Roberts and Jol (2000), FitzGerald and van Heteren (1999), Smith et al. (1999), Tronicke et al. (1999), Vanderburgh et al. (1998), van Heteren et al. (1996, 1998), van Overmeeren (1994, 1998), van Heteren and van de Plassche (1997), Harari (1996), Meyers et al. (1996), Bristow (1995), Dominic et al. (1995), Dott and Mickleson (1995), Zenero et al. (1995), FitzGerald et al. (1992), Baker (1991), Strand Petersen and Andreasen (1989), Leatherman (1987), Ulriksen (1982)
Aeolian	Botha et al. (2003), Buynevich and FitzGerald (2003), van Dam et al. (2002a,b, 2003), van Dam (2001, 2002), Clemmensen et al. (1996, 2001), Neal and Roberts (2000, 2001), Bailey and Bristow (2000), Bristow et al. (2000a,c, 1996), Jol et al. (2000), Junck and Jol (2000), McGourty and Wilson (2000), van Dam and Schlager (2000), Vanderburgh et al. (1998), van Overmeeren (1994, 1998), Grant et al. (1997), Greaves et al. (1996), Harari (1996), Schenk et al. (1993), Fisher et al. (1992b)
Delta	Pelpola and Hickin (2003), Roberts et al. (2003), Nitsche et al. (2002), Sandberg et al. (2002), Beres et al. (2000), Jol et al. (1996a,b, 2000), Smith and Jol (1992, 1995b, 1997), Jol (1995), Soldal et al. (1994), Jol and Smith (1991), Ulriksen (1982)
Alluvial fan	Ékes and Friele (2003), Ékes and Hickin (2001), Friele et al. (1999), Mills and Speece (1997)
Lake	Carreón-Freyre et al. (2003), Pipan et al. (2000b), Grant et al. (1998), Dott and Mickleson (1995), Mellet (1995), Jol and Smith (1991)
Peatland	Holden et al. (2002), Slater and Reeve (2002), Poole et al. (1997), Lapen et al. (1996), Jol and Smith (1995), Theimer et al. (1994), Hänninen (1992), Warner et al. (1990), Worfield et al. (1986)
Slope	Degenhardt and Giardino (2003), Degenhardt et al. (2003), Leopold and Völkel (2003), Sass and Wollny (2001), Volkel et al. (2001), Barnhardt and Kayen (2000), Bruno and Marillier (2000), Hruska and Hubatka (2000), Olson and Doolittle (1985)
Carbonates	Pedley and Hill (2003), Orlando (2003), Xia et al. (2003), Al-fares et al. (2002), McMechan et al. (1998, 2002), Singh and Chauhan (2002), Asprion and Aigner (2000), Dagallier et al. (2000), Kruse et al. (2000), Orlando (2000), Pedley et al. (2000), Pipan et al. (2000a), Doolittle and Collins (1998), Sigurdson and Overgaard (1998), Meschede et al. (1997), Dominic et al. (1995), Liner and Liner (1995), Pratt and Miall (1993)
Volcanic	Cagnoli and Ulrych (2001a,b), Cagnoli and Russell (2000), Rust and Russell (2000), Russell and Stasiuk (1997)
Faults, joints and folds in sediments	Anderson et al. (2003), Bakker and van der Meer (2003), Green et al. (2003), Liberty et al. (2003), Orlando (2003), Rashed et al. (2003), Reiss et al. (2003) Rossetti (2003), Slater and Niemi (2003), Al-fares et al. (2002), Jackobsen and Overgaard (2002), McMechan et al. (2002), Audru et al. (2001), Demanet et al. (2001), Lehmann et al. (2001), Overgaard and Jakobsen (2001), Reicherter (2001), Reicherter and Reiss (2001), Bano et al. (2000), Beres et al. (2000), Orlando (2000), Pipan et al. (2000a), Busby and Merritt (1999), Yetton and Nobes (1998), Liner and Liner (1995, 1997), Meschede et al. (1997), Cai et al. (1996), Lønne and Lauritsen (1996), Wyatt and Temples (1996), Wyatt et al. (1996), Benson (1995), Smith and Jol (1995a), Pratt and Miall (1993)

Due to some overlap, papers can appear in more than one category, for example those investigating coastal aeolian dunes are placed in both the 'Coastal' and 'Aeolian' categories. The glacial category includes deformation structures, but not fluvioglacial sediments or studies related to the internal structure of ice sheets or glaciers.

paper, although much of the GPR research performed is of direct or indirect relevance.

Although the rise in use of GPR in sedimentological studies can be attributed to its wider availability since the 1980s, its use by the research community is also related to the ease and rapidity of data collection, the ability to collect subsurface information away from outcrops or boreholes, and the apparent familiarity of the images, due to GPR's analogy with the established seismic reflection technique. The power of seismic reflection data was demonstrated to geologists when new interpretation techniques associated with seismic stratigraphy (Mitchum et al., 1977) revolutionised regional sedimentological studies in the late 1970s/early 1980s, and subsequently led directly to the concepts associated with the new geological science of sequence stratigraphy (for a review of the history and controversies surrounding seismic and sequence stratigraphy consult Miall and Miall, 2001).

Seismic reflection and GPR data are often analogous in terms of wave propagation kinematics (Ursin, 1983; Carcione and Cavallini, 1995) and reflection and refraction responses to subsurface discontinuities (McCann et al., 1988; Fisher et al., 1992a). Consequently, the broad assumptions that underpin processing and interpretation of seismic reflection data (Sangree and Widmier, 1979; Yilmaz, 1987, 2001) should also apply to GPR. With respect to interpretation, the basic assumption in both techniques is that, *at the resolution of the survey and after appropriate data processing*, reflection profiles will contain accurate information regarding the nature of a sediment body's primary depositional structure. In other words, the form and orientation of bedding and sedimentary structures in the plane of the survey will be adequately represented by recorded reflections, and any nongeological reflections can be readily identified and removed by data processing, or by simply discounting them from the interpretation. Although this assumption is a seemingly simple basis for the interpretation of radar reflection profiles, the degree to which it can be assumed to be true is dependent upon a wide range of factors. These include the nature of the sediment body under investigation, the groundwater regime, the type of terrain immediately adjacent to the survey line, the nature and appropriateness of any data processing undertaken, the interpretation techniques employed, and the overall understanding and experience of the researcher(s) with respect to GPR, and hence their appreciation of the other factors.

Geophysicists and sedimentologists want to extract accurate and meaningful sedimentological information from GPR profiles, but so do geomorphologists, soil scientists, hydrogeologists, archaeologists, environmental scientists and others with an interest in the structure of the shallow subsurface. Due to GPR's relatively recent development and acceptance, and the wide range of potential uses, experience of GPR end-users is wide and their subject backgrounds diverse. This point was emphasised at 'GPR in Sediments' (Geological Society, London, 20–21 August 2001) the first international conference on the applications of GPR in sedimentological studies (Bristow and Jol, 2003). From the papers presented and comments made by delegates in open discussion sessions, it was clear that appreciation of the GPR technique was highly variable across the user, and potential-user, base. On the basis of this observation and a comprehensive review of the literature, it is clear that overall understanding of the value and limitations of GPR is not as high as that generally displayed by the seismic reflection community for their analogous technique, where robust data collection, processing and interpretation methods have been developed, particularly since the 1970s.

It is not the purpose of this paper to review the use of GPR in sedimentology in terms of the actual sedimentological information extracted and the conclusions drawn. At this stage in the development of the use of GPR in sedimentological studies, this seems premature. Instead, it will attempt to consider in detail the basis for the use of GPR in sedimentology, the problems and pitfalls of data collection and processing, and the development of techniques for the interpretation of radar reflection profiles that maximise the sedimentological information obtained and prevent or minimise incorrect interpretations. Such an approach appears timely; an increasing number of sedimentological studies are attempting to utilise GPR (Fig. 1, Table 1), and yet the basis for the processing and interpretation of their data is often unclear and many misinterpretations or overinterpretations are evident.

Given the background outlined above, the aims of this paper are as follows:

(1) to introduce those theoretical aspects that are fundamental to understanding the GPR technique and

its use in sedimentology, in a manner that is suitable for the wide user-base;

(2) to outline the fundamental limitations of the GPR technique, in particular by examining how unprocessed or poorly processed radar reflection profiles can often seriously misrepresent the nature of the subsurface sedimentary structure, and by considering the causes and nature of nongeological reflection events that further complicate subsequent data processing and sedimentological interpretation;

(3) to examine the ways in which appropriate data processing can enhance the interpretability of radar data, by producing reflection profiles that more accurately depict the subsurface sedimentary structure;

(4) to critically evaluate the assumptions that underlie interpretation of GPR data for sedimentological research purposes;

(5) to show how systematic interpretation of appropriately processed GPR profiles, through the application of a strictly defined radar stratigraphy approach, can maximise the sedimentological information extracted and minimise interpretation pitfalls.

To earth scientists familiar with the seismic reflection technique, the need for an understanding of the basic principles underlying data acquisition, processing techniques that convert data into the most meaningful representation of the subsurface possible, and robust interpretation techniques that maximise geological information return, might seem obvious. However, it is clear that, as yet, the GPR community engaged in sedimentological research does not fully share this common vision. This can only inhibit future research and wider appreciation of the technique within the earth-science community. This paper is, therefore, offered as a contribution to the on-going debate regarding the future direction of GPR research in sedimentology.

2. Data collection

Geophysical reflection data are of four main types: common offset, common mid (or depth) point, common source and common receiver (Fig. 2). Common-offset surveys (Fig. 2a) are most frequently used in GPR studies, with commercial radar systems consisting of either a single transmitting and receiving antenna, or two, separate, transmitting and receiving antennae. In the latter systems, a fixed spacing is employed between the antennae, typically with both orientated in the same direction (i.e. copolarised). In conventional surveys, antennae are perpendicular to the survey line, with their broad sides orientated towards each other. With such an antenna configura-

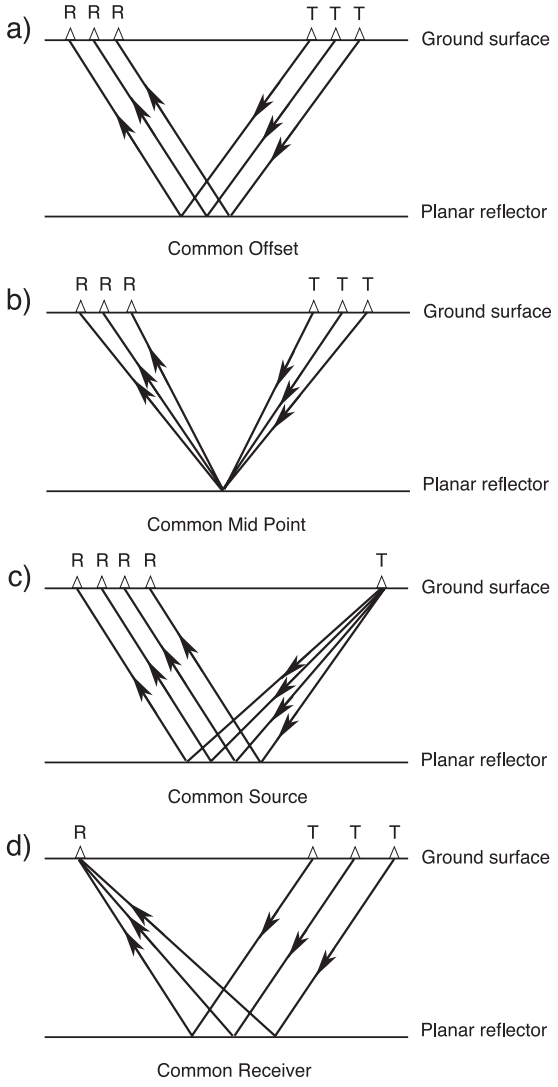

Fig. 2. The four main types of geophysical reflection survey. T = transmitter, R = receiver. Modified from Daniels (1996).

tion the survey is said to be copolarised, perpendicular broadside. However, other potential configurations do exist and these may provide important additional information (van Gestel and Stoffa, 2001; Jol et al., 2002; Lutz et al., 2003). During surveying, antennae are either dragged along the ground and horizontal distances recorded on a time-base, which can be converted to a distance-base through manual marking, or they are moved in a stepwise manner at fixed horizontal intervals (the 'step size'). Step-mode operation generates more coherent and higher amplitude reflections, as antennae are stationary during data acquisition. This allows more consistent coupling between antennae and the ground, with the added benefit of better trace stacking (Annan and Davis, 1992).

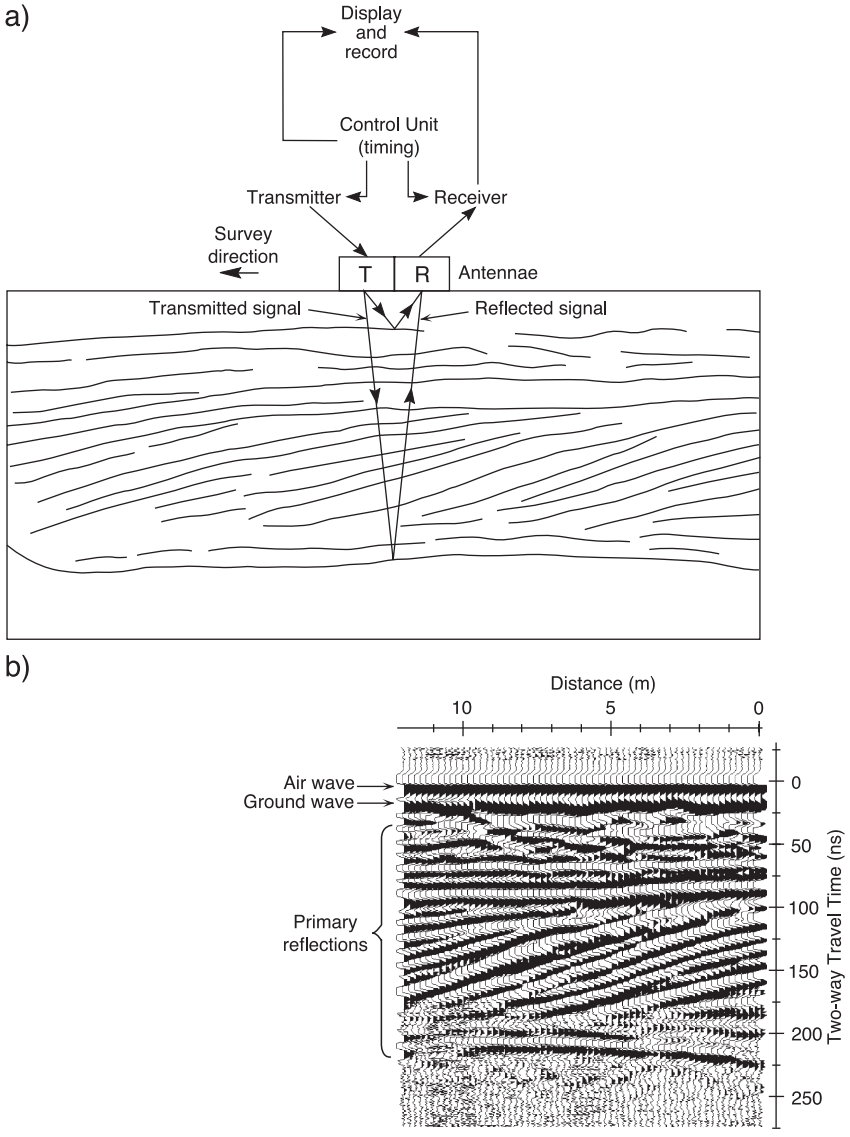

Fig. 3. GPR data acquisition and the resulting radar reflection profile. (a) Data acquisition at an individual survey point, showing GPR system components and subsurface reflector configuration. (b) Radar reflection profile resulting from sequential plotting of individual traces from adjacent survey points. Position of the airwave, ground wave and primary reflections are indicated. Modified from Neal and Roberts (2000).

As data are recorded during surveying, horizontally sequential reflection traces build up a radar reflection profile (Fig. 3). Each trace results from the GPR system emitting a short pulse of high-frequency electromagnetic energy, typically in the MHz range, that is transmitted into the ground. As the electromagnetic wave propagates downwards it experiences materials of differing electrical properties, which alter its velocity. If velocity changes are abrupt with respect to the dominant radar wavelength, some energy is reflected back to the surface. The reflected signal is detected by the receiving antenna. In systems with a single antenna, it switches rapidly from transmission to reception. The time between transmission, reflection and reception is referred to as two-way travel time (TWT) and is measured in nanoseconds (10^{-9} s). Reflector TWT is a function of its depth, the antenna spacing (in systems with two antennae), and the average radar-wave velocity in the overlying material.

Reflections from subsurface discontinuities are not the only signals recorded on a radar trace. The first pulse to arrive is the airwave (Fig. 4), which travels from transmit antenna to receive antenna at the speed of light (0.2998 m ns^{-1}). The second arrival is the ground wave (Fig. 4), which travels directly through the ground between the transmit and receive antennae. The air and ground waves mask any primary reflections in the upper part of a radar reflection profile (Fig. 3). Lateral waves can also be present (Fig. 4) and result from shallow reflections that approach the surface at the appropriate critical angle and are subsequently refracted along the air–ground interface (Clough, 1976). It should be noted that reflections associated with lateral waves are not correctly placed in time (depth) with respect to the interface that generated them.

Most sedimentological studies utilise common-offset, 2-D radar reflection profiles to characterise the subsurface. Where there is significant lateral variability in internal structure, pseudo-3-D or truly 3-D surveys may be desirable. Pseudo-3-D surveys involve collecting data on regular or irregular survey grids, usually in two mutually perpendicular directions, and often display results in fence diagrams (for example, Gawthorpe et al., 1993; Bridge et al., 1995; Bristow, 1995; Aigner et al., 1996; Bristow et al., 1996, 1999, 2000b; Asprion and Aigner, 1997, 1999; Leclerc and Hickin, 1997; Roberts et al., 1997; Pedley et al., 2000; Neal and Roberts, 2001; Russell et al., 2001; Holden et al., 2002; Skelly et al., 2003). In true

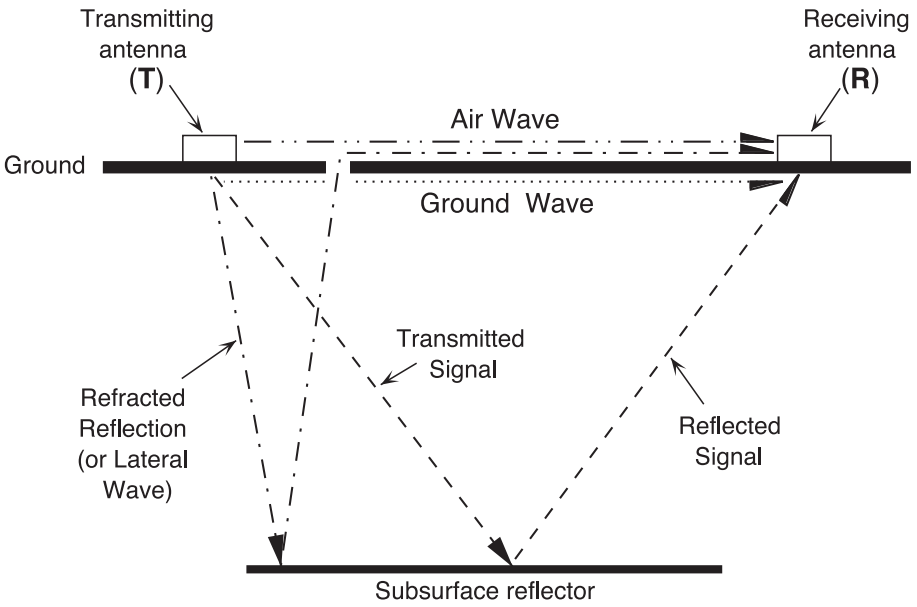

Fig. 4. Ray paths between transmitting and receiving antennae for the airwave, the ground wave, a lateral wave and a reflected wave. Modified from Fisher et al. (1996).

3-D surveys, transect lines are so closely spaced that data for individual traces overlap. 3-D data cubes can be generated from these surveys (for example, Beres et al., 1995, 1999, 2000; McMechan et al., 1997; Sigurdson and Overgaard, 1998; Lehmann and Green, 1999; Junck and Jol, 2000; Lehmann et al., 2000; Sénéchal et al., 2000; Corbeanu et al., 2001; Szerbiak et al., 2001; Jol et al., 2002; Nitsche et al., 2002; Heinz and Aigner, 2003). Collecting true 3-D data is particularly time consuming, largely because of time required to accurately record the position and elevation of data points. Lehmann and Green (1999) attempted to overcome this problem by developing a semiautomated system that records coordinates during radar data collection using a self-tracking laser theodolite. Other experiments have combined the use of GPR with Global Positioning Systems (GPS) (e.g. Urbini et al., 2001; Freeland et al., 2002). Jol and Bristow (2003) consider other practical difficulties in performing GPR field surveys for sedimentary research purposes.

Using two separate antennae, common mid-point (CMP) surveys can also be performed. Antennae are moved apart sequentially at fixed horizontal intervals (Fig. 2b). Resulting increases in TWT are used to calculate average radar-wave velocities to a given reflection (Annan and Davis, 1976; Reynolds, 1997). Once average velocities have been obtained, TWT can be converted to depth estimates.

Common-source or common-receiver surveys (Fig. 2c and d) are rarely performed in GPR studies, unlike in seismic reflection where multi-fold surveys are standard. GPR experiments by Fisher et al. (1992b), Greaves et al. (1996) and Pipan et al. (1999), using standard seismic reflection data-processing techniques and software, indicate that such surveys have a number of advantages over common-offset (single-fold) data collection. These include improved signal-to-noise ratio, reduction of coherent noise, increased depth of penetration, greater reflection continuity and more accurate spatial positioning. However, improvements come at the cost of increased field and processing times, due to the additional data acquired and the need for access to seismic data processing software. Consequently, benefits are only likely to outweigh costs when higher than normal resolution or depth of penetration are required (Fisher et al., 1992b), or where results unobtainable using single-fold data-processing techniques are achieved (Pipan et al., 1999).

3. Theoretical background and causes of subsurface GPR reflections

The material properties that control the behaviour of electromagnetic energy in a medium are dielectric permittivity (ε), electrical conductivity (σ) and magnetic permeability (μ). When an alternating electric field is applied to a material, those electric charges that are bound, and, therefore, unable to move freely, still respond to the applied field by undergoing a small amount of displacement. When the resulting internal electric field balances the external electric field, the charges stop moving (Olhoeft, 1998). This charge separation in distance is called polarisation and can be of various types (Powers, 1997): circular orbits of electrons become elliptical (electronic polarisation), charged molecules undergo slight distortion (molecular polarisation), neutrally charged dipole molecules rotate into alignment with the applied field (orientational polarisation), and ions accumulate at interfaces (interfacial polarisation). Polarisation processes store electric field energy, the amount stored during each cycle of the alternating electric field determines the real dielectric permittivity at that frequency (Powers, 1997). In addition, a small amount of energy is lost as heat due to resistance to the transportation of charge resulting from polarisation processes. The amount of energy dissipated determines the imaginary component of the dielectric permittivity at that frequency (Powers, 1997). The real and imaginary dielectric permittivities are often quoted relative to the dielectric permittivity of free space (i.e. a region where there is no matter and no electromagnetic or gravitational fields). Dielectric permittivity is measured in units of electrical capacitance (farads) per metre, and represents a measure of the material's ability to store electrical charge.

Dielectric permittivity is in part dependent upon frequency of the applied, alternating electric field (Powers, 1997; Olhoeft, 1998). At low frequencies, charges move the full distance required to balance the applied field, but only spend a fraction of the time moving and the rest waiting for the field to reverse (Olhoeft, 1998). This results in maximum energy

storage and minimum energy loss. At high frequencies, polarity reversals occur much more quickly and charge movement may not be complete before the field reverses. This results in charge storage proportional to the distance moved and a proportionally small energy loss through dissipation (Olhoeft, 1998). At a certain intermediate frequency a charge will move the full distance required to balance the external field in the same time as one cycle of that field. This will produce maximum energy loss and energy storage that is an average of the high and low frequency limits (Powers, 1997; Olhoeft, 1998). Clearly, each polarisation process will vary in its ability to respond to the applied electric field and the net effect will be very much dependent upon the medium involved. In porous media, grain edges or pore walls may also limit electrical charge motions (Olhoeft, 1998).

With respect to water, maximum energy losses occur around 10–20 GHz (GHz = 10^9 Hz), and are caused by relaxation (= dissipation) processes associated with the dipolar nature of the water molecule (Powers, 1997). This effectively limits the upper frequency range for GPR systems. At low frequencies, a significant relaxation frequency often associated with rocks and sediments, and of unknown origin, is around 10 MHz (Powers, 1997).

Conductivity is a measure of the ability to transport charge on application of a static electric field. These charge motions are in addition to those associated with polarisation phenomena and occur throughout each half cycle of an alternating electric field, irrespective of its frequency. With respect to GPR, the most important conduction-based energy losses occur due to ionic charge transport in water and electrochemical processes associated with cation exchange on clay minerals (Olhoeft, 1998).

Due to the nature of ε and σ, as frequency of an applied field changes the energy dissipated through charge transport and the energy stored in charge displacements also changes. Hence, conduction losses can also be frequency dependent. For typical earth materials, below a transition frequency of 10–300 MHz energy losses due to σ greatly exceed energy stored by polarisation processes and propagation will be dispersive. This limits low-frequency applications of GPR. Above the transition frequency, energy losses due to conduction are approximately independent of frequency. High-frequency propagation is instead limited by scattering losses, which become particularly important when wavelengths approach the size of the particles (Powers, 1997). Scattering is also influenced by electromagnetic contrast between object and host, object shape, object orientation relative to electromagnetic-field polarisation vectors, and antennae geometry (Olhoeft, 1998). Most GPR systems are designed to perform within a frequency range of 50 MHz–1 GHz.

Magnetic permeability is essentially the magnetic equivalent of dielectric permittivity and is a measure of magnetic field energy stored and lost through induced magnetisation (Powers, 1997). Magnetic permeability can, like dielectric permittivity, be divided into its real and imaginary parts and is often expressed relative to the magnetic permeability of free space. Magnetic permeability is measured in inductance (henrys, H) per metre. All substances respond to an applied magnetic field and various types of magnetic behaviour exist (Walden et al., 1999). Diamagnetic and paramagnetic behaviour are weak compared to ferromagnetism, which occurs in substances where unpaired electrons exist in atoms that are closely spaced. Consequently, strong coupling (of various types) occurs between unpaired electron spins and ferromagnetic substances can display spontaneous magnetisation (Walden et al., 1999). Materials displaying such behaviour are normally compounds of the transition metals, particularly iron, nickel and cobalt. On application of a magnetic field, complex responses are encountered that are a function of: the precise type of ferromagnetism (ferromagnetism senso stricto, anti-ferromagnetism, ferrimagnetism or canted anti-ferromagnetism), crystal form, grain size and grain shape (Walden et al., 1999). In naturally occurring materials, the strongest magnetic response is usually seen in ferromagnetic oxides or sulphides, particularly iron and iron-titanium oxides such as magnetite, maghaematite, haematite, goethite and various titanomagnetites. Laboratory experiments at GPR frequencies have identified important magnetic relaxation losses associated with both natural and artificial iron-rich sands. However, the majority of natural magnetic minerals have never undergone measurement (Olhoeft, 1998).

In addition to energy losses due to ε, σ, μ and scattering, losses also occur due to geometric spreading. As energy propagates downward from the transmitting antenna it spreads in an ever-expanding cone,

causing power to decrease as the inverse square of distance.

Velocity (v) of an electromagnetic wave is a function of its frequency (f), the speed of light in free space, and the host medium's relative dielectric permittivity (ε_r), relative magnetic permeability (μ_r) and σ. Mathematically it is defined as:

$$v = \frac{c_0}{\sqrt{\varepsilon_r \mu_r \frac{1+\sqrt{1+(\sigma/\omega\varepsilon)^2}}{2}}}, \quad (1)$$

where c_0 is the electromagnetic wave velocity in a vacuum (3×10^8 m s^{-1}), and $\sigma/\omega\varepsilon$ is a loss factor, where $\omega = 2\pi f$ is angular frequency (rad s^{-1}).

For low-loss materials, such as clean sand and gravel, the influence of σ over the GPR frequency range is minimal and it is assumed that $\sigma/\omega\varepsilon \approx 0$ (Davis and Annan, 1989; Reynolds, 1997). As little is known about magnetic response at radar frequencies, the influence of μ_r is also assumed to be negligible, and is given a value corresponding to nonmagnetic material ($\mu_r = 1$). As a result, Eq. (1) can be simplified to:

$$v = \frac{c_0}{\sqrt{\varepsilon_r}} \quad (2)$$

As the electromagnetic wave propagates through a medium, its amplitude (A) shows an exponential decline from its initial value (A_0) as it travels distance z, as follows:

$$A = A_0 e^{-\alpha z}, \quad (3)$$

where α is the attenuation constant. For low-loss materials this constant is frequency independent, such that:

$$\alpha = \frac{\sigma}{2}\sqrt{\mu/\varepsilon} \quad (4)$$

It can be seen from Eq. (4) that conductivity exerts the greatest influence over the attenuation constant (Theimer et al., 1994).

Based on the assumptions that lead to Eqs. (2) and (4), a number of statements can be made with respect to behaviour of natural earth materials. Freshwater has a high ε in comparison to air and typical rock-forming minerals (Olhoeft, 1981). As a consequence, freshwater content exerts a primary control over dielectric properties of common geologic materials (Topp et al., 1980; Davis and Annan, 1989). Generally in such rocks, sediments and soils, lower ε results in higher v, and lower σ results in lower α (Table 2). However, these relationships break down if the assumptions outlined above are violated, for instance by introducing high-conductivity substances, such as seawater and certain types of clays, or significant amounts of magnetic material, such as magnetite or haematite.

When a propagating electromagnetic wave encounters a significant subsurface discontinuity with respect to ε_r, μ_r or σ, some energy is reflected. Reflection strength is proportional to the magnitude of change (Reynolds, 1997; van Dam, 2001). The amount of energy reflected, with respect to signal amplitude, is given by the reflection coefficient (R). Assuming that σ and μ_r contrasts are negligible:

$$R = \frac{\sqrt{\varepsilon_{r2}} - \sqrt{\varepsilon_{r1}}}{\sqrt{\varepsilon_{r2}} + \sqrt{\varepsilon_{r1}}} \quad (5)$$

where ε_{r1} and ε_{r2} are the relative dielectric permittivity of adjacent layers 1 and 2, or:

$$R = \frac{\sqrt{v_2} - \sqrt{v_1}}{\sqrt{v_2} + \sqrt{v_1}}, \quad (6)$$

where v_1 and v_2 are the velocity of adjacent layers 1 and 2. In all cases, the value of R will lie in the range $+1$ to -1. Modeling of reflection coefficients for a range of subsurface discontinuities, associated with a variety of geological phenomena in unconsolidated sediments, indicate radar is sensitive to changes in the sediment/air/freshwater ratio (Baker, 1991). Changes in the amount and type of fluid occupying pore spaces, minor changes in porosity, changes in the sediment grain type, and changes in grain shape, orientation and packing all give significant reflections (Table 3). Consequently, features such as the water table, sedimentary structures and lithological boundaries should all be visible with GPR. Ability to image primary sedimentary structure and lithological boundaries is of particular importance to sedimentological applications of GPR. Sedimentary bedding is a product of changes in sediment composition and changes in the size, shape, orientation and packing of grains (Fig. 5), and results in corresponding changes in porosity (Collinson and Thompson, 1989). The rela-

Table 2
Examples of the electrical properties of some common geologic materials at 80–120 MHz (based primarily on van Heteren et al., 1998, but with additional data from Davis and Annan, 1989; Theimer et al., 1994; van Overmeeren, 1994)

Medium	Relative dielectric permittivity (ε_r)	Electromagnetic-wave velocity (m ns^{-1})	Conductivity (mS m^{-1})	Attenuation (dB m^{-1})
Air	1	0.3	0	0
Fresh water	80	0.03	0.5	0.1
Seawater	80	0.01	30,000	1000
Unsaturated sand	2.55–7.5	0.1–0.2	0.01	0.01–0.14
Saturated sand	20–31.6	0.05–0.08	0.1–1	0.03–0.5
Unsaturated sand and gravel	3.5–6.5	0.09–0.13	0.007–0.06	0.01–0.1
Saturated sand and gravel	15.5–17.5	0.06	0.7–9	0.03–0.5
Unsaturated silt	2.5–5	0.09–0.12	1–100	1–300[a]
Saturated silt	22–30	0.05–0.07	100	1–300[a]
Unsaturated clay	2.5–5	0.09–0.12	2–20	0.28–300[a]
Saturated clay	15–40	0.05–0.07	20–1000	0.28–300[a]
Unsaturated till	7.4–21.1	0.1–0.12*	2.5–10	[b]
Saturated till	24–34	0.1–0.12*	2–5	[b]
Freshwater peat	57–80	0.03–0.06	<40	0.3
Bedrock	4–6	0.12–0.13	10^{-5}–40	7×10^{-6}–24

From Neal and Roberts (2000).
[a] Unsaturated and saturated values not differentiated (van Heteren et al., 1998).
[b] Values not available.

tionship between primary radar reflections and primary bedding underpins use of GPR in sedimentological studies, particularly with respect to clastic sediments where physical processes typically dominate.

Numerous GPR studies have broadly confirmed the relationship between primary radar reflections and primary bedding (Table 1). This has been achieved either by performing direct visual comparison be-

Table 3
Reflection coefficient modeling for typical changes in sediment water content, porosity, lithology, grain shape and grain orientation

Layer 1 Layer 2	Porosity (%)	ε_r	Reflection coefficient (+1 to −1)	Geological significance
Dry sand	35	3.1		
Saturated sand	35	20.7	−0.44	Water table
Dry sand	35	3.1		5% porosity change in dry sand
Dry sand	30	3.27	−0.013	
Saturated sand	35	20.7		5% porosity change in saturated sand
Saturated sand	30	17.7	+0.04	
Saturated sand	35	20.7		lithology change to high-porosity peat
Peat	70	46.5	−0.2	
Dry sand	35	3.1		dry heavy-mineral placer deposit
Dry heavy-mineral sand	35	19.9	−0.43	
Saturated sand	35	20.7		saturated heavy-mineral placer deposit
Saturated heavy-mineral sand	35	53	−0.23	
Round grains	33	23.5		
Platey grains	33	16.9	+0.08	grain-shape change
Isotropic grain packing	33	22.5		orientation change for platey grains
Anisotropic grain packing	33	16.9	+0.7	

Reflection coefficients indicate the proportion of energy theoretically reflected from an interface. Values range from +1 to −1, the sign indicating polarity of the reflected wave. Modified from Baker (1991).

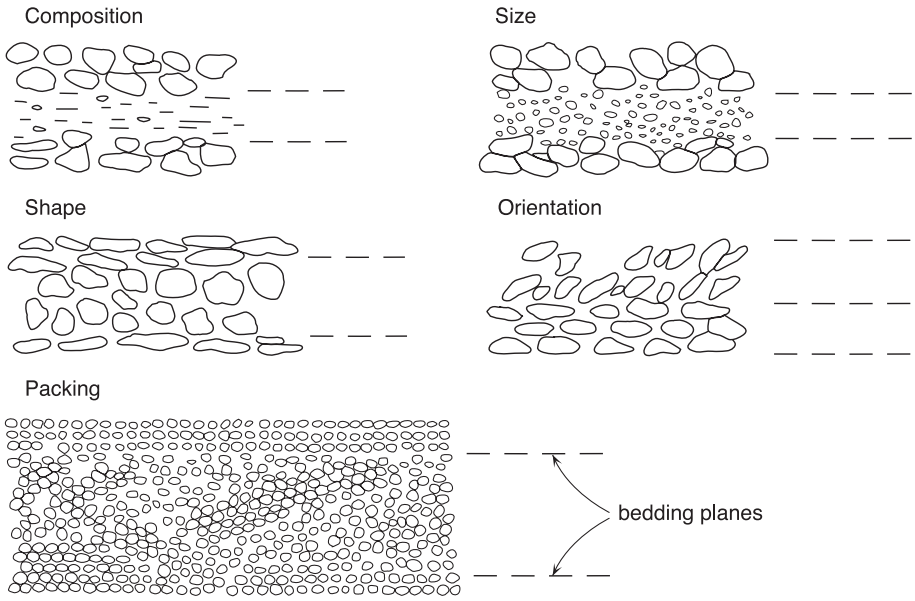

Fig. 5. Bedding in sediments and sedimentary rocks resulting from changes in composition, size, shape, orientation and packing of sediment grains. Redrawn from Collinson and Thompson (1989).

tween radar reflection profiles and underlying sedimentary structure or, perhaps less satisfactorily, by obtaining reflection geometries recognisable to the interpreter as resulting from primary sedimentary structure. However, only more recently, with the work of van Dam and Schlager (2000), van Dam (2001) and van Dam et al. (2002a,b, 2003) has a more fundamental examination been undertaken of the causes of GPR reflections in sediments. In the aeolian coversands they were studying, these workers found that changes in ε_r, associated with variations in water content, were most significant in causing reflections and that changes in μ_r and σ were not particularly significant. Variations in water content were related to both changes in sediment porosity and a particular sediment's ability to hold water. Presence of organic material, iron-oxide precipitates and finer grained sediment had all caused water content, and hence ε_r, to increase. Organic material occurred as distinct soil horizons in the coversands that marked important bounding surfaces within the sedimentary sequence. It was, therefore, effectively enhancing reflections related to primary sedimentary structure. A similar effect has been noted in coastal aeolian dune deposits (Clemmensen et al., 2001; Neal and Roberts, 2001).

Small textural variations associated with primary bedding in unsaturated aeolian sediment were shown by van Dam (2001) and van Dam et al. (2003) to result in changes in ε_r capable of causing clear radar reflections. This was again due to changes in water content, which was itself controlled by the size distribution and connectivity of sediment pore networks. Results also confirmed the assertion of Annan et al. (1991) that sharpness of a reflection is a function of transition-zone width (i.e. distance over which ε_r changes) relative to dominant wavelength. Wavelengths must be less than approximately three times the size of the transition zone to obtain a sharp reflection. Above this there is typically dispersion and generation of more diffuse reflections.

Goethite iron-oxide precipitates, occurring either in bands or irregular layers, were shown by van Dam (2001) and van Dam et al. (2002a) to result in significant reflections in the coversands they studied. This was due to the higher water retention capacity of goethite with respect to the host quartz sand, which resulted in higher ε_r. Neither μ_r or σ were significantly altered by presence of goethite and were not, therefore, responsible for reflections. Diagenetic precipitation of iron oxides in unconsolidated sediments is related to flow of pore water. Sedimentary structure,

various discontinuities and overall regional flow patterns help determine flow path and, hence the nature and form of precipitates. Where precipitation was found along primary bedding, reflection strength was enhanced due to the higher ε_r contrast and reflection patterns accurately represented the nature of bedding (van Dam, 2001; van Dam et al., 2002a). However, where iron-oxide bands cut across depositional bedding or irregular precipitations were developed, reflection patterns were more complex, with reflections from precipitates masking, or interfering with, reflections from primary bedding.

The findings of van Dam and Schlager (2000), van Dam (2001) and van Dam et al. (2002a,b, 2003) have important implications, because in certain instances they call into question the assumption that primary reflections in radar profiles obtained from sedimentary sequences represent primary depositional structure. The influence of secondary iron-oxide precipitation is particularly important because this is a common feature in many unconsolidated sand and/or gravel-dominated sedimentary sequences.

The influence of diagenetic precipitates and other diagenetic processes is likely to be even more significant in sedimentary rocks, although so far this has not been investigated in any detail. In addition, subsequent surface fracturing and preferential weathering in exposed outcrops are also likely to produce reflections unrelated to primary sedimentary structure (Corbeanu et al., 2001). Some of these problems can potentially be reduced with careful data processing (Szerbiak et al., 2001).

Fractures and other deformation structures also generate reflections unrelated to primary sedimentary structure, as they usually represent major electromagnetic discontinuities within a sediment or rock body. Furthermore, they will also disturb bedding continuity. Faults, joints and folds have been identified in sediments and sedimentary rocks by numerous GPR investigations (Table 1). The presence of such features can make radar reflection profiles very difficult to interpret sedimentologically and even lead to misinterpretations when they are not properly identified.

Another common non-sedimentary feature in radar profiles from unconsolidated sediments is a distinct reflection from the water table. The detection of the water table is common at lower radar frequencies because thickness of the capillary zone is small compared to radar wavelength. Consequently, there is sufficient contrast between unsaturated and saturated sediments to reflect an easily detectable proportion of incident wave energy (Table 2). The water table is usually a horizontal or very-gently dipping surface that cross-cuts primary sedimentary structure (for example, Beres et al., 1995; Birkhead et al., 1996; Harari, 1996; van Heteren et al., 1998; van Overmeeren, 1998; Smith et al., 1999; Tronicke et al., 1999; Vandenberghe and van Overmeeren, 1999; Neal and Roberts, 2000, 2001; Russell et al., 2001), although distinct ‘steps’ can occur under certain ground conditions (van Overmeeren, 1997).

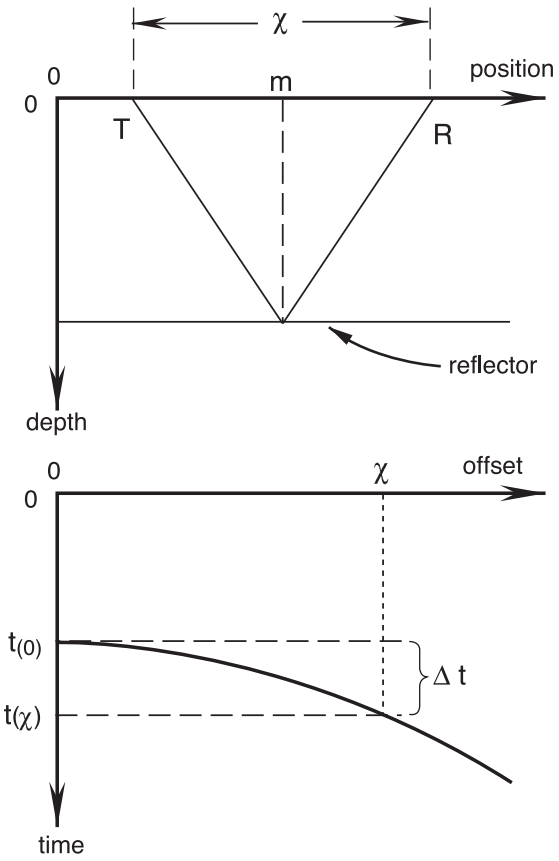

Fig. 6. Normal moveout resulting from a separation (x) between the transmitter (T) and receiver (R). The time $t_{(x)}$ for a reflection with a T–R separation x is larger (by Δt) than $t_{(0)}$, which would be observed at zero offset (i.e. if the antennae were coincident). With increasing antenna separation, the reflection from the horizontal reflector displays hyperbolic normal moveout. Modified from Fisher et al. (1992a).

Although it is generally true that in sediments and sedimentary rocks reflections parallel bedding, it is clear that some reflections can result from subsurface features unrelated to primary sedimentary structure. Consequently, at each study site there is a need for a clear and realistic assessment of the non-sedimentary features likely to be present. Preferably this should occur prior to data collection, and certainly before data processing and interpretation.

4. Inherent limitations of unprocessed GPR data

4.1. Time-zero drift

This occurs when the first break in a common-offset radar reflection profile (the airwave) changes position from trace to trace during data collection. It causes misalignment not only of the air and ground waves, but also the primary and secondary reflections beneath. Drift commonly occurs when console electronics are markedly colder or warmer than ambient air temperature, such as when a GPR system is operated outdoors having just been removed from storage (Sensors and Software, 1999a). This problem is usually eliminated after the console's internal temperature has stabilised with respect to the external temperature (Bano et al., 2000). Damaged cables may also induce similar, but more erratic, time shifts (Sensors and Software, 1998).

4.2. Common-offset data collection

Although common-offset surveying is the most popular, convenient and quickest way of obtaining radar reflection profiles, there is an inherent limitation

Table 4
Comparison between two-way travel time (TWT) and depth for a zero-offset GPR profile and common-offset profiles with antenna separations of 0.5, 1 and 2 m

Zero Offset		Common Offset					
0 m antenna separation		0.5 m antenna separation (e.g. 200 MHz)		1 m antenna separation (e.g. 100 MHz)		2 m antenna separation (e.g. 50 MHz)	
TWT (ns)	depth (m)	TWT (ns)	depth (m)	TWT (ns)	depth (m)	TWT (ns)	depth (m)
0	0	4.1	0.25	8.3	0.5	16.5	1.0
1.7	0.1	4.5	0.27	8.4	0.51	16.7	1.01
3.3	0.2	5.3	0.32	8.9	0.54	16.9	1.02
5.0	0.3	6.4	0.39	9.6	0.58	17.2	1.04
6.6	0.4	7.8	0.47	10.6	0.64	17.9	1.08
8.3	0.5	9.3	0.56	11.7	0.71	18.5	1.12
9.9	0.6	10.7	0.65	12.9	0.78	19.3	1.17
11.6	0.7	12.2	0.74	14.2	0.86	20.2	1.22
13.2	0.8	13.9	0.84	15.5	0.94	21.2	1.28
14.9	0.9	15.4	0.93	17.0	1.03	22.3	1.35
16.5	1.0	17.0	1.03	18.5	1.12	23.3	1.41
24.8	1.5	25.1	1.52	26.1	1.58	29.8	1.80
33.1	2.0	33.4	2.02	34.0	2.06	37.0	2.24
41.3	2.5	41.5	2.51	42.2	2.55	44.5	2.69
49.6	3.0	49.8	3.01	50.3	3.04	52.2	3.16
82.6	5.0	82.8	5.01	83.1	5.03	84.3	5.10
115.7	7.0	115.9	7.01	116.0	7.02	116.9	7.07

A single, constant velocity of 0.121 m ns^{-1} and horizontal reflectors are assumed. As a consequence of antenna separation, reflections on the common-offset profiles are displaced downwards, i.e. they appear at greater depth than their true (zero offset) position. This is due to significantly longer travel times to reflectors at shallow depth. This effect reduces with increasing depth, such that beneath the air and ground waves only a small difference exists between depths on the zero-offset and common-offset profiles, relative to total depth and vertical resolution. This is illustrated by reference to the 7-m-thick zone above the water table in the 200, 100 and 50 MHz common-offset profiles presented in Fig. 7, which have estimated vertical resolutions of 0.23, 0.4 and 0.56 m, respectively.

Area obscured by the air and ground waves in the 200, 100 and 50 MHz radar profiles shown in Fig. 7.

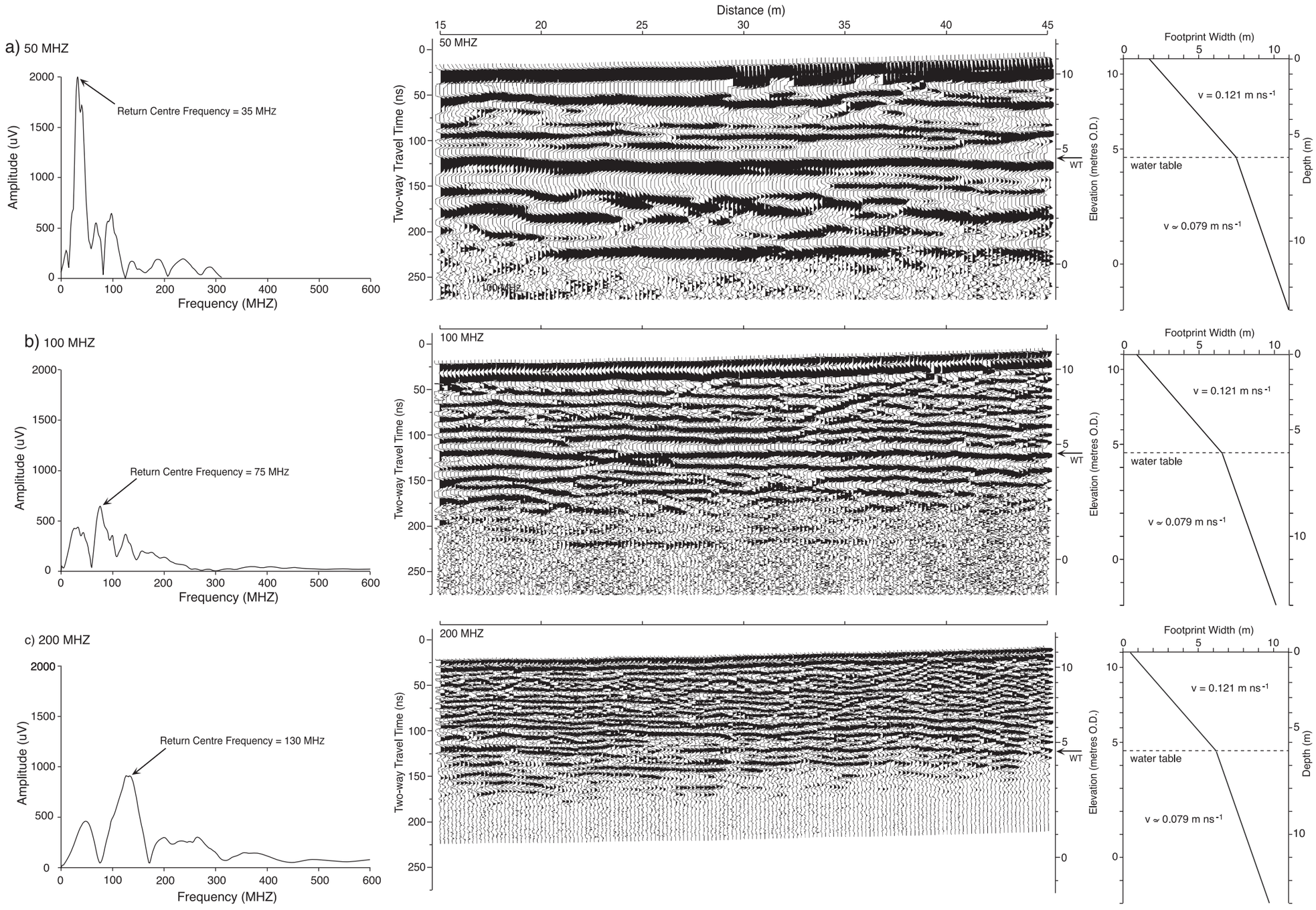

Fig. 7. Return-frequency spectrums, radar reflection profiles and radar-footprint size variations with depth for data collected along the same shore-parallel transect across sand-and-gravel-rich beach ridge-plain deposits, Beckfoot, outer Solway Firth, northwest England using antennae with nominal centre frequencies of (a) 50 MHz, (b) 100 MHz and (c) 200 MHz. Note expansion of the elevation axis beneath the water table (WT) due to the decrease in radar wave velocity.

to this mode of data acquisition. As antennae are not coincident, image distortion occurs (Fisher et al., 1992a), because reflection travel times are too long with respect to depth of the reflector that generated them (Fig. 6). Table 4 illustrates this by reference to the GPR profiles in Fig. 7, which were collected at three different antenna frequencies and spacings. Difference between travel time at a given offset and at zero offset is called normal moveout. The effect of normal moveout becomes less significant with increasing travel time (depth), as the time taken for the radar wave to travel from the transmitter, to the reflector and then back to the receiver increasingly approaches, but never truly meets, the zero-offset time (i.e. the time taken with zero transmitter–receiver separation). However, the situation becomes more complex if significant velocity variations occur with depth or reflectors are dipping (Yilmaz, 1987, 2001). However, Yilmaz (1987, 2001) also notes that as long as the average (root mean squared) velocity to a reflector is known, the degree of offset is less than reflector depth, and dips of reflectors in the line of the survey are shallow ($<15°$), hyperbolic normal moveout (Fig. 6) is still a reasonable approximation.

4.3. Signal saturation

Due to the short time interval between transmitter 'shots' during surveying and large energy input from the airwave, ground wave and near-surface reflections, receivers become signal saturated (Fisher et al., 1996). When this occurs, a slowly decaying, low-frequency 'wow' is induced on the trace that is superimposed on higher frequency reflections (Sensors and Software, 1999a). The wow's magnitude depends on ground conditions and antenna separation (Sensors and Software, 1998).

4.4. Depth of penetration

It has already been demonstrated that propagating electromagnetic waves undergo energy losses in the subsurface. These limit the depth that radar waves can penetrate at a particular frequency or location. The frequency-dependent nature of attenuation (Davis and Annan, 1989) means that, in general, the higher the antenna's frequency, the shallower the depth of penetration (Fig. 7). Practical implications of this relationship for sedimentological studies have been examined by Jol (1995), Smith and Jol (1995b) and Jol et al. (2002).

4.5. Horizontal and vertical resolution

In seismic reflection, resolution has two common definitions (Knapp, 1990). These can be directly applied to radar data. The first relates to the ability to determine reflector position in space or time. In terms of vertical resolution, this is a function of the wavelet sharpness or pulse width. By this definition, and for practical purposes, vertical resolution is proportional to frequency, i.e. as frequency increases so does vertical resolution (Knapp, 1990). The second definition of resolution relates to ability to resolve two closely spaced features. With respect to vertical resolution, this is controlled by wavelength (Knapp, 1990). Wavelength (λ) is governed by wave frequency and velocity:

$$\lambda = \frac{v}{f} \tag{7}$$

The return centre frequency (the most common frequency detected by the receiving antenna) is typically lower than the nominal centre frequency for the transmit antenna (Fig. 7). This is because any antenna transmits across a range of frequencies (Conyers and Goodman, 1997) and higher frequencies are preferentially attenuated as waves propagate through the earth, resulting in longer average wavelengths (Jol, 1995; Bano, 1996). Consequently, more realistic vertical resolution estimates are obtained using return centre frequency. It is evident from Eq. (7) that if the return centre frequency is higher then λ decreases and vertical resolution, by the second definition, increases. In order to increase vertical resolution, by the two definitions given above, the high-frequency content of the data must be enhanced. This has an additional benefit in that repetitive thin beds (beds of similar dimension to the wavelength) tune response to frequencies harmonic with bed thinness. Hence, thinner beds are resolved if there are higher frequencies in the bandwidth (Knapp, 1990).

Wave theory indicates that the best vertical resolution that can be achieved is one-quarter of dominant wavelength (Sheriff, 1977). Within that vertical distance any reflections will interfere in a constructive

manner and result in a single, observed reflection (Fig. 8). Vertical resolution of a radar reflection profile has important implications for its sedimentological interpretation, as it will determine the scale of sedimentary structure that can be observed. In particular, it will determine whether laminae, lamina-sets, beds or bedsets can be imaged (Fig. 9). Given that the thickness

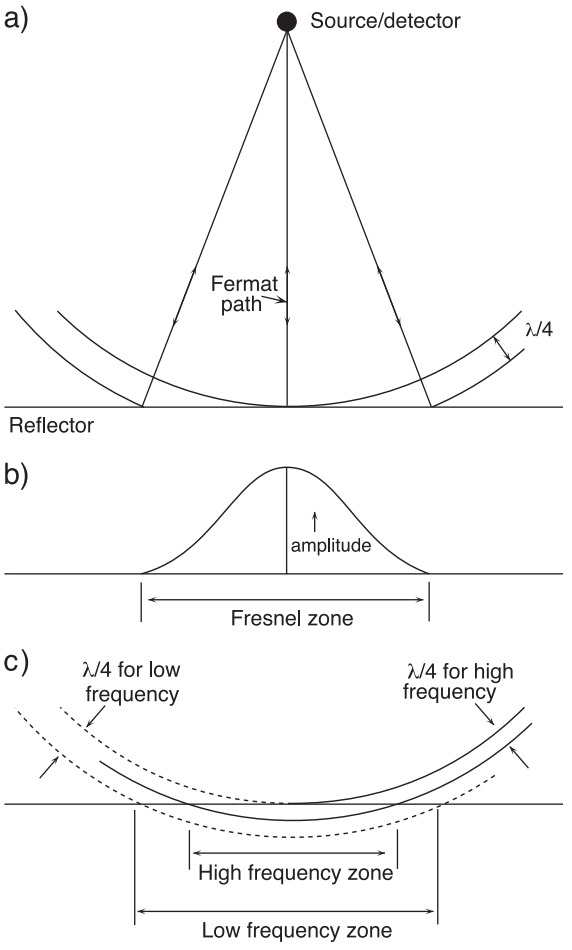

Fig. 8. Horizontal resolution as determined by Fresnel zone width. (a) Electromagnetic waves propagate through the ground in an ever-expanding cone, with the cone's apex at the transmitting antenna. All reflections within one-quarter of the dominant wavelength will interfere constructively to form a single reflection. (b) Waves closest to the Fermat path contribute most to a reflection's amplitude. (c) Fresnel-zone width is a function of reflector depth and frequency-dependent wavelength. The higher the frequency (and shorter the wavelength) the higher the horizontal resolution. Modified from Emery and Myers (1996).

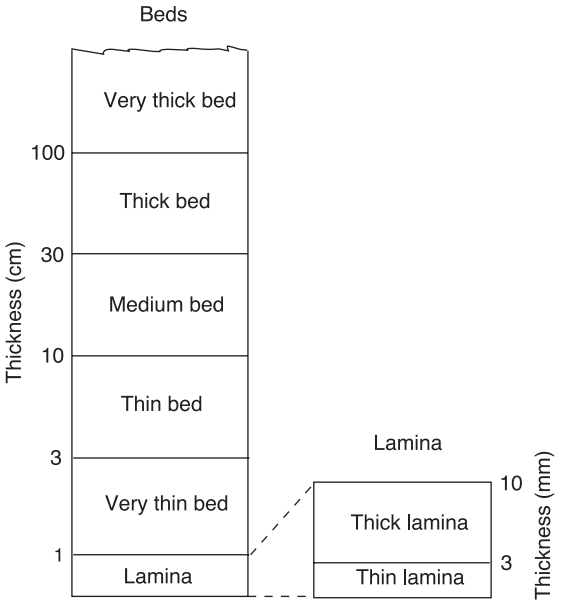

Fig. 9. Practical distinction between laminae and beds in terms of thickness. Redrawn from Boggs (1995).

of individual laminae is regarded by many as <0.01 m (McKee and Weir, 1953; Collinson and Thompson, 1989; Bridge, 1993; Boggs, 1995) and maximum vertical resolutions so far recorded in low-loss materials such as sand and gravels with high-frequency antennae are between 0.02 and 0.08 m (e.g. Neal et al., 2002b, 2003, with 900 MHz antennae), sets of laminae, beds and bedsets are most likely to be resolved.

In the case of a spherical wave front, a suitable assumption in seismic profiling, horizontal resolution is governed by the width of the first Fresnel zone (Fig. 8). Fresnel zone width is a function of wavelength and depth to a particular reflector (Sheriff, 1977; Reynolds, 1997). Depth is important because radiated energy expands laterally as it propagates downwards, such that horizontal resolution decreases downwards. However, energy transmission into the ground is fundamentally different in radar. GPR antennae are dipoles and generate polarised wavefields that show strong directionality to amplitudes (Engheta et al., 1982; Roberts and Daniels, 1996; Lehmann et al., 2000). Radiated energy creates an electromagnetic field within 1.5 wavelengths of an antenna (Engheta et al., 1982; Conyers and Goodman, 1997). Conse-

quently, ground within this zone is essentially part of the antenna and defines the 'near-field' zone (Conyers and Goodman, 1997). Beyond the 'near-field' zone is the 'far-field' zone in which energy is transmitted. Shape of the propagating radar wave front is complicated by the way in which the wavefield couples with the ground (Engheta et al., 1982; Lehmann et al., 2000) and is elongated in the direction of the survey line when copolarised, perpendicular broadside surveying is undertaken. Also, the higher the ε_r of the ground the more focused the radar beam (Annan et al., 1975; Conyers and Goodman, 1997; Reynolds, 1997). The receiving pattern of an antenna is exactly the same as the transmitting pattern, and shows the same degree of directionality for given ground conditions (Roberts and Daniels, 1996). A method and equation (Eq. (8)) for estimating the approximate size of the radar footprint (area illuminated on a buried surface), based on subsurface ε_r, radar wavelength and depth to a horizontal reflector, is shown in Fig. 10. A practical illustration of the increasing size of the radar footprint with depth is given in Fig. 7 for three antenna frequencies.

For a given frequency, the width of the long axis of the radar footprint estimated using Eq. (8) (Fig. 10) is always wider than that which would be derived for a spherical wave front (i.e. the width of the conventional circular Fresnel zone), although widths approach each other at high values of ε_r. However, as the radar footprint is elliptical in shape, its short axis is narrower than that associated with the circular Fresnel zone, except at very low values of ε_r. Where dipping surfaces are encountered, shape and size of the footprint is further complicated by orientation of the radiating wave front with respect to reflector dip and strike (Moran et al., 2000), although there is no simple way of estimating this.

The decrease in horizontal resolution with depth noted above, and illustrated in Fig. 7, has important implications for interpretation of radar profiles in sedimentary research. Based on a radar profile collected over fluvioglacial sands and gravels that were subsequently excavated, Heinz (2001) noted that stratification in the lower part of the section was poorly imaged compared to similar stratification in the upper part. Heinz (2001) also demonstrated, using forward modeling based on the detailed sedimentology of excavated exposures, that the scale of the feature that can be resolved is limited by antenna frequency, if it is assumed ground conditions at a particular location are invariant over the time scale of an individual survey.

A further consideration with respect to horizontal resolution is the horizontal spacing between traces on

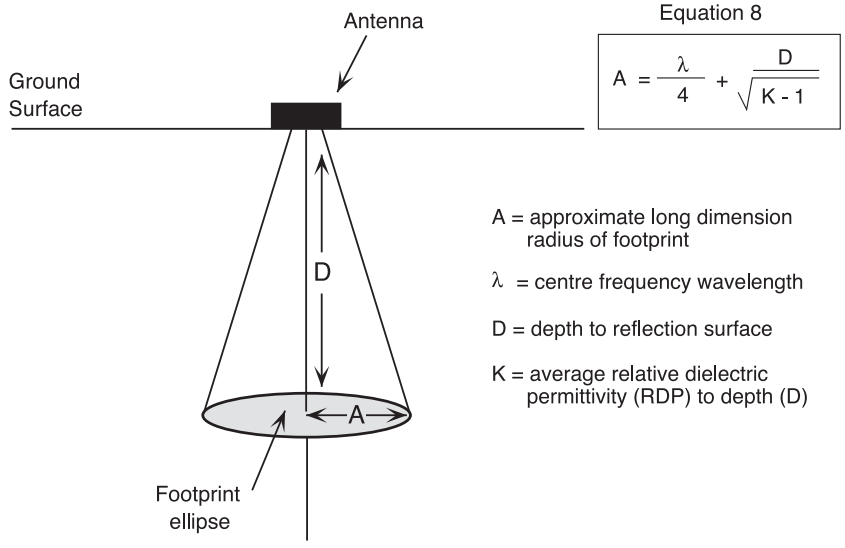

Fig. 10. Calculating radar-footprint size on a horizontal reflector. Modified from Conyers and Goodman (1997) and Annan (personal communication, 2002).

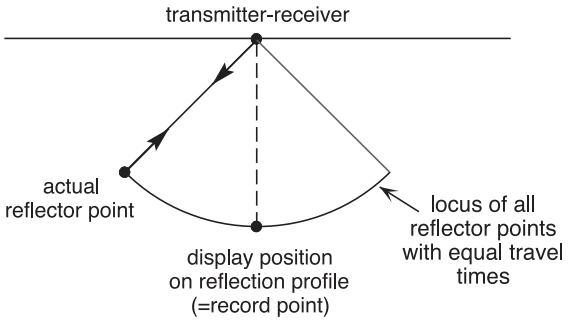

Fig. 11. At any particular reflection time, a reflector point may lie anywhere on the radar wave front. On an unmigrated reflection profile the record point is mapped directly beneath the transmitter–receiver. Modified from Kearey and Brooks (1991).

the radar reflection profile. This is a function of the step size used when originally collecting the radar data (see Section 2). In selecting a step size the aim is to horizontally sample the subsurface sedimentary structure such that it is adequately represented on the final radar image. The step size chosen is both a function of the frequency of the antenna(e) used and the nature of the sedimentary structure. GPR manufactures often recommend conservative maximum step sizes for their different antennae that are appropriate for any ground conditions and survey objectives (e.g. Sensors and Software, 1999a). The higher the frequency of the antenna(e) the smaller the suggested maximum step size. However, in practice the recommended step size can often be increased, especially where the sedimentary structures have low to moderate dip. The most effective way of determining the most appropriate step size for a given survey is through a series of initial field trials. Woodward et al. (2003) found that for the fluvial sedimentary features they were investigating to be resolved with accuracy, reflections from them needed to appear on at least 10 adjacent radar traces.

4.6. Diffractions, distortions, dip displacements and out-of-line reflections

The simple impression given by 2-D radar reflection profiles that reflections recorded on a given trace were obtained from directly beneath the survey point (Fig. 3) is incorrect. This is because, as already noted, radar antennae radiate and receive electromagnetic energy in a complex 3-D cone. Consequently, a reflection on a trace can originate anywhere on the radar wave front (Fig. 11). The effects that result include (Yilmaz, 1987, 2001; Robinson and Çoruh, 1988; Kearey and Brooks, 1991):

(1) down-dip movement of reflector points generated on dipping reflectors, such that a record surface is created that has an apparent dip shallower than the reflector that generated it (Fig. 12);
(2) generation of diffractions by isolated reflector points (Fig. 13) and strongly curved reflectors (Fig. 14), often obscuring primary reflections;

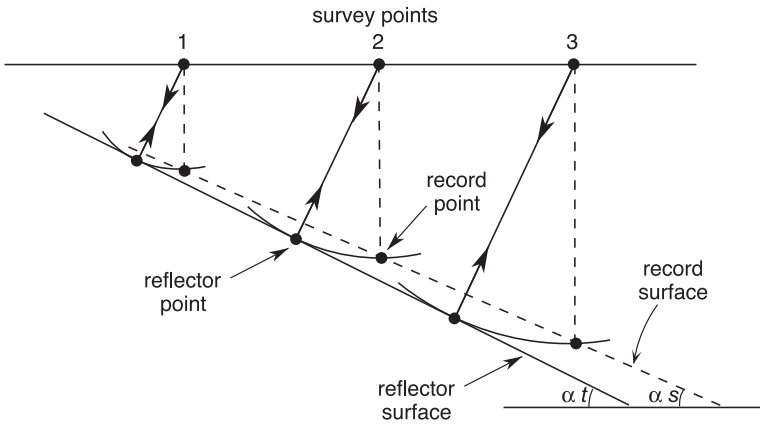

Fig. 12. On an unmigrated reflection profile, reflector points from a planar, dipping reflector (dip = α_t) have undergone down-dip movement and the resulting record surface has a shallower dip (α_s). Modified from Kearey and Brooks (1991).

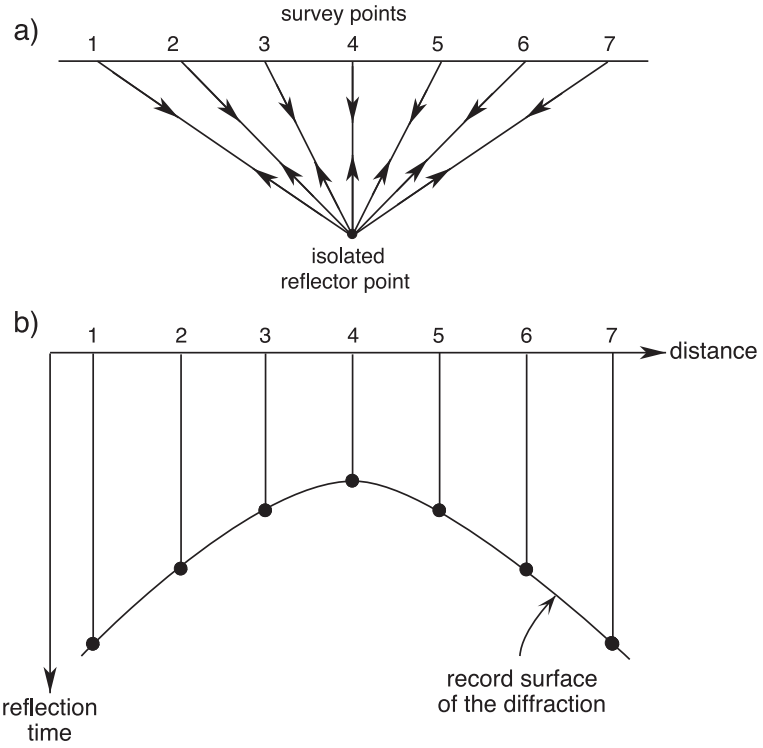

Fig. 13. Generation of a diffraction on an unmigrated reflection profile from an isolated reflector point. (a) Reflection paths to and from the reflector point, at survey points 1 to 7. (b) Diffraction on the resulting unmigrated radar reflection profile, caused by mapping record points directly beneath each survey point. Modified from Kearey and Brooks (1991).

(3) distortions caused by undulating reflectors, such that record surfaces depict synclinal features that are narrower, and anticlines that are broader, than in reality.
(4) generation of out-of-plane reflections.

The extent to which subsurface diffractions, distortions and out-of-line reflections develop in an unprocessed radar profile is a function of the shape, orientation, dip and spatial location of the reflector that generated them and nature of the radiating wave front. These features again have important implications for the interpretation of radar reflection profiles. First, dips will be underestimated (Fig. 12), with the amount of underestimation (in degrees) increasing with increasing dip, such that for reflector surfaces perpendicular to the plane of a radar reflection profile:

$$\sin \alpha_t = \tan \alpha_s \quad (9)$$

where α_s is the dip of the record surface and α_t is the true dip of the reflector (Kearey and Brooks, 1991, p. 70).

Second, objects that act as isolated reflector points (Fig. 13), such as man-made pipes and cables perpendicular to the survey line (Fig. 15a), or individual sediment grains that are large with respect to radar wavelength, e.g. cobbles and boulders in gravel-sized sediment (Fig. 15b), will generate diffractions that can obscure primary reflections (Naegeli et al., 1996; Papziner and Nick, 1998; Busby and Merritt, 1999). In fluvial sediments, diffractions caused by lateral truncation of various heterogeneities have also been identified (Beres et al., 1999). Vandenberghe and van Overmeeren (1999) used synthetic-radar-profile modeling to account for linear sets of diffractions generated by intersecting fluvial channels, channel bottoms and the edge of horizontal beds eroded by a channel. Faults and joints can also result in diffractions (Wyatt et al., 1996; Overgaard and Jakobsen, 2001).

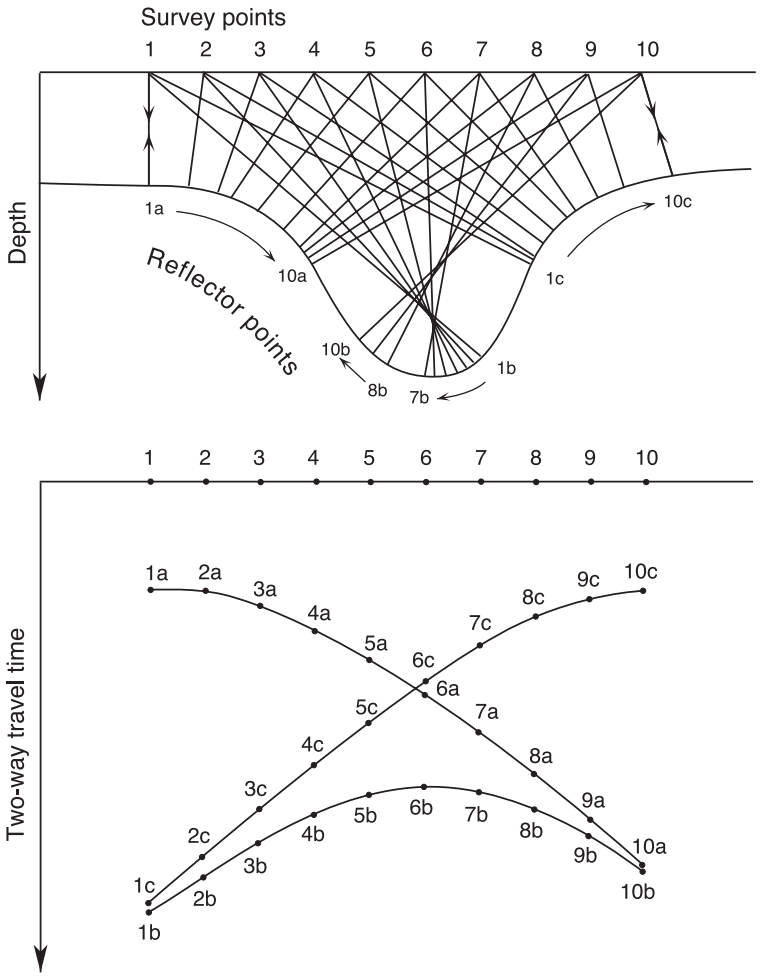

Fig. 14. Record surfaces generated by a concave reflector whose curvature exceeds that of the radiating wave front. Waves from survey points 1 to 10 have at least three reflector points (a, b, c) on the reflector surface. The resulting unmigrated radar reflection profile shows a complex 'bow-tie' pattern generated by three, separate, curved record surfaces. Modified from McQuillin et al. (1979).

Third, where concave-up, curved bedding is encountered, such as trough cross-bedding, whether it can be imaged in unprocessed data will depend upon its relationship to wave front curvature. Where bedding curvature exceeds wave front curvature a 'bow-tie' record surface pattern will be generated, because reflections will originate from at least three discrete reflector points (Fig. 14). These 'bow-tie' patterns are a poor representation of the reflector that generated them, and it will be difficult to interpret the presence of such curved features with confidence. Even where bedding curvature is less than wave front curvature, the image will still be distorted due to down-dip movement of the record surface, such that troughs appear narrower than in reality.

Fourth, out-of-plane reflections, from both isolated point reflectors and discrete reflector surfaces, are particularly hard to identify in the 2-D radar reflection profiles used in many sedimentological studies. Lehmann et al. (2000) utilised the strongly directional nature of the energy radiated by GPR antenna to design surveys that would identify out-of-plane reflections from various natural subsurface features in a suite of fluvioglacial sediments. Such an approach clearly has significant potential in other studies, par-

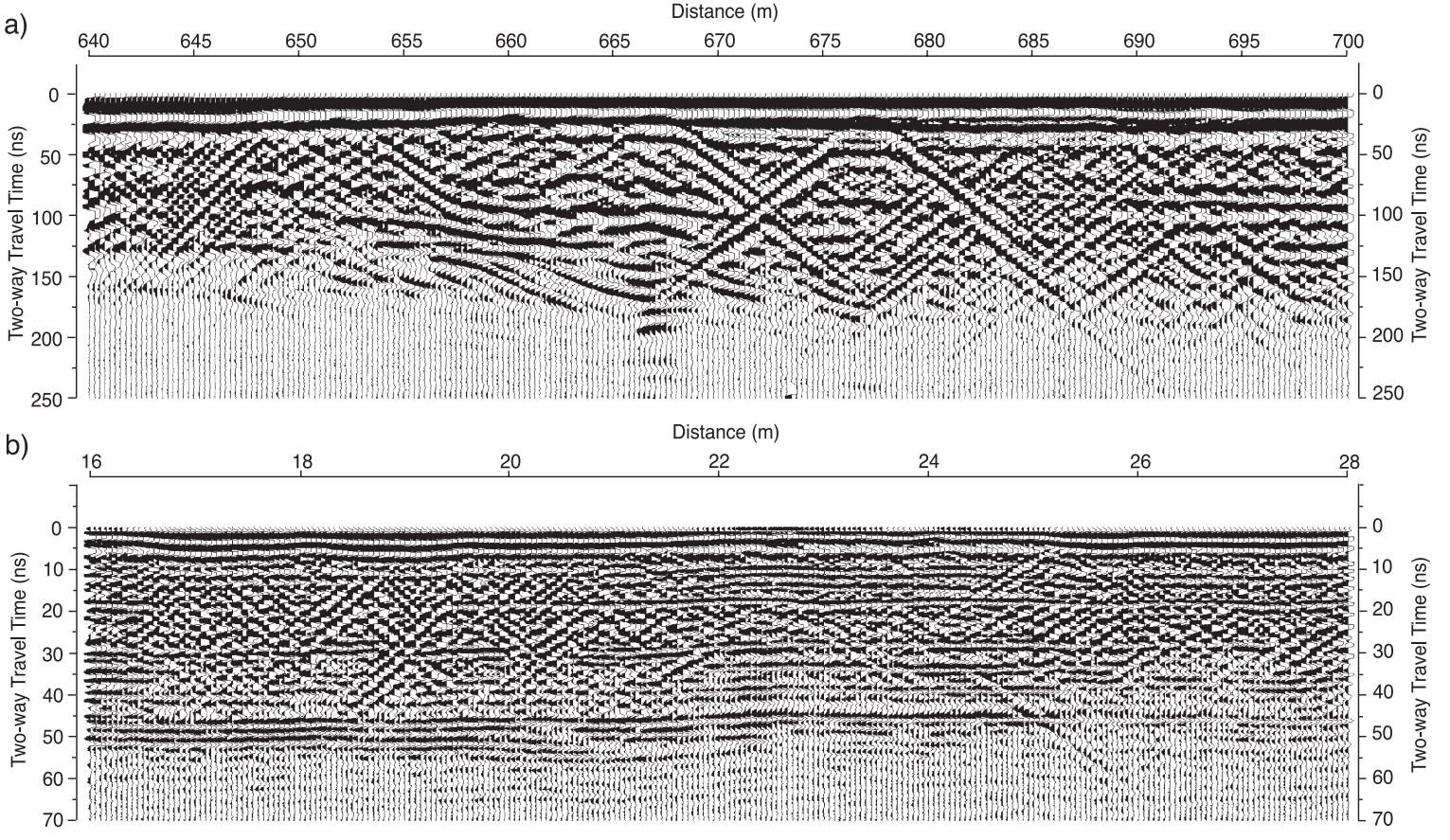

Fig. 15. (a) Unmigrated 100 MHz radar reflection profile showing a complex sequence of cross-cutting diffractions. These have resulted from communication cables and pipes (associated with a sprinkler system) both buried in the shallow subsurface (ca. 1 m) at the Royal Birkdale Golf Club, Sefton, northwest England. The golf course is on coastal dunes, but many reflections resulting from the dunes' primary sedimentary structure, which mainly appear to be dipping gently to the right, are obscured by the steeply dipping diffraction tails. The profile has an AGC gain applied with a maximum limiting value of 500, and no horizontal or vertical averaging. (b) Complex sequence of cross-cutting diffractions in an unmigrated, shore-parallel, 450 MHz radar reflection profile from a small, mixed-sand-and-gravel beach-ridge strandplain at Aldeburgh, Suffolk, southeast England. The diffractions partially obscure a set of horizontal reflections resulting from the primary sedimentary structure of the beach deposits. Diffractions are believed to be caused by large sediment grains (e.g. cobbles) throughout the upper part of the sedimentary sequence. The profile has an AGC gain applied with a maximum limiting value of 125, and no horizontal or vertical averaging.

ticularly where sedimentary structure shows marked three-dimensional heterogeneity.

4.7. Ambient and systematic electromagnetic noise

GPR systems are essentially wideband receivers and are, therefore, susceptible to interference from various man-made sources including television transmitters, FM radio transmitters, mobile (cell) phones and their transmission towers, walkie-talkies and other types of radio communication (Conyers and Goodman, 1997; Olhoeft, 1999, 2000). Fig. 16 shows interference affecting individual traces on a reflection profile collected immediately adjacent to a military airbase. The GPR operators noted that the interference coincided with take-off and landing of planes, and its random nature in time suggests the noise was related to radio communications. In some instances random background noise can be reduced by trace stacking at the time of data collection (Olhoeft, 1999), or by choosing an antenna frequency significantly different to that of the noise (Conyers and Goodman, 1997). However, the former increases data collection times and the latter may compromise the initial survey objectives.

Systematic noise can also be generated in radar profiles, the most common of which are 'ringing' multiples. These are multiple 'reflection' events of various origins and are normally dominated by a single frequency that obscures primary reflections (Sensors and Software, 1998). Ringing can result from power overloads on antennae and other system noise, leading to horizontal bands, typically of lower frequency (Young et al., 1995; Geophysical Survey Systems, 1996; Conyers and Goodman, 1997). Ringing is common where wire cables are used to connect the transmitter and receiver to the console, because they can act as a second antenna or radiator (Annan and Davis, 1992). This effect is significantly reduced by using fibre-optic cables instead (Annan and Davis, 1992). Ringing can also occur when radar signals bounce back and forth between a high-conductivity reflector and an antenna (Geophysical Survey Systems, 1996; Sensors and Software, 1998). Neal et al. (2002a) recorded high-frequency ringing during surveying of the middle and lower upper part of a mixed-sand-and-gravel beach and ascribed it to presence of highly conductive saline groundwater. Conductive clays also generate similar high-frequency ringing (Fig. 17).

4.8. Surface reflections

Although GPR antennae direct much of their electromagnetic energy into the subsurface, some is also lost into the air. As in the subsurface, when radar waves in air strike an object or planar surface with high electrical contrast, part of the signal is reflected and detected by the receiver. Consequently, not all reflections on radar profiles are necessarily from subsurface features. This is particularly the case when unshielded antennae are used. Shielding tries to prevent unwanted surface reflections by placing metal plates immediately above the antennae to act as reflectors. However, success is marginal unless shields are three to four times the size of the antenna element (A.P. Annan, personal communication, 2002). Consequently, shielded antennae tend to be smaller and, therefore, of higher frequency. For example, the company Sensors & Software manufacture two GPR systems commonly used for sedimentological applications: the PE100 system utilises unshielded antennae ranging from 12.5 to 200 MHz, whereas the PE1000 system operates with shielded antennae ranging from 110 to 1200 MHz.

Common causes of surface reflections include power lines and poles, trees, metallic fences, large boulders, walls and irregular topography (Sun and Young, 1995; Bano et al., 1999, 2000; van der Kruk and Slob, 2000). As in the subsurface, unshielded antennae radiate energy in a 3-D pattern, such that as they record along a survey line, travel time to surface features varies systematically. Consequently, diffractions and linear record surfaces are generated on the radar profile (Fig. 18). Surface scattering can obscure, or be confused with, primary reflections.

The precise nature of the surface reflection response will be dependent upon antenna frequency; the size, shape and orientation of the surface object, and the objects location in relation to survey line orientation. Due to variations in coupling between an antenna's radiated energy and the ground, different electrical ground conditions will result not only in different radiation patterns and strengths in the subsurface (see Section 4.5), but also in the air. Van der Kruk and Slob (2000) note this will have a particular

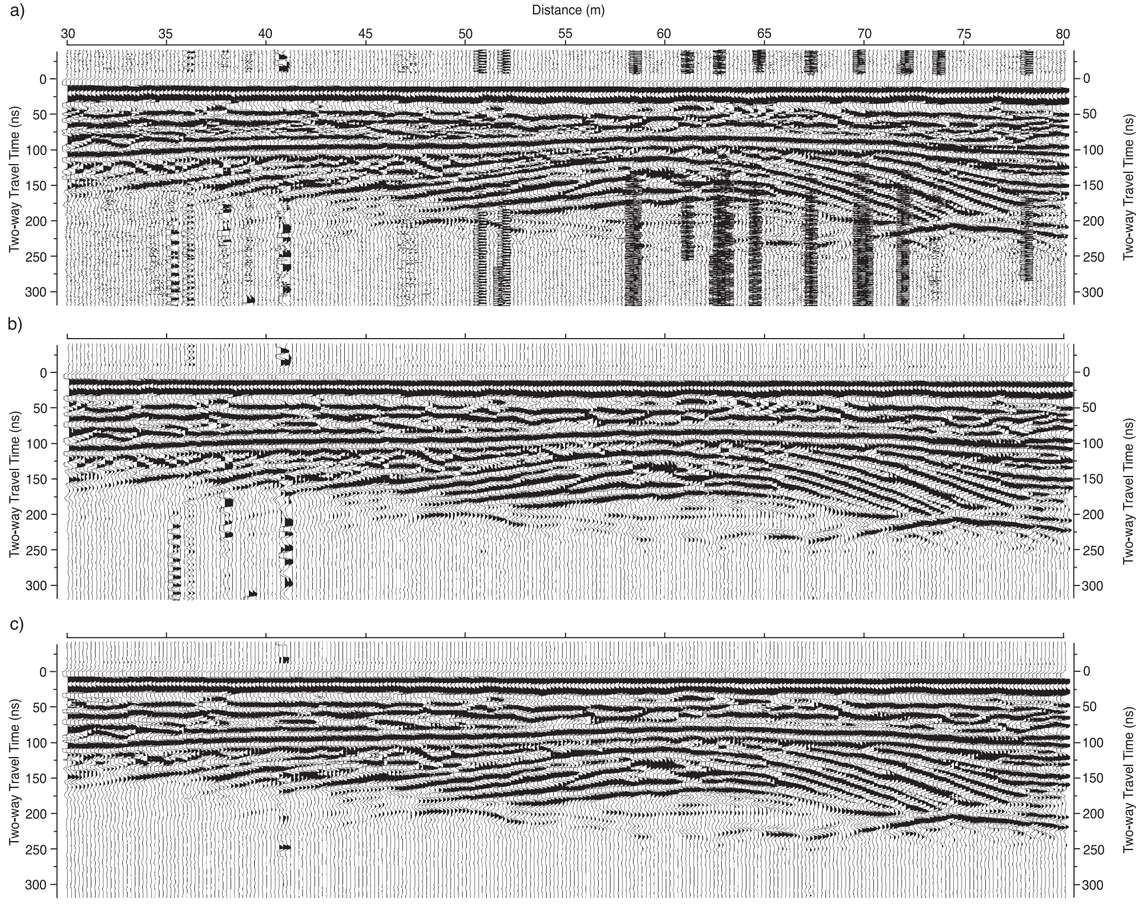

Fig. 16. (a) Unmigrated and unfiltered 100 MHz radar reflection profile showing high-frequency ambient noise resulting from aircraft radio communications at Woodvale, Sefton, northwest England. Noise partially obscures primary reflections from this stabilised coastal-dune sequence. (b) The noise can be almost entirely removed by time-domain, low-pass, frequency filtering with a cutoff of 125 MHz, although a lower frequency component remains between 35 and 41 m. (c) The lower frequency noise can be removed by spatial filtering using an alpha-mean trim filter, which is particularly useful for removing single 'bad' traces (Sensors and Software, 1998). All profiles have an AGC gain applied with a maximum limiting value of 1000, and no horizontal or vertical averaging.

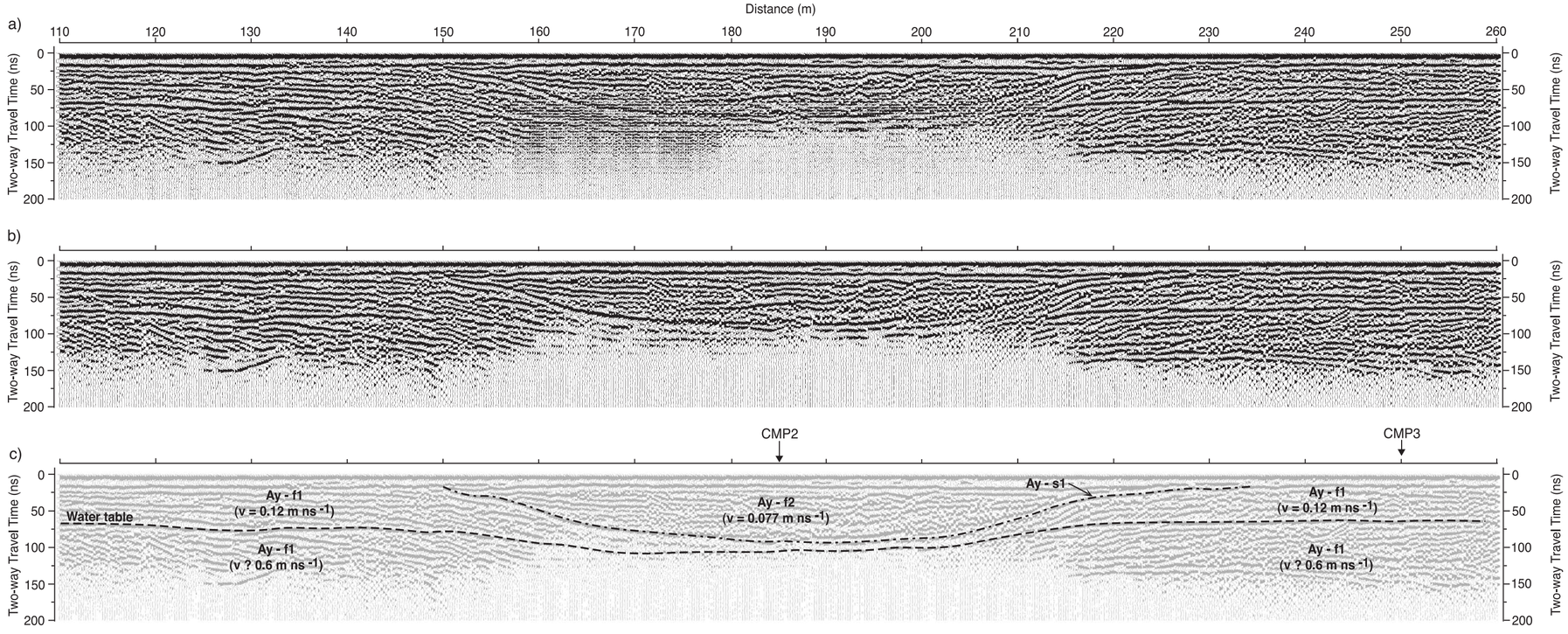

Fig. 17. (a) Unmigrated and unfiltered 100 MHz radar reflection profile from the Ayres coastal foreland, Isle of Man, showing systematic high-frequency ringing between approximately 158 and 212 m and beneath a two-way travel time of approximately 50 ns. Noise is associated with a lens-shaped subsurface structure filled with a complex mixture of unsaturated, sandy and silty clay, sand, and sand and gravel (Ay-f2 in (c)). The lens sits within a sequence of clean sands and gravels (Ay-f1 in (c)). Ringing is occurring due to the presence of conductive clays in the lens' sediments. (b) The effects of ringing in the profile can be removed by time-domain, low-pass, frequency filtering with a cutoff of 187 MHz. (c) Velocity structure for the profile, based on two common mid-point surveys (CMP2 and CMP3), identification of the water table (WT) and radar-stratigraphy interpretation that identified one radar surface (Ay-s1) and two radar facies (Ay-f1 and Ay-f2). All profiles have an AGC gain applied with a maximum limiting value of 1000, and no horizontal or vertical averaging.

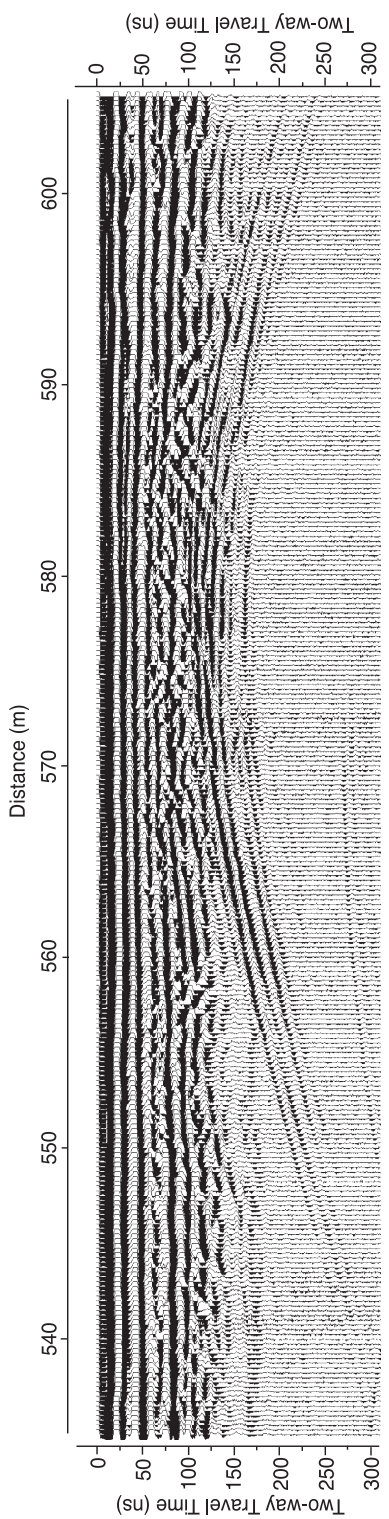

Fig. 18. 100 MHz unmigrated radar reflection profile showing a broad diffraction (beneath a two-way travel time of 100 ns across the whole profile shown) resulting from surface scattering. The diffraction obscures some primary reflections in the coastal dune sequence surveyed and was caused by a large dune hillock adjacent to the transect line on the Hillside Golf Club, Sefton, northwest England. The profile has an AGC gain applied with a maximum limiting value of 400, and no horizontal or vertical averaging.

impact on the amplitude of surface reflections. They also demonstrate that the nature of a reflection response to a surface reflector is highly dependent upon survey line orientation, because of the polarised nature of the radiated electromagnetic waves. In order to minimise surface reflections, van der Kruk and Slob (2000) recommend the emitted electric field is polarised perpendicular to surface objects, i.e. under standard radar reflection profiling, vertical features such as trees should be at the ends of survey lines, whereas walls should be perpendicular to the survey line. By contrast, horizontal features, such as fence wire, should parallel the survey line. However, constraints placed on survey line orientation may compromise initial objectives. If this is the case, surface reflections will have to be identified and accounted for during interpretation.

Detailed records of the positions and extent of all surface features likely to cause reflections will aid their identification on a radar profile (Sun and Young, 1995). Diffractions are relatively easy to identify (Fig. 18), as these hyperbolic events display moveout at the velocity of air, which is much higher than the velocity associated with subsurface materials (Sun and Young, 1995; Bano et al., 1999, 2000; van der Kruk and Slob, 2000; McMechan et al., 2002). However, surface reflections from large, planar or linear objects (e.g. walls, metallic fences and quarry walls), which run parallel or subparallel to the survey line, are more difficult to recognise (Lehmann et al., 2000; van der Kruk and Slob, 2000). Where these are present, a CMP survey can be performed on the transect line, with surface reflections being identified on the resulting CMP profile by moveout at the velocity of air (Sun and Young, 1995; van der Kruk and Slob, 2000). Alternatively, Lehmann et al. (2000) used data from two separate reflection profile surveys, utilising different antenna orientations, to identify the out-of-plane reflection from a quarry wall.

4.9. Vertical and lateral variations in subsurface radar-wave velocity

GPR data are recorded on a fixed and invariant time base (Fig. 3). Depths can only be estimated on a radar reflection profile if the velocities of the radar waves are known. Where a single, average velocity is sufficient to characterise the subsurface (e.g. many unsaturated sands and gravels), then TWT can undergo simple linear conversion to depth and an image is not distorted. However, where significant changes in velocity occur with depth, the radar profile becomes distorted because the depth scale is expanding and contracting with increasing TWT. This problem is well illustrated in any GPR section with a water table. Low-loss unsaturated sediments typically have significantly higher radar-wave velocities than equivalent saturated sediments (Table 2). As radar waves pass through the water table into saturated sediment they slow down. As a result, the depth scale on the radar profile has to expand to take account of this (Fig. 7; Neal and Roberts, 2000). However, the profile remains visually distorted, with, for example, reflection dips appearing to increase below the water table.

Similar changes in velocity can also occur laterally, particularly if subsurface sediment type changes along the survey line. For example, in Fig. 17 two main types of sediment are present above the water table. Lens-shaped radar facies Ay-f2 is a complex mixture of unsaturated sandy and silty clay, sand, and sand and gravel, with an average radar velocity of 0.077 m ns^{-1}. By contrast, the unsaturated sand and gravel of Ay-f1 is characterised by a velocity of 0.12 m ns^{-1}. These large velocity variations have led to significant lateral distortion of the radar image, with the water table appearing progressively deeper as Ay-f2 thickens. More importantly from a sedimentological perspective, however, reflection configurations that characterise the radar facies and radar surfaces have also been systematically distorted. These effects cannot be easily corrected and often have to be compensated for in a qualitative manner during interpretation.

A number of other studies have indicated that significant vertical and lateral velocity variations occur in sediments and sedimentary rocks, even over relatively short distances. Greaves et al. (1996) estimated velocities of between 0.06 and 0.125 m ns^{-1} from 35 CMP gathers along a 450 m transect across a complex, 30-m-deep sequence of fluvial and aeolian sediments of glacial origin. Hubbard et al. (1997) used crosshole radar tomography to obtain velocities of between 0.125 and 0.145 m ns^{-1} for unconsolidated, unsaturated gravelly sands in boreholes 4 m apart and 4 m deep. Tronicke et al. (2002a) also used tomographic radar data to detect velocity variations of up to 50% (approximately 0.1 to 0.15 m ns^{-1}), largely in a

vertical direction, along an 18 m transect in unsaturated glaciofluvial sands and gravels. The velocity variations were interpreted as resulting from changes in porosity, and silt and clay content. In contrast, Tronicke et al. (2002b) found lateral velocity variations of only 0.012 m ns^{-1} (0.068 to 0.08 m ns^{-1}) using crosshole radar along a 30 m transect through a sequence of saturated postglacial sand and gravels. Binley et al. (2001) measured largely vertical velocity variations of 0.045 m ns^{-1} (0.085 and 0.13 m ns^{-1}) for a 12-m-thick sequence of unsaturated medium-grained fluvial sandstone, using crosshole radar in boreholes 5 m apart. Low-velocity zones were associated with thin layers of discontinuous siltstone and interlaminated fine/medium sandstone, which had led to either greater water retention or ponding. Hammon et al. (2002) also used crosshole radar, to a depth of 16 m in boreholes 14 m apart, to detect lateral and vertical velocity variations of up to 0.1 m ns^{-1} (0.05 to 0.15 m ns^{-1}) in an unsaturated fluvial sandstone with thin layers of intraclast conglomerate and mudstone. Zones of low-velocity were correlated with the mudstones.

4.10. Topographic variation along the survey line

Another problem associated with the fact that GPR data are recorded on a time base is that elevation changes along a survey line are not taken into account. This can lead to significant distortions of the subsurface image if uncorrected (Fisher et al., 1996). This problem is made worse because the radiated energy from a transmitter (given the constraints on directionality outlined previously) always propagates outwards from the antenna at right angles to the surface. Therefore, on slopes energy is no longer directed vertically downwards, but instead has a horizontal component that increases with increasing dip of the slope. This is generally a problem on slopes greater than 6°, due to resulting mislocation of subsurface reflections (Lehmann and Green, 2000).

5. Data processing

The basic aim of processing GPR data, just as in processing reflection seismic or many other types of geophysical data, is to try and overcome the inherent limitations of the basic survey data, such that you obtain more realistic subsurface information. This then allows more confident interpretation in terms of geological or sedimentological meaning. Clearly some limitations cannot be overcome once data has been collected, as they are dependent upon site characteristics and/or the data collection configuration used (e.g. depth of penetration, step size). Also some data enhancements must be performed at the time of data collection (e.g. trace stacking at individual survey points to remove ambient noise).

Due to the analogies between seismic reflection and GPR, many seismic reflection processing techniques can be used without modification on radar data (Fisher et al., 1992a; Maijala, 1992; Rees and Glover, 1992; Young et al., 1995; Fisher et al., 1996; Annan, 1999; Pipan et al., 1999), although there are a number of notable exceptions. However, it was not until the advent of digital-data collection that GPR could fully exploit seismic processing (Annan and Davis, 1992; Fisher et al., 1992b; Young et al., 1995; Greaves et al., 1996). Seismic reflection processing has become extremely sophisticated, its development having been facilitated by strong financial backing from oil and gas exploration companies. As a result, numerous software packages are commercially available, which can perform almost any data manipulation required (Annan, 1999). However, the GPR-research community has been relatively slow to take up the numerous opportunities offered by such packages. This perhaps reflects the combined effects of the limited geophysical background of some GPR users, the often limited financial support available for GPR-based research projects, and the fact that in commercial applications benefit-to-cost ratios of a project very quickly approach unity (Annan, 1999), leaving little time for more complex data processing.

In the following section, the main types of processing that have been, or could be, applied to GPR data in sedimentological studies will be discussed and, where appropriate, their relative strengths and weaknesses will be assessed. The nature and order of any processing that might be applied to a set of GPR data will be dependent upon the site characteristics, the radar system and software system(s) employed and the survey's overall objective. Clearly, the processing options presented here are not exhaustive and those discussed will not be appropriate for all data sets.

Annan (1999) outlines other processing techniques applicable to radar data, although the benefits of their routine use in sedimentological studies have yet to be demonstrated.

5.1. Time-zero-drift correction

In order to correct for misalignment of the first break that can occur in a radar reflection profile (see Section 4.1), GPR software packages often contain routines that perform automatic realignment. They do this by physically moving individual traces up or down by the required amount of TWT. As a threshold is required to identify the first break, problems can occur when data are particularly noisy, because it may be difficult to define consistently across all traces. Successful realignment causes all reflections beneath to become correctly aligned and is, therefore, often the first piece of data processing performed.

5.2. Normal-moveout corrections

As noted in Section 4.2, common-offset radar reflection profiles are distorted with respect to depth, particularly in their upper part. Normal-moveout corrections can be applied to remove this effect and create zero-offset traces (Fisher et al., 1992a; Fisher et al., 1996). Although generation of zero-offset traces is necessary for some more-advanced data processing, e.g. certain types of migration (Fisher et al., 1996), normal-moveout corrections are often not performed during GPR studies. This is because depth distortion is small in that part of the radar profile containing primary reflections (i.e. in the area beneath that obscured by the air and ground waves, see Table 4), and many other processing steps appear to work adequately with common-offset data (e.g. Young et al., 1995).

If common-offset data are to be used for further processing, time zero must be moved from the first-break position, as this marks the arrival at the receiver of the airwave generated by the transmitter. Consequently, the airwave was generated at some finite time before it was detected by the receiver. In order to get a more realistic TWT, and hence depth estimate, for the primary reflections, time-zero must be moved up trace (i.e. back in time) to the point at which the initial pulse was generated at the transmitting antenna. The adjustment required can be calculated if the antenna spacing is known, as the velocity of radar waves in air is constant (0.2998 m ns^{-1}). An antenna spacing of 1 m would, for example, require an adjustment in time zero of approximately -3.3 ns from the first break.

5.3. Signal-saturation correction

Due to low-frequency ‘wow’ induced by signal saturation of the receiving antenna (see Section 4.3) a ‘dewow’ filter is usually applied to radar data after acquisition. Dewow is a high-pass filter ideally optimised to allow the spectral peak for a specific antenna centre-frequency to pass with fidelity, but suppress the low-frequency ‘wow’ (Sensors and Software, 1998). However, such filtering can occasionally create two artifacts: a precursor to the first break or, where wow is particularly large, blank areas in the trace where the signal exceeded the electronics’ clipping level (Sensors and Software, 1998). The former can sometimes be removed by using a different high-pass filter and the latter can be removed by reducing wow, usually by increasing antenna separation (Sensors and Software, 1998).

5.4. Application of gains and filters

As radar-signal strength generally decreases with increasing travel time, due to progressive attenuation, it is usually necessary to increase the strength of weaker signals at later times. This is achieved by applying gain to data. Gain is a time-variant scaling and various scaling functions can be utilised (Yilmaz, 1987, 2001; Geophysical Survey Systems, 1996; Sensors and Software, 1998). Where continuity of stratigraphic horizons is of central interest, it is often desirable to show all recorded information in traces, irrespective of amplitude (Annan, 1999). Consequently, in many sedimentological studies data are plotted and interpreted with automatic gain control (AGC). AGC applies gain, within user-defined limits, that is inversely proportional to signal strength, and thus attempts to equalise all signals (Yilmaz, 1987, 2001; Geophysical Survey Systems, 1996; Sensors and Software, 1998). Information regarding relative amplitudes is lost. To preserve relative amplitudes, gains can be applied, once more within user-defined limits, that attempt to take into account signal decay

due to geometric spreading and exponential dissipation of energy (Yilmaz, 1987, 2001; Young et al., 1995; Fisher et al., 1996; Sensors and Software, 1998).

Although application of gain is useful for data display and as an important precursor to some more-advanced processing procedures, it also has the undesirable effect of amplifying various types of ambient and systematic noise (Yilmaz, 1987, 2001). As a result, application of gain should be carefully considered, with the objective of obtaining relevant information regarding subsurface structure without introducing artifacts (Annan, 1999).

Filters are designed to alter the shape of individual traces through mathematical manipulation, enhancing or eliminating certain features (Sensors and Software, 1998). Typical features requiring removal from GPR profiles include the low-frequency wow referred to in Section 5.3 (‘dewow‘ is a type of time filter), and ambient and systematic noise (see Section 4.7). There are essentially two types of filter: time filters act vertically and are applied to individual traces sequentially, whereas spatial filters act with respect to horizontal position and use adjacent traces (Sensors and Software, 1998).

There are many different types of filter and discussion of their characteristics and designs is well beyond the scope of this paper. However, in many sedimentological studies, practitioners often use simple vertical and horizontal running-average filters. These act to reduce random or high-frequency noise, with horizontal averaging having the added effect of emphasising horizontal or gently dipping reflections and removing more steeply dipping ones. Both filters tend to increase the apparent interpretability of radar profiles. However, such averaging effectively reduces horizontal and vertical resolution, and can also distort or remove important dipping reflections, especially when over-judiciously applied.

Perhaps more useful in removing ambient or systematic noise is more direct frequency filtering, which attempts to remove a specified frequency band from the data set. This is well illustrated by reference to the two examples presented previously, illustrating ambient (Fig. 16a) and systematic noise (Fig. 17a). Ambient noise in Fig. 16a can be almost entirely removed by frequency filtering (Fig. 16b). Coherent noise present in Fig. 17a can be entirely removed by time-domain, low-pass, frequency filtering (Fig. 17b). In both cases, frequency filtering has preserved the main character of primary reflections, albeit with a slight decrease in vertical resolution, and enhanced their visibility, continuity and, hence, interpretability. If necessary, lower frequency noise still present in Fig. 16b can be removed by spatial filtering (Fig. 16c). However, filtering of this sort does lead to an effective decrease in horizontal resolution, as a form of horizontal averaging is taking place.

Many other options exist for filtering GPR data, with the type of filter employed being very much dependent upon the overall objective. Simple data processing such as gain application and filtering should not radically modify the data set. Their purpose should be to enhance basic aspects of the data that are of interest to a given study (Annan, 1999). In sedimentological applications, form and orientation of primary reflections is normally of paramount importance and basic processing should seek to enhance, but not distort, these features.

5.5. Velocity profile estimates

Good subsurface-radar-wave velocity information is important for converting TWT to an accurate estimation of depth. Velocity can be estimated in a number of ways, including measuring TWT to an horizon or buried object of known depth; direct laboratory measurements on field samples; using time-domain-reflectometry probes in the field; measuring travel time between two wells using borehole radar; transillumination surveys between two parallel exposures; iterative migration and CMP surveys (Annan and Davis, 1976; Topp et al., 1980; Fisher et al., 1992a; Greaves et al., 1996; Conyers and Goodman, 1997; Reynolds, 1997; Binley et al., 2001; Hammon et al., 2002; Tronicke et al., 2002a).

The standard approach to velocity estimation in many studies is the CMP survey (Fig. 2b), as it is entirely noninvasive and can be supplemented by subsequent ground truthing (Annan and Davis, 1976; Beres and Haeni, 1991; Tillard and Dubois, 1995; Greaves et al., 1996; van Overmeeren et al., 1997). Velocities are derived as in seismic reflection, using normal-moveout principles (Yilmaz, 1987, 2001; Robinson and Çoruh, 1988). To obtain the most reliable estimates, reflection events from surfaces that

are horizontal in the plane of the survey should be used (Beres and Haeni, 1991; Tillard and Dubois, 1995), such that the CMP survey also becomes a common depth-point (CDP) survey (Yilmaz, 1987, 2001). A typical CMP profile is shown in Fig. 19. The profile was collected with 50 MHz antennae centred on the mid-point CMP1 in Fig. 7c. As reflections in the equivalent radar reflection profile are horizontal (Fig. 7c), the CMP profile is ideal for estimating radar-wave velocities. An individual reflection event can be picked manually and the average velocity (v_1) to and from it is obtained using:

$$v_1 = \sqrt{[(x_2^2 - x_1^2)/(t_{x_2}^2 - t_{x_1}^2)]}, \quad (10)$$

where t_{x_1} and t_{x_2} are the two-way travel times to the reflection event at antenna separations x_1 and x_2, respectively (Robinson and Çoruh, 1988, p. 89).

In Fig. 19, the most significant event is the water-table reflection, with the average velocity down to it being 0.121 m ns^{-1}. Velocity below the water table was estimated to be 0.079 m ns^{-1}, based on the known velocity above the water table and average velocities down to various reflections below the water table. However, this value should be treated with caution due to difficulties associated with calculating interval velocities (Tillard and Dubois, 1995). Once velocity structures for radar reflection profiles have been obtained, TWT can be converted to estimations of depth or elevation. The two-layer velocity structure derived for the profiles in Fig. 7 leads to a split elevation scale at the water table, and also indicates that the image is visually distorted in the vertical plane. Such distortion can lead to problems with interpretation (see Section 4.9). In addition to being performed manually, most seismic and some GPR software contain automatic-velocity-analysis programs (e.g. Sensors and Software, 1999b).

As noted in Section 4.9, in addition to varying vertically, velocity can also vary horizontally, leading to lateral distortion of the resulting radar reflection profile. If significant lateral velocity variation is suspected, a number of CMP surveys will have to be performed to adequately characterise it (e.g. Greaves et al., 1996). This will then allow qualitative or quantitative correction for this effect, either before or during interpretation.

5.6. Deconvolution

Deconvolution is an analytical process designed to remove the effect of a previous filtering operation (Yilmaz, 1987, 2001; Kearey and Brooks, 1991). In both seismics and radar, deconvolution attempts to remove filtering effects resulting from propagation of a source wavelet through a layered earth, and the recording system response (Kearey and Brooks, 1991; Turner, 1994). In seismics, this includes dereverberation to remove ringing multiples associated with water layers, deghosting to remove the multiple associated with the base of the weathered layer, and whitening or spiking deconvolution to equalise amplitudes of the different frequency components. The intended effect of the deconvolution process is to shorten pulse length and, therefore, improve vertical resolution (Kearey and Brooks, 1991).

Unfortunately, application of deconvolution filters employed in seismic processing has met with limited success with radar signals (e.g. Fowler and Still, 1977; Payan and Kunt, 1982; LaFlèche et al., 1991; Maijala, 1992; Todoeschuck et al., 1992; Fisher et al., 1996; Arcone et al., 1998). Annan (1999) believes this is because prior to deconvolution the radar wavelet is often as compressed as can be realistically achieved, and some underlying assumptions used for wavelet estimation in seismics do not apply. Turner (1992, 1994) attempted to overcome the latter by designing deconvolution filters based on more realistic assumptions about radar-wave behaviour in the subsurface. In particular, Turner (1992, 1994) designed a time-variant deconvolution filter that addressed the fact that the frequency-dependent nature of attenuation is far greater than in seismics. This substantially improved vertical resolution in the radar data presented.

More recently, Xia et al. (2003) employed deterministic deconvolution, which requires detailed knowledge of the source wavelet characteristics, to improve the resolution of radar reflection profiles collected from a limestone with shale partings. This improved resolution allowed greater correlation between beds identified in adjacent quarry walls and reflections on the radar profiles. Overall, however, Annan (1999) believes that deconvolution is difficult to apply systematically to GPR profiles, can lead to various data artifacts, and often does not lead to a major improvement in resolution, although it can be

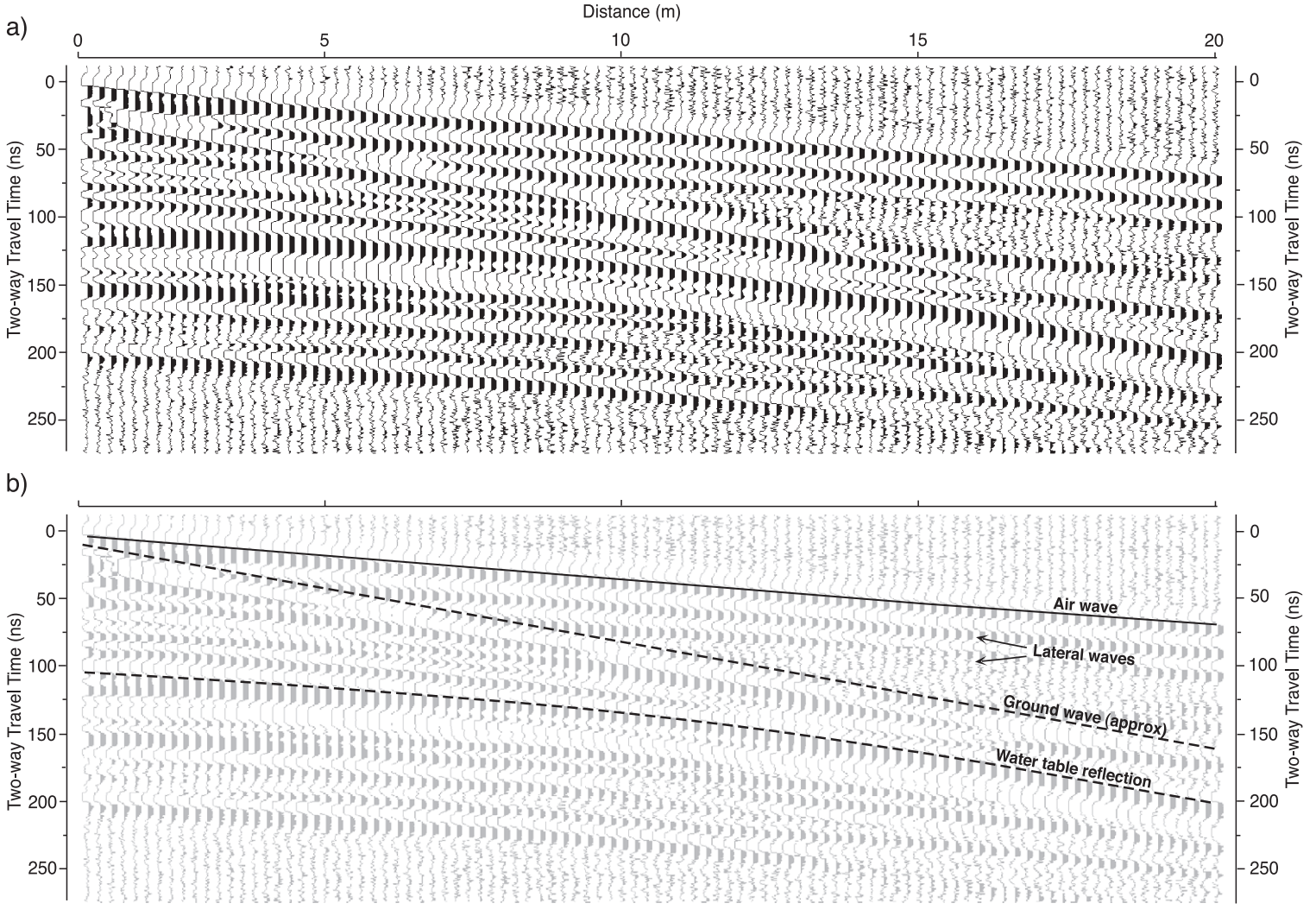

Fig. 19. (a) 50 MHz radar profile for a common mid-point survey centred on CMP1 in Fig. 7a. The profile has been plotted to allow manual picking of reflection events for velocity analysis, using Eq. (10). (b) CMP profile interpretation, showing position of the airwave, strong lateral waves that partially obscure the ground wave and a water-table reflection. With increasing antenna separation (i.e. distance), the planar water-table reflector has caused hyperbolic normal moveout of the resulting reflection. Therefore, it is ideal for performing velocity analysis. The profiles have an AGC gain applied with a maximum limiting value of 150, and no horizontal or vertical averaging.

useful where reverberation is a significant problem. As a result, deconvolution of radar data should be approached with caution and should perhaps not be viewed as an essential processing step unless a specific problem demands it.

5.7. Surface-reflection removal

Reflections from various surface features can be superimposed on radar profiles, obscuring primary reflections (see Section 4.8). Sun and Young (1995) and Bano et al. (1999, 2000) used simple geometrical modeling and synthetic radar profiles to separate surface-scattering events from both primary sedimentary structure in a sandstone and tectonic features in fluvial sediments. Sun and Young (1995) also demonstrated that migration (see Section 5.8) at the velocity of radar waves in air, and careful interpretation of CMP profiles, can also distinguish surface and primary reflections.

In most instances, mere identification of surface reflections is sufficient to allow full radar profile interpretation. However, where they are very strong or particularly numerous, it may be desirable to remove these unwanted reflections. Sun and Young (1995) modified a seismic processing stream to successfully remove a series of surface-scatter hyperbola from a reflection profile collected over a sequence of fractured carbonates.

5.8. Topographic correction

As noted in Section 4.10, radar data collected in the field does not take into account topographic variation along a survey line. This can be corrected by moving traces up and down by an appropriate TWT relative to a common datum, based on knowledge of the velocity, and, therefore, depth profile of the uppermost part of the radar profile (Geophysical Survey Systems, 1996; Sensors and Software, 1996a). In order to do this, survey line topography must be adequately characterised. Topographic surveys are typically performed using either a total station/laser theodolite or differential GPS, as these have the required vertical accuracy and allow relatively rapid data collection. Spatial sampling in such surveys should ensure that all significant breaks in slope are accounted for. Topographic corrections can also be performed relative to a reflection that is known, or believed to be, horizontal across a survey line.

5.9. Migration

Migration attempts to remove diffractions, distortions, dip displacements and out-of-line reflections resulting from the fact that radar antennae radiate and receive electromagnetic energy in a complex 3-D cone (see Section 4.6). It can, therefore, be viewed as a form of deconvolution that increases spatial resolution (Yilmaz, 1987, 2001). Migration was performed on the first seismic reflection data, collected in 1921 (Sheriff and Geldart, 1995), and has been routine in seismic processing ever since. Fisher et al. (1992a) indicate seismic migration techniques can only be used on GPR data when the same assumptions apply. Consequently, wave-propagation kinematics must satisfy the laws of geometrical optics and propagation must be linear and nondispersive. These conditions are met when electrical conductivities are low (<10 mS m^{-1}) and frequencies are in the normal range for GPR (Fisher et al., 1992a). Consequently, seismic migration techniques are generally regarded as having direct application to most radar data (Fisher et al., 1992a,b; Maijala, 1992; Fisher et al., 1996; Sensors and Software, 1996b).

The goal of migration is to make the reflection profile look like the geological structure in the plane of the survey. It attempts to correctly position subsurface reflection events. However, due to various uncertainties, in practice a significantly improved, but still imperfect image, is usually achieved (Hatton et al., 1986). Such improvements are likely to be very beneficial in sedimentological studies, where the nature and form of stratigraphic units and primary sedimentary structure is of utmost importance. Compare and contrast, for instance, unmigrated and migrated 100 MHz GPR profiles from aeolian deposits associated with a large, coastal, trough blowout (Fig. 20). Complex diffractions in the upper part of the unmigrated image lie above a laterally continuous and essentially horizontal reflection (Fig. 20a). Following migration using the program of Sensors and Software (1996b), which utilises the frequency–wave number approach of Stolt (1978), these diffractions are collapsed to reveal a more realistic arrangement of subsurface reflections (Fig. 20b). The image is further

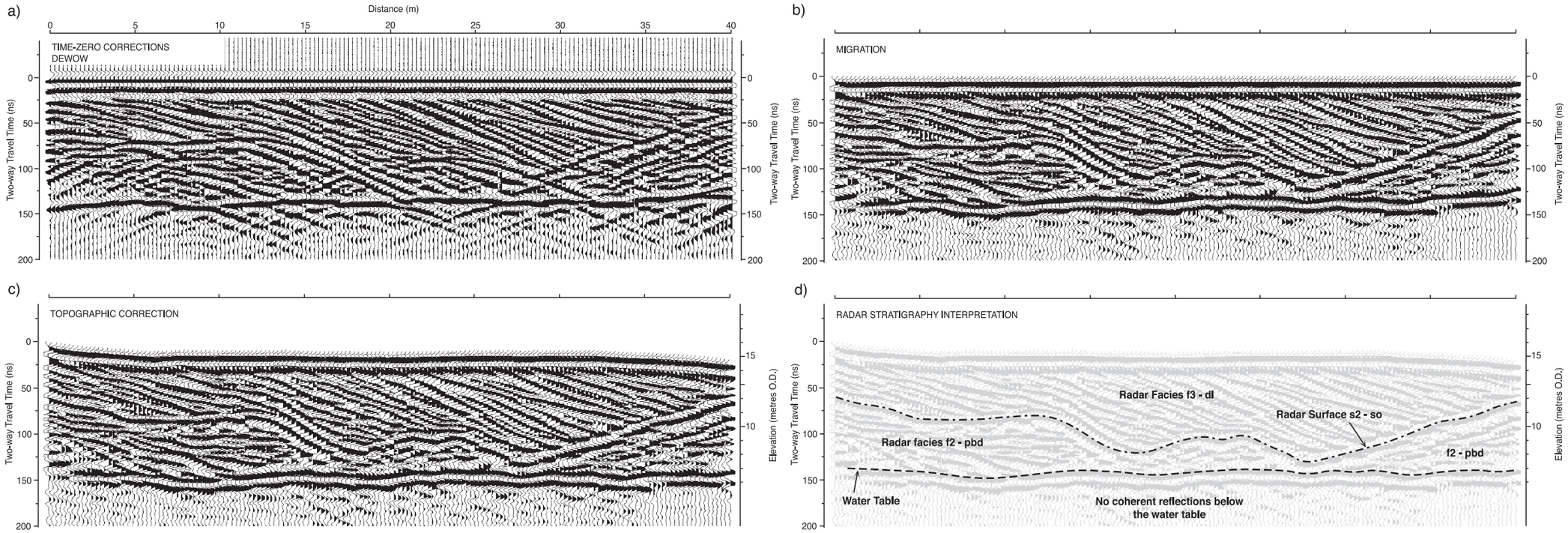

Fig. 20. Processing and interpretation sequence for a 100 MHz radar reflection profile collected from a large, coastal, trough blowout at Raven Meols, Sefton, northwest England, as part of a study by Neal and Roberts (2001). (a) Time-zero corrections and 'Dewow' filter. (b) Stolt frequency–wave number migration using a velocity of 0.132 m ns^{-1}. (c) Topographic correction. (d) Radar-stratigraphy interpretation. See Table 6 for a full radar-stratigraphy description and its sedimentological interpretation. All profiles have an AGC gain applied with a maximum limiting value of 400, and no horizontal or vertical averaging.

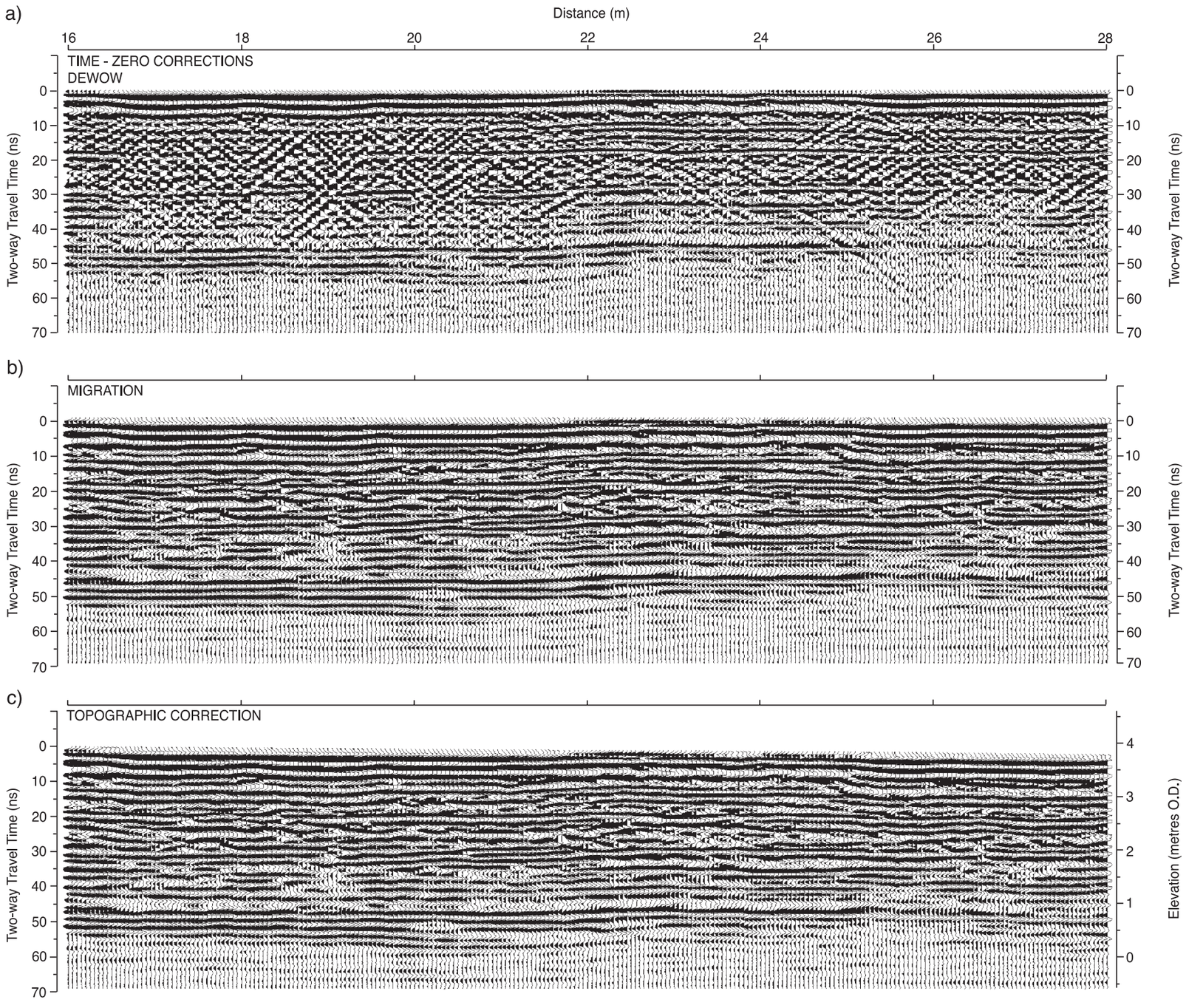

Fig. 21. Processing sequence for the migration and topographic correction of the 450 MHz radar reflection profile shown in Fig. 15b. (a) Time-zero corrections and 'Dewow' filter. (b) Stolt frequency–wave number migration using a velocity of 0.131 m ns^{-1}. (c) Topographic correction. All profiles have an AGC gain applied with a maximum limiting value of 125, and no horizontal or vertical averaging.

enhanced by subsequent topographic correction (Fig. 20c). The horizontal reflection forming the base of the unmigrated profile is seen to actually consist of two reflections. Auger holes indicate this double reflection is caused by a water table (Neal and Roberts, 2001). Above the water-table reflection, migration has revealed a second laterally continuous reflection, which displays a complex topography (radar surface s2-so, Fig. 20c). Auger holes show this is a soil separating two aeolian sands (Neal and Roberts, 2001). The soil's irregular topography had led to distortion of the unmigrated image through broadening where it was gently convex-up and narrowing where it was gently concave-up, and through generation of 'bow-tie' diffractions where it was strongly concave-up (see Section 4.6 and Fig. 14). Migration successfully corrects for these effects. Above the soil reflection are a series of more-steeply dipping reflections, interpreted as resulting from sets of cross-bedding (Neal and Roberts, 2001). Comparison of the unmigrated and migrated profiles indicates migration has resulted in dip increases broadly consistent with theoretical predictions (Eq. (9)).

A second example of the benefits of migration is presented in Fig. 21. This 450 MHz GPR data set was collected from a mixed-sand-and-gravel beach-ridge strandplain, as part of a study by Neal et al. (2002a). The profile was acquired along a beach-ridge crest, parallel to the coast and depositional strike. As a result of survey orientation, the majority of primary reflections in the unmigrated image appear horizontal, although they are often partially obscured by a series of cross-cutting diffraction hyperbolae that consistently have their apexes in the profile's upper part (Fig. 21a). Profile migration, again using the program of Sensors and Software (1996b), results in collapse of the diffraction hyperbolae and increased lateral continuity to primary reflections (Fig. 21b). Subtle changes to reflection orientation are achieved by subsequent topographic correction of the migrated profile (Fig. 21c). Diffractions in the unmigrated profile are believed to have been generated by coarse gravel in the upper part of the beach, with large (with respect to a radar wavelength of approximately 0.3 m), individual sedimentary particles acting as isolated reflector points. Fisher et al. (1992a,b), Liner and Liner (1995), Vandenberghe and van Overmeeren (1999), Beres et al. (2000); Lehmann and Green (2000), Lehmann et al. (2000), Rust and Russell (2000) and Neal and Roberts (2001) all provide further practical illustrations of the advantages of various types of migration to sedimentological GPR data.

Despite the advantages outlined above, and the fact that migration has been beneficial to radar data collected from both contemporary sediments and sedimentary rocks (Fisher et al., 1992a,b; Maijala, 1992; Beres et al., 1995, 1999, 2000; Bridge et al., 1995; Liner and Liner, 1995; Fisher et al., 1996; Wyatt et al., 1996; Grant et al., 1997; van Overmeeren, 1998; Vandenberghe and van Overmeeren, 1999; Lehmann and Green, 2000; Lehmann et al., 2000; Pipan et al., 2002a,b; Rust and Russell, 2000; Sénéchal et al., 2000; Corbeanu et al., 2001; Heinz, 2001; Neal and Roberts, 2001; Overgaard and Jakobsen, 2001; Russell et al., 2001; Szerbiak et al., 2001; Hammon et al., 2002; Neal et al., 2002a,b, 2003; Nitsche et al., 2002; Tronicke et al., 2002a; Cardenas and Zlotnik, 2003; Degenhardt et al., 2003; Heinz and Aigner, 2003; Orlando, 2003; Pedley and Hill, 2003; Skelly et al., 2003), its use in sedimentary research is by no means routine. Furthermore, there is often little or no justification within many research articles for its omission, and many studies fail to fully acknowledge or take into account potential limitations of the unmigrated sections they present. Therefore, it appears appropriate to take a closer look at migration, by outlining the basic types of migration routine and their relative strengths and weaknesses.

There are essentially two types of migration, time migration and depth migration (Hatton et al., 1986; Yilmaz, 1987, 2001; Kearey and Brooks, 1991; Sheriff and Geldart, 1995). Time migration is appropriate where lateral velocity variations are small to moderate (Yilmaz, 1987, 2001). In seismics, migrated sections are commonly processed and displayed in time, because depth conversion is never completely accurate due to velocity uncertainties, and interpreters like to compare migrated and unmigrated sections to evaluate how 'successful' migration has been (Yilmaz, 1987, 2001). The latter point emphasises the subjective aspect of migration processing, in that processors are likely to have preconceived ideas about how the final migrated profile will appear, and this will lead to bias in the processing parameters chosen (Annan, 1999).

Where lateral velocity variations are large, depth migration is required to obtain a true subsurface

picture (Yilmaz, 1987, 2001). However, success will be dependent upon how well velocity variations are characterised. Table 5 outlines the principal types of migration that can be employed, and the advantages and limitations of each. In GPR processing, time-migration algorithms are typically employed. In sedimentological studies, Kirchoff migration (Lehmann and Green, 2000; Lehmann et al., 2000; Corbeanu et al., 2001; Heinz, 2001; Russell et al., 2001; Szerbiak et al., 2001; Hammon et al., 2002; Tronicke et al., 2002a; Degenhardt et al., 2003; Heinz and Aigner, 2003), Stolt frequency–wave number migration (van Overmeeren, 1998; Vandenberghe and van Overmeeren, 1999; Rust and Russell, 2000; Neal and Roberts, 2001; Overgaard and Jakobsen, 2001; Neal et al., 2002a,b, 2003; Orlando, 2003; Skelly et al., 2003), phase-shift frequency–wave number migration (Beres et al., 1999; 2000; Sénéchal et al., 2000) and a combination of phase-shift frequency–wave number and frequency–space migration (Fisher et al., 1992b) have all been successfully employed to help clarify subsurface structure.

Irrespective of the migration algorithm, success in achieving its goal will be dependent upon how closely the profile approximates a zero-offset section; the signal-to-noise ratio, and the accuracy of velocities used, with sensitivity to velocity errors increasing with increasing dip (Yilmaz, 1987, 2001). An additional problem arises because migration can be either 2-D or 3-D. In 2-D migration, it is assumed that the radar profile does not contain any energy from outside the plane of the transect. However, this is not the case,

Table 5
The principal types of migration method, listed in order of their historical development, and with their advantages and limitations

Migration type	Method	Comments
Semicircle superposition	Amplitude mapping at sample points in a time section onto a semicircle in a depth section using wave front charts	Performed before digital computers
Diffraction summation	Summing amplitudes along diffraction hyperbola whose curvature is governed by the medium's velocity	First computer implementation of migration
Kirchoff summation	Same as diffraction summation, but with added amplitude and phase corrections applied before summing	Accurate for dips up to 90° Only vertical velocity variations accounted for Sensitive to spatial extent of the summation (=aperture width)
Finite difference	Finite-difference solutions to the scalar wave equation	60° is maximum dip that can be migrated Vertical and lateral velocity variations accounted for Produces less migration noise Sensitive to the depth step size (measured in TWT) over which calculations are performed Less sensitive to velocity errors than Kirchoff-summation and frequency–wave number migration
Frequency–wave number (f–k): Stolt	Fourier transforms to facilitate coordinate transformations from frequency to vertical wave number axis, while keeping the horizontal wave number unchanged	Accurate for dips up to 90° Requires one, constant velocity Profiles stretched to account for vertical velocity variations Often the most economical method
Frequency–wave number (f–k): phase shift	Imaging principle invoked by summing over the frequency components of the extrapolated wavefield at each depth step	Accurate for dips up to 90° Vertical velocity variations accounted for Sensitive to depth step size, as in finite-difference migration Similar sensitivity to velocity errors as Kirchoff summation
Frequency–space (f–x)	Finite-difference technique implemented in the hybrid domain of frequency–space based on continuous fractions expansion	Accurate for dips up to 80° Vertical and lateral velocity variations accounted for Sensitive to depth step size Often easiest method for depth migration

Based on Yilmaz (1987), with additional information from Sheriff and Geldart (1995).

because energy is radiated in three dimensions (see Section 4.6). This can lead to variations in migration quality both in and between sections, due to spatially variable 3-D effects not correctly treated by 2-D migration. These problems can only be overcome by initial acquisition of 3-D GPR data sets and their subsequent 3-D migration (e.g. Beres et al., 1995, 1999, 2000; Lehmann et al., 2000; Pipan et al., 2000a;

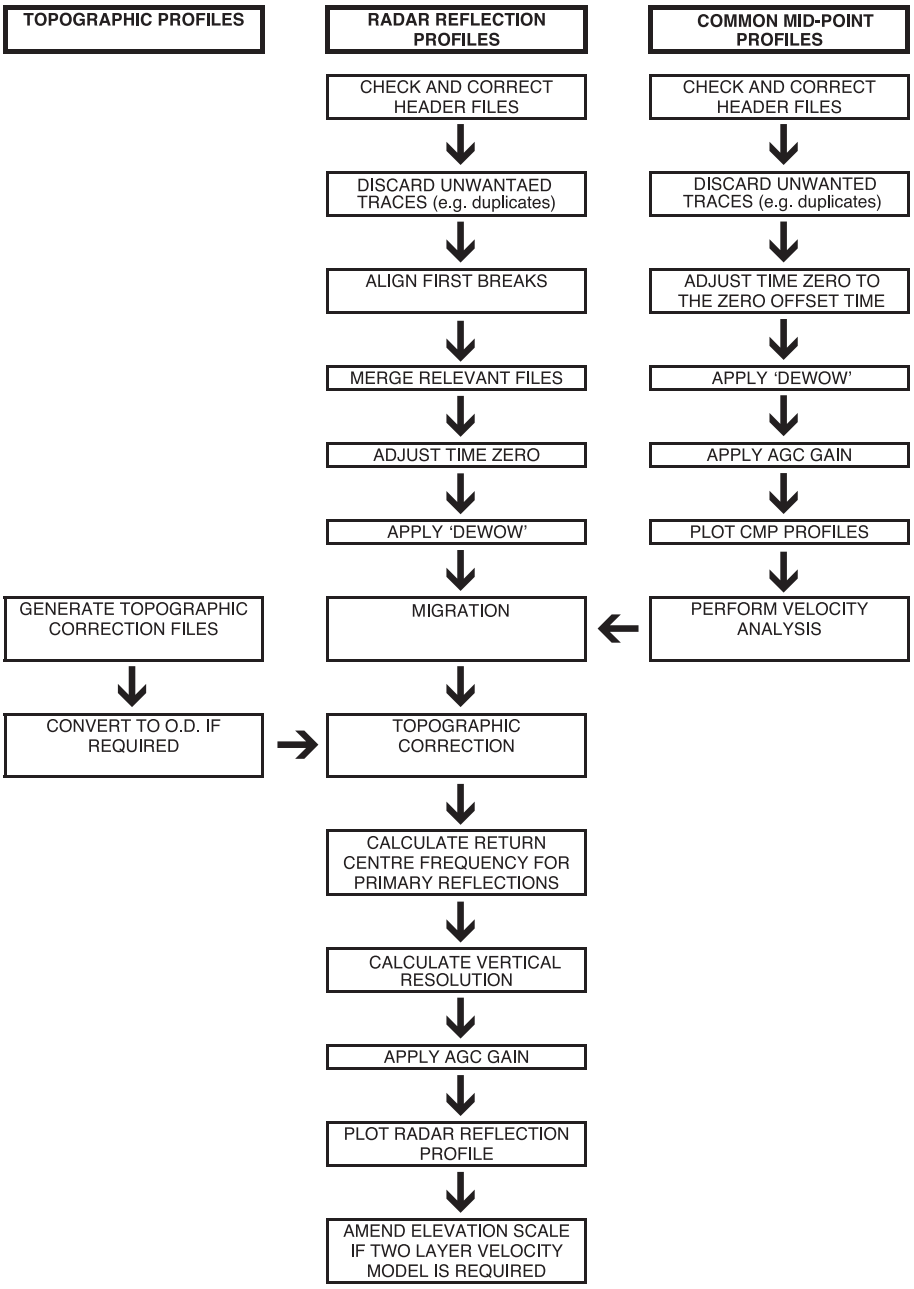

Fig. 22. Flow diagram of the processing sequence applied using PulseEKKO software (Sensors and Software, 1996a,b, 1998) to produce the final migrated, topographically corrected radar reflection profiles presented in this paper (Figs. 20c, 21c and 25a).

Sénéchal et al., 2000; Corbeanu et al., 2001; Szerbiak et al., 2001; Nitsche et al., 2002).

An important advance for sedimentological studies has been the development of a topographic-migration algorithm for radar (Lehmann and Green, 2000), as many profiles, particularly those collected over individual landforms, show significant variations in elevation (e.g. aeolian dunes, slope deposits). On slopes, radiated energy from a GPR antenna has a horizontal component that increases with increasing dip (see Section 4.10). During migration this is not fully accounted for if a horizontal data-acquisition surface is assumed, or if conventional elevation corrections (see Section 5.8) are applied before migration. This can lead to reflections being significantly out of position on migrated sections where slopes exceed approximately 6° (Lehmann and Green, 2000). Neal et al. (2002b) noted such problems on a conventionally migrated GPR profile collected over a relatively steep-sided (up to 32°) chenier beach-ridge, where interpretability was significantly reduced compared to migrated data collected where there was limited topographic variation. The topographic migration of Lehmann and Green (2000) was developed from seismic algorithms designed to deal with the effects of mountainous terrain and utilises Kirchoff-summation methods. For successful migration, lateral and vertical coordinates of traces should be known within 10% of dominant radar wavelength and subsurface velocities need to be within 10% to 20% of their true values (Lehmann and Green, 2000).

5.10. Data processing streams

A data processor is confronted by three main tasks (Yilmaz, 1987):

(1) selecting an appropriate sequence of processing steps;
(2) choosing an appropriate set of parameters for each processing step;
(3) evaluating output resulting from each processing step and identifying problems caused by incorrect parameter selection.

Yilmaz (1987) demonstrates how different processors can produce significantly different end products from the same initial data set, because of different decisions made. Fisher et al. (1992b) and Greaves et al. (1996) demonstrate this point very well with respect to radar, with their different approaches to the processing of the same multi-offset data. A processor's ability to make the right choices is often as important as effectiveness of the processing algorithms in determining final image quality. Processing, therefore, cannot be entirely objective, with some considering it more of an art than a science (Yilmaz, 1987).

A wide range of options are available and processors choose different ones depending upon algorithms available, objectives of the study, and their experience and ability. This means accurate records of all processing steps performed should be maintained. The data processing stream employed in preparation of the final, migrated, topographically corrected, radar images presented in this paper is shown in Fig. 22. Unfortunately, there are numerous examples in the GPR literature where little or no processing information is given. This clearly undermines the potential validity of interpretations drawn from the final reflection profiles, as readers cannot assess for themselves the likely extent to which they are an accurate representation of true subsurface structure.

6. Radar reflection profile interpretation

Soon after the realisation that GPR could provide useful data for stratigraphic and sedimentological studies, various authors suggested that the principles of seismic stratigraphy could be applied to the interpretation of radar reflection profiles (Baker, 1991; Beres and Haeni, 1991; Jol and Smith, 1991). Jol and Smith (1991) first used the term 'radar stratigraphy' for this new interpretation technique, although Gawthorpe et al. (1993) were the first to fully define the concept and its relationship to seismic stratigraphy.

Seismic stratigraphy was developed by the petroleum industry in the 1970s, principally by the Exxon Research Group, as a means of systematically interpreting seismic data to determine the stratigraphy and depositional environment of sedimentary rock formations (Mitchum et al., 1977). It took many years to develop an appropriate methodology, which was tested on a worldwide database (Hardage, 1987). Development of this approach was to be of profound importance to the science of stratigraphy, leading to concepts

associated with sequence stratigraphy and controversies over the role of eustatic sea-level change in controlling the overall depositional framework (Miall and Miall, 2001). However, the principles underlying seismic stratigraphy are remarkably simple and it is unnecessary to delve into the more controversial aspects of its subsequent use in order to apply the technique. The basic concept that underpins the interpretation regime is that seismic reflections parallel bedding surfaces at the survey resolution (Mitchum et al., 1977; Sangree and Widmier, 1979). This is generally true, because of the tendency for stratified sediments to show greater continuity of lithology, and, therefore, physical properties, parallel to depositional surfaces rather than across them, although it is acknowledged that lateral variations do occur (Sangree and Widmier, 1979). This general principle underwent considerable testing by seismic stratigraphy's proponents. However, it is acknowledged that there are exceptions to parallelism between bedding and reflections. These include reflection events from non-stratigraphic reflectors such as fluid contacts and diagenetic surfaces, diffraction patterns, out-of-line reflections and occasional effects associated with the finite resolution of seismic pulses (Sangree and Widmier, 1979; Hardage, 1987). As Sangree and Widmier (1979) note 'it is our experience that reflections do parallel beds within the limitations of seismic resolution. The seismic interpreter must learn to handle problems, exceptions, and pitfalls'.

Originally in seismic stratigraphy, reflection profiles were subdivided into *seismic sequences* by surfaces of discontinuity (*seismic sequence boundaries*) defined by systematic reflection terminations (Mitchum et al., 1977). Reflection termination types include erosional truncation, toplap, onlap and downlap. However, with development of sequence stratigraphy in the 1980s and the very specific meaning attached to the word 'sequence' in terms of changes in relative sea level (van Wagoner et al., 1990), *seismic sequences* are now known as *seismic packages* and *seismic sequence boundaries* are now called *seismic surfaces*. Seismic packages are interpreted as depositional units consisting of genetically related strata, which are bounded top and bottom by unconformities or their correlative conformities, as defined by seismic surfaces (Mitchum et al., 1977). The term *seismic facies* has remained unchanged since its definition and describes the two or three-dimensional sets of reflections lying between seismic surfaces. Seismic-facies reflections are characterised by their distinctive configuration, amplitude, continuity, frequency and internal velocity (Mitchum et al., 1977). A standard terminology exists to describe seismic package external form, and the configuration, amplitude, continuity and frequency of reflections (Mitchum et al., 1977; Sangree and Widmier, 1979; Hardage, 1987). Analysis of seismic-facies characteristics allows direct interpretation of environmental setting, depositional processes and lithofacies (Mitchum et al., 1977; Roksandic, 1978; Sangree and Widmier, 1979; Hardage, 1987).

Unlike in the development of seismic stratigraphy, early pioneers of radar stratigraphy could not have tested the approach on a large, worldwide data set, as one did not exist at that time (ca. 1991). Instead, they recognised that the principle assumption underlying seismic stratigraphy also applied to radar data collected from sedimentary environments, i.e. reflections paralleled bedding, albeit on a much finer scale. Numerous studies over the last decade have confirmed this general observation (see Section 3).

That the same interpretation technique is likely to be applicable on two very different scales reflects the fact that sedimentary sequences, particularly those dominated by clastic sediments, appear to display a hierarchy of depositional units, from individual laminae to whole sedimentary basins (Miall, 1991). Despite this enormous range of scales, physical contrasts that define sedimentary units are essentially the same, and units have similar forms and internal structures (Miall, 1991). Therefore, *radar surfaces*, *radar packages* and *radar facies* (Neal et al., 2002b), which are defined in the same way as the equivalent terms in seismic stratigraphy, are the building blocks of the radar stratigraphy for a GPR reflection profile (Fig. 23). Although common in the GPR literature, the terms 'radar sequence' and 'radar sequence boundaries' should not be used, because, as was the case originally in seismics, these cause confusion due to the specific meaning of 'sequence' in sequence stratigraphy.

Although much of the terminology associated with seismic stratigraphy can be directly applied to the definition of a radar stratigraphy, it is recommended here that some of the descriptive terminology employed is modified. This is because in both seismic and radar stratigraphy there has been a tendency to

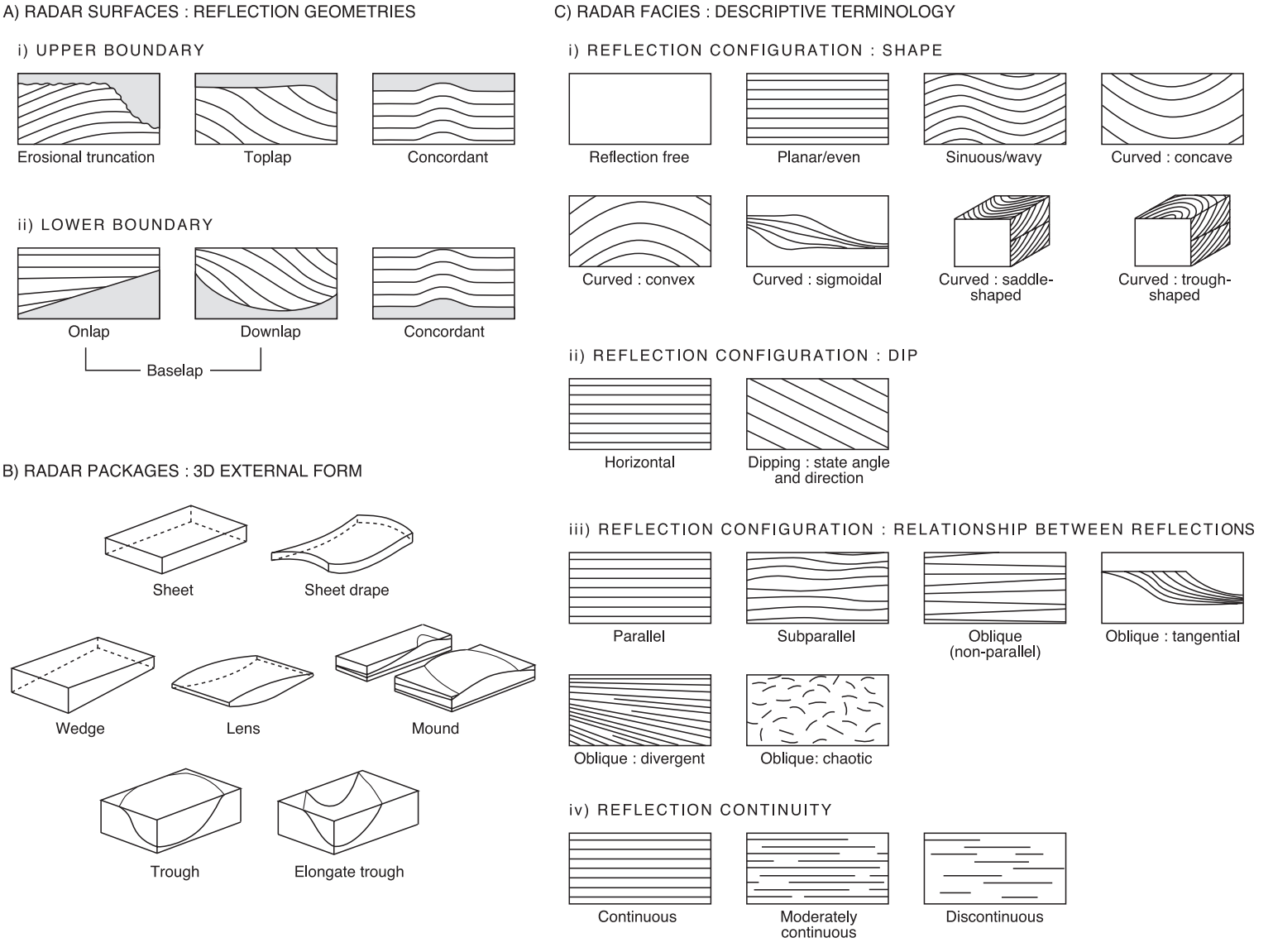

Fig. 23. Terminology to define and describe radar surfaces, radar packages and radar facies. Modified in part from Mitchum et al. (1977), Campbell (1967) and Allen (1982).

mix descriptive and interpretive terms, particularly with respect to definition of facies (e.g. 'migrating-wave facies' or 'prograded-fill facies'), which can clearly be misleading if the context in which these terms are used is not clear. Also, where purely descriptive terms have been used, they have often been poorly defined. Consequently, it is recommended that radar facies reflection configurations are described in terms of the:

(1) shape of reflections;
(2) dip of reflections;
(3) relationship between reflections;
(4) reflection continuity.

Basic terms to describe these attributes are shown in Fig. 23 and are derived in part from terms used in seismic stratigraphy (Mitchum et al., 1977), but also partly from attempts to describe and classify sedimentary structures (Campbell, 1967; Allen, 1982). Radar surfaces can also be described using this terminology, excluding, of course, that defining the relationship between reflections.

In radar stratigraphy, as in seismic stratigraphy, there are inevitably violations to the general principle that reflections parallel bedding. These include reflections generated by the water table and diagenetic horizons, diffractions generated by isolated reflector points, out-of-line reflections, reflections generated by faults and joints, surface reflections, and ambient and systematic noise. As in seismic stratigraphy, it falls to the interpreter to deal with these problems, by developing ways of identifying, removing or discounting reflections that are not related to primary sedimentary structure. Such methods have already been discussed (Section 5).

In sedimentological studies carried out at the scale and resolution of GPR surveys, definition of sedimentary facies and bounding surfaces is fundamental to interpretation (Reading, 1996). Bedding and sedimentary structure are often important elements in defining facies. Bounding surfaces represent depositional breaks in the sedimentary sequence and define the external form of facies. Relationships between sedimentary facies are critical for interpretation at the environmental level, particularly in eliminating alternative interpretations (Reading, 1996). Facies associations are thus the essential building blocks of facies analysis and contacts between individual facies (as defined by bounding surfaces) allow definition of architectural elements (Reading, 1996).

Only a relatively small number of GPR studies have fully applied the principles of radar stratigraphy, i.e. radar surfaces, radar packages and radar facies have all been identified on the radar reflection profiles, after discounting or removing reflections unrelated to primary sedimentary structure. In doing so, these studies have subsequently demonstrated or inferred that radar facies represent aspects of the broader sedimentary facies (namely their bedding and internal structure) and that radar surfaces represent bounding surfaces (e.g. Jol and Smith, 1991; Smith and Jol, 1992; Gawthorpe et al., 1993; Huggenberger, 1993; Bristow, 1995; Beres et al., 1999; Neal and Roberts, 2000, 2001; Corbeanu et al., 2001; Heinz, 2001; Neal et al., 2001, 2002a,b, 2003; Szerbiak et al., 2001; Russell et al., 2001; Hornung and Aigner, 2002; O'Neal and McGeary, 2002; Heinz and Aigner, 2003; Skelly et al., 2003). Thus, at the resolution of the GPR survey, it has been possible to interpret sedimentary facies and facies associations from radar reflection profiles and thus help determine environment of deposition and formative processes. It has proved a particularly powerful technique where sedimentary structure is a fundamental criteria for definition of sedimentary facies, as is usually the case in clastic sediments and rocks.

Two examples will be presented to demonstrate how radar stratigraphy is defined and how subsequent environmental interpretations may be derived. The first example uses a previously unpublished 100 MHz radar profile collected by Neal and Roberts (2001), as part of their study of coastal-dune blowout deposits. This profile was presented earlier to demonstrate benefits of migration and topographic correction (Fig. 20a–c). Using the principles of radar stratigraphy, and at the survey's vertical resolution (0.4 m), it is possible to identify one major radar surface (s2-so) and two major radar facies (f2-pbd and f3-dl) on the migrated and topographically corrected image (Fig. 20d). These give the deposits a relative chronology. The water table at the base of the interpretable profile is not related to primary sedimentary structure and can be discounted from the radar-stratigraphy interpretation. Once radar surfaces and radar facies have been defined they can be described using objective, radar-

Table 6
Description and interpretation of the radar stratigraphy for Raven Meols blowout (see Fig. 20d)

	Description	Geological interpretation
Radar facies f2-pbd	Series of cross-cutting reflections with limited lateral continuity. Reflections have low to moderate apparent dips that toplap s2-so.	Aeolian deposits of the pre-blowout dunes (pbd), characterised by a complex series of cross-strata separated by numerous bounding surfaces.
Radar surface s2-so	Laterally continuous, undulating reflection with complex topography.	Thin soil (so) representing a former vegetated surface.
Radar facies f3-dl	Laterally continuous, subparallel, moderate to high-angle reflections that downlap s2-so. Occasional low-angle cross-cutting relationships between reflections.	Aeolian deposits of the blowout's depositional lobe (dl), displaying packets of well-developed cross-strata with occasional third-order bounding surfaces.

stratigraphy terminology (Table 6). As this radar profile was collected from a contemporary environment, current depositional context can be used to help interpret the radar stratigraphy sedimentologically. In this instance, such information is complemented by data from field exposures, trenches, auger holes and historical aerial photographs to arrive at the final interpretation (Table 6). A unique labeling system (Fig. 24) has been used for the radar surfaces and radar facies (Fig. 20, Table 6) that summarises both their sequence of development and sedimentological interpretation. Neal and Roberts (2001) used a series of intersecting, similarly interpreted radar profiles to

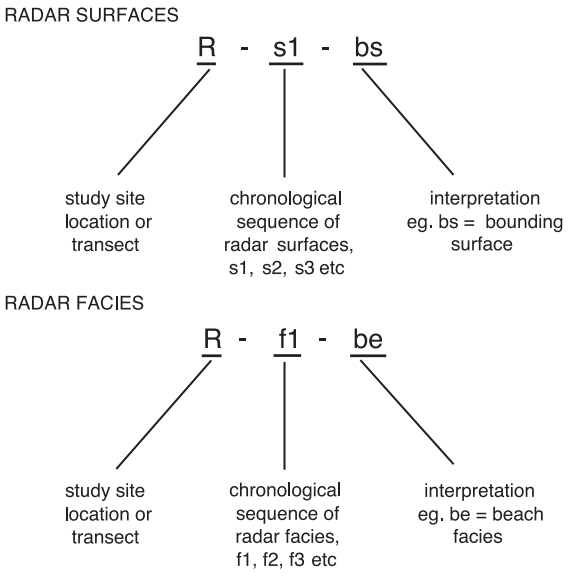

Fig. 24. Suggested labeling system for radar surfaces and radar facies on reflection profiles, which summarises both their sequence of development and sedimentological interpretation. The study-site location or transect name/number can be omitted if required.

reconstruct the three-dimensional internal structure of the blowout deposits. In older Holocene or Quaternary deposits, various dating methods can convert a relative chronology defined by a radar stratigraphy into an absolute chronology.

The second example comes from a study by Neal et al. (2002a), who collected 450 MHz data from a recently formed (< 120 years), mixed-sand-and-gravel, beach-ridge strandplain. Migration of the data has already been discussed with reference to a shore-parallel reflection profile (Fig. 21). As the shore-parallel profiles are dominated by horizontal reflections (Fig. 21), migrated cross-shore profiles contain reflections showing the true dip of reflectors that generated them, i.e. the cross-shore profiles parallel sedimentary dip. Consequently, there is no need to employ three-dimensional surveying techniques, as in the previous example, to confidently determine the true orientation and dip of primary bedding. The profiles collected had a high vertical resolution (0.08 m) and Neal et al. (2002a) were able to define and objectively describe a complex radar stratigraphy for the upper beach deposits consisting of 33 radar packages (Fig. 25). Direct ground truthing was not possible at the site, because the upper beach gravel was not suitable for trenching. However, additional information to aid interpretation was available from the deposits' current environmental context, data from a previous beach-profile monitoring program along the same survey line, and description of similar deposits in the literature. Using these in conjunction with the radar stratigraphy, it was possible to interpret the radar surfaces as bounding surfaces (bs) that separated radar facies resulting from primary sedimentary structure associated with berm-ridge (br), overtop (ot) and mixed overtop/overwash (ot/ow) deposits (Fig. 25).

On this basis, it was possible to reconstruct the strandplain's depositional history and identify likely conditions leading to beach-ridge development.

The examples presented above have demonstrated that radar stratigraphy is a powerful technique for the systematic description of reflections generated by primary depositional structure (sets of laminae, beds, bedsets, bounding surfaces and architectural elements). Definition of radar stratigraphy allows subsequent detailed environmental interpretation, particularly when combined with ground truthing or other forms of suitable data. However, its use in GPR-based sedimentological studies has been far from straightforward. Since its inception in 1991, the overriding emphasis, with the exception of the small number of studies described above, has been on characterisation and interpretation of radar facies, with radar surfaces and radar packages typically not being defined. This overemphasis on radar facies analysis, rather then true radar stratigraphy, led to the common misconception that any radar reflection pattern constituted a radar facies. As a result, use of radar facies to describe reflections not related to primary sedimentary structure and stratigraphy became commonplace. Terms such as 'water-table radar facies' and 'hyperbolic' or 'diffraction radar facies' can be found throughout the GPR literature. In addition, radar surfaces have also been described as radar facies. The term 'palaeosol radar facies' has been used on several occasions, despite the fact that the 'facies' is defined by only a single reflection, i.e. it is a radar surface at the resolution of the radar profile. These examples are clearly in violation of the correct use of the term radar facies and, therefore, the true principles of radar stratigraphy.

Further confusion to the interpretation of radar profiles has also been caused by use of interpretive facies names, such as 'channel-fill facies' and 'progradational-beach facies'. Such an approach is valid if the context in which it is used is clearly understood, i.e. it is an interpretation of a nonunique set of reflection characteristics and their relationship to other nonunique sets of reflections, in a given or suspected depositional context. However, if this context is not made clear, use of interpretive facies names has the danger of suggesting that particular depositional environments or sub-environments are characterised only by certain radar facies.

The reasons for the adoption of the much-looser concept of radar facies analysis during much of the 1990s may well reflect several interrelated factors:

(1) initial papers to suggest that radar stratigraphy provided a suitable framework for radar profile interpretation appear to have unintentionally overemphasised the importance of identifying radar facies, as opposed to the radar surfaces that demarcate them, as the facies were seen as key to interpreting the depositional environment and sedimentary processes;
(2) many studies in the 1990s were performed on data that had not undergone more advanced processing procedures, particularly migration. Migrated radar profiles are normally much more suitable for full radar-stratigraphic interpretation because they provide a more coherent and realistic image of the subsurface (see Section 5.9). When seismic stratigraphy was developed, migration of seismic profiles was routine and standard;
(3) the potential significance of out-of-line reflections and certain nongeological reflections, such as those from surface objects and ambient/systematic noise, was only beginning to be explored during the 1990s. As a result, these appear to have gone unrecognised in some instances, making definition of a full radar stratigraphy difficult and the use of just radar facies more appealing;
(4) in certain, very specific circumstances, a radar facies analysis approach can be more appropriate. Where active bedform migration does not take place or is limited, such as in vegetated coastal dunes and some carbonate systems, lateral facies changes can occur that are not defined by bounding surfaces. Consequently, resulting radar facies are not bounded by radar surfaces (e.g. Bristow et al., 2000c; Dagallier et al., 2000).

Many of the problems outlined above have begun to be addressed. Considerable research has been carried out with respect to identification and removal of out-of-line reflections, diffractions, surface reflections and ambient/systematic noise (see Sections 5.4 and 5.7). Simple migration programs are now provided with most GPR-system software (e.g. Geophysical Survey Systems, 1996; Sensors and Software, 1996b) and more advanced seismic processing packages,

which can perform a variety of migration types, are commercially available and often PC based. Furthermore, seismic interpretation and 3-D-modeling software can be used to automatically pick and characterise radar surfaces (Sénéchal et al., 2000; Heinz, 2001; Heinz and Aigner, 2003), potentially making identification simpler.

As a consequence of these developments, and as noted earlier, a series of recent studies have reassessed use of the radar stratigraphy approach to interpretation of radar profiles, mainly using migrated data from sand and/or gravel-rich sediments and rocks (Beres et al., 1999; Neal and Roberts, 2000, 2001; Corbeanu et al., 2001; Heinz, 2001; Neal et al., 2001, 2002a,b, 2003; Szerbiak et al., 2001; Russell et al., 2001; Heinz and Aigner, 2003; Skelly et al., 2003). These studies met with considerable success, allowing much more detailed and confident sedimentological interpretation of the radar data than would have been possible using radar facies analysis.

Considering these developments, it now seems timely to abandon the less-robust radar facies analysis approach to interpretation and generate data appropriate for radar stratigraphy interpretation. In order to do this, processors and interpreters will have to: (1) have a full appreciation of inherent limitations to their data; (2) be able to process their data to an appropriate level; (3) develop skills to identify reflections not related to primary depositional structure, (4) understand the principles of radar stratigraphy and its implementation. It is perhaps in the area of data processing that the biggest challenges lie for GPR users. However, with the ever-developing power of personal computers and increasing commercial availability of seismic and radar-specific data processing software, high levels of processing capability are becoming available to all. It is up to the GPR community to take advantage of these opportunities.

7. Conclusions

GPR has found a wide range of applications in the field of sedimentology over the last two decades. This is because in correctly processed profiles and at the resolution of the survey, primary reflections generally parallel primary depositional structure. Using GPR wisely, it is possible to image the two and three-dimensional structure of a range of sedimentary structures in unconsolidated sediments and sedimentary rocks, including sets of laminae, beds, bedsets, bounding surfaces and architectural elements. However, in order to do this accurately, many of the inherent limitations to the field data must be acknowledged and where possible overcome by careful and systematic data processing. More advanced data processing, such as migration, which is essential to obtain correctly positioned subsurface reflections, is only just beginning to be performed on a regular basis by GPR researchers. GPR processing packages are supplied with commercial radar systems and these are sometimes adequate to perform all the data manipulations necessary. However, there are strong analogies between GPR and seismic reflection, and radar data can also be imported into the wide range of commercial seismic processing software.

It is recommended that appropriately processed data are interpreted sedimentologically using the principles of radar stratigraphy, as defined in this paper. Radar stratigraphy allows the definition of radar packages, through delineation of radar surfaces (identified by systematic reflection terminations), and description of radar facies, which are the sets of reflections lying between radar surfaces. Where it has been possible to define a full radar stratigraphy, which is principally in clastic sediments or sedimentary rocks, researchers have demonstrated or inferred that radar surfaces correspond to bounding surfaces and radar facies represent aspects of the broader sedimentary facies. Supplementary information, such as geological context, the relationship between the various radar surfaces and facies, data from ground truthing, and data from subsequent laboratory analyses, can then be used in conjunction with the radar stratigraphy to furnish a full sedimentological interpretation. Less robust interpretation techniques such as radar facies analysis, which does not define the radar surfaces that bound the facies or the resulting radar packages, should be abandoned as a primary interpretive tool, except in very specific instances.

In order to apply radar stratigraphy successfully, an interpreter must have a thorough understanding of a wide and complex range of factors, including: the scientific principles that underlie the GPR technique,

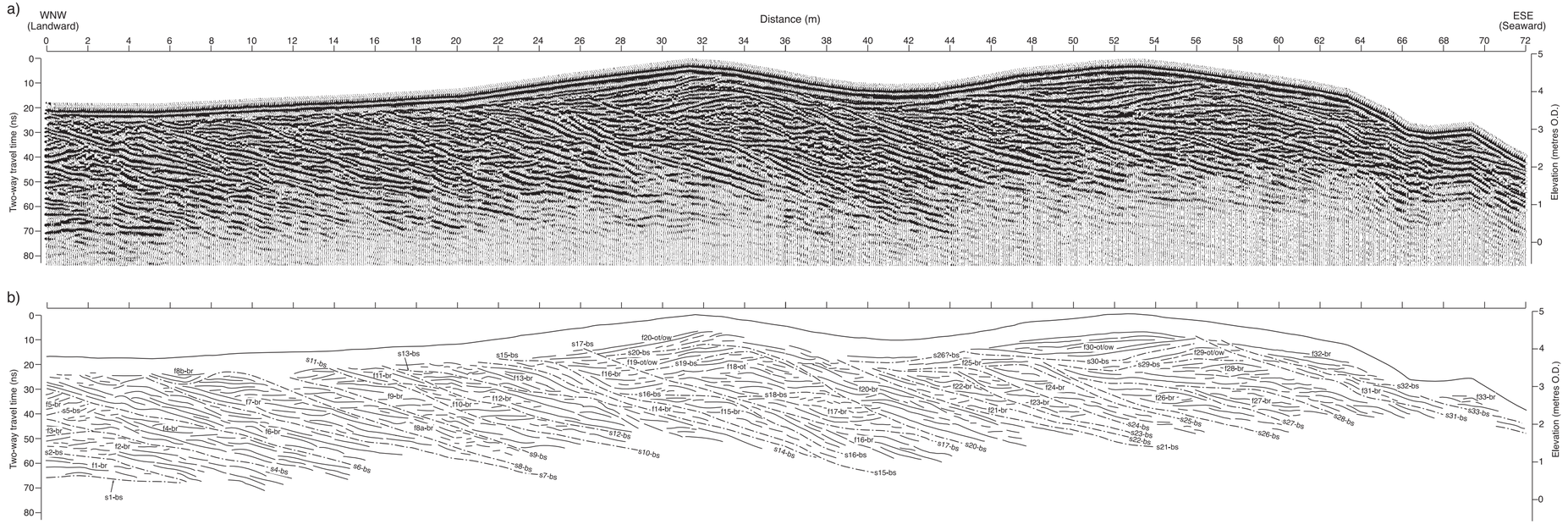

Fig. 25. (a) Migrated and topographically corrected 450 MHz radar reflection profile from a beach-ridge strandplain at Aldeburgh, Suffolk, southeast England. The profile has an AGC gain applied with a maximum limiting value of 250, and no horizontal or vertical averaging. (b) Radar-stratigraphy interpretation defining 33 sequential radar surfaces (s1–s33) and radar facies (f1–f33). Sedimentological interpretation indicates radar surfaces correspond to bounding surfaces (bs) and radar facies represent either berm-ridge (br), overtop (ot) or mixed overtop/overwash (ot/ow) deposits. Modified from Neal et al. (2002a).

the effects of the data collection configuration used, the effects of survey-line topographic variation, the effects of the technique's finite resolution (both vertical and horizontal) and depth of penetration, the causes of reflections unrelated to primary depositional structure, and the nature and appropriateness of each processing step undertaken. Data processing should aim to provide, within the limitations of the field data and processing routines employed, an accurate record of the subsurface location and orientation of reflections caused by primary sedimentary structure. Only with this more thorough approach to data collection, processing and interpretation will the full utility of the radar-stratigraphy interpretation approach be tested, and the full potential of GPR in sedimentary research be realised.

Acknowledgements

This research was supported by NERC Geophysical Equipment Pool Loans 555, 556, 638 and 639, the Environment Agency, the Isle of Man's Centre for Manx Studies, the Isle of Man Government and the University of Wolverhampton. Robert Arklay, Roger Dackombe, Martin Fenn, Gemma Fenn, Melanie Neal, Nigel Pontee, Clive Roberts, Magic Shirt and Jane Washington-Evans provided field assistance. Kay Lancaster prepared the diagrams. Assistance provided by the Sefton Coastal Ranger Service, the Sefton Coast Life Project, Tony Smith of Sefton Metropolitan Borough Council, Brian Irving of the Solway Rural Initiative, Roy Stoddard and John Davies of Suffolk Coastal District Council, Alison Collins of English Nature and many local landowners is gratefully acknowledged. Peter Fenning and Andy Brown of Earth Science Systems, Kimpton, and the staff of the NERC Geophysical Equipment Pool, Edinburgh, are thanked for technical and logistical support.

References

Aigner, T., Asprion, U., Hornung, J., Junghans, W.-D., Kostrewa, R., 1996. Integrated outcrop analogue studies for Triassic alluvial reservoirs: examples from southern Germany. J. Pet. Geol. 19, 393–406.

Alexander, J., Bridge, J.S., Leeder, M.R., Collier, R.E.Ll., Gawthorpe, R.L., 1994. Holocene meander-belt evolution in an active extensional basin, southwestern Montana. J. Sediment. Res., B 64, 542–559.

Al-fares, W., Bakalowicz, M., Guérin, R., Dukhan, M., 2002. Analysis of the karst aquifer structure of the Lamalou area (Hérault, France) with ground penetrating radar. J. Appl. Geophys. 51, 97–106.

Allen, J.R.L., 1982. Sedimentary Structures: Their Character and Physical Basis. Volume 1. Developments in Sedimentology, vol. 30A. Elsevier, Amsterdam.

Anderson, W.P., Evans, D.G., Snyder, S.W., 2000. The effects of Holocene barrier-island evolution on water-table elevations, Hatteras Island, North Carolina, USA. Hydrogeol. J. 8, 390–404.

Anderson, K.B., Spotila, J.A., Hole, J.A., 2003. Application of geomorphic analysis and ground-penetrating radar to characterization of paleoseismic sites in dynamic alluvial environments: an example from southern California. Tectonophysics 368, 25–32.

Annan, A.P., 1999. Practical Processing of GPR Data. Sensors and Software, Ontario.

Annan, A.P., Davis, J.L., 1976. Impulse radar sounding in permafrost. Radio Sci. 11, 383–394.

Annan, A.P., Davis, J.L., 1992. Design and development of a digital ground penetrating radar system. In: Pilon, J. (Ed.), Ground Penetrating Radar. Geol. Surv. Can. Pap. 90-4, 15–23.

Annan, A.P., Waller, W.M., Strangway, D.W., Rossiter, J.R., Redman, J.D., Watts, R.D., 1975. The electromagnetic response of a low-loss, 2-layer, dielectric earth for horizontal electric dipole excitation. Geophysics 40, 285–298.

Annan, A.P., Cosway, S.W., Redman, J.D., 1991. Water table detection with ground penetrating radar. Expanded Abstracts Soc. Explor. Geophysicists Annual Meeting, SEG, Tulsa, OK, pp. 494–496.

Arcone, S.A., Lawson, D.E., Delaney, A.J., Strasser, J.C., Strasser, J.D., 1998. Ground-penetrating radar reflection profiling of groundwater and bedrock in an area of discontinuous permafrost. Geophysics 63, 1573–1584.

Asprion, U., Aigner, T., 1997. Aquifer architecture analysis using ground-penetrating radar: Triassic and Quaternary examples (S. Germany). Environ. Geol. 31, 66–75.

Asprion, U., Aigner, T., 1999. Towards realistic aquifer models: three-dimensional georadar surveys of Quaternary gravel deltas (Singen Basin, SW Germany). Sediment. Geol. 129, 281–297.

Asprion, U., Aigner, T., 2000. An initial attempt to map carbonate buildups using ground-penetrating radar: an example from the Upper Jurassic of SW-Germany. Facies 42, 245–252.

Audru, J.-C., Bano, M., Begg, J., Berryman, K., Henrys, S., Nivière, B., 2001. GPR investigations on active faults in urban areas: the Georisc-NZ project in Wellington, New Zealand. Earth Planet. Sci. 333, 447–454.

Augustinus, P.C., Nichol, S., 1999. Ground-penetrating radar imaging of Pleistocene sediments, Boco Plain, western Tasmania. Aust. J. Earth Sci. 46, 275–282.

Bailey, S., Bristow, C.S., 2000. The structure of coastal dunes: observations from ground penetrating radar (GPR) surveys. In: Noon, D.A., Stickley, G.F., Longstaff, D. (Eds.), Proceedings of the Eighth International Conference on Ground Penetrating Radar. SPIE, Billingham, vol. 4084, pp. 660–665.

Baker, P.L., 1991. Response of ground-penetrating radar to bound-

ing surfaces and lithofacies variations in sand barrier sequences. Explor. Geophys. 22, 19–22.
Baker, G.S., Steeples, D.W., Schmeissner, C., Pavlovic, M., Plumb, R., 2001. Near-surface imaging using coincident seismic and GPR data. Geophys. Res. Lett. 28, 627–630.
Bakker, M.A.J., van der Meer, J.J.M., 2003. Structure of a Pleistocene push moraine revealed by GPR: the eastern Veluwe Ridge, The Netherlands. In: Bristow, C.S., Jol, H.M. (Eds.), Ground Penetrating Radar in Sediments. Geol. Soc. London Spec. Publ. 211, 143–151.
Bano, M., 1996. Constant dielectric losses of ground-penetrating radar waves. Geophys. J. Int. 124, 279–288.
Bano, M., Pivot, F., Marthelot, J.-M., 1999. Modeling and filtering of surface scattering in ground-penetrating radar waves. First Break 17, 215–222.
Bano, M., Marquis, G., Nivière, B., Maurin, J.C., Cushing, M., 2000. Investigating alluvial and tectonic features with ground-penetrating radar and analyzing diffraction patterns. J. Appl. Geophys. 43, 33–41.
Barnhardt, W.A., Kayen, R.E., 2000. Radar structure of earthquake-induced, coastal landslides in Anchorage, Alaska. Environ. Geosci. 7, 38–45.
Benson, A.K., 1995. Applications of ground penetrating radar in assessing some geological hazards: examples of groundwater contamination, faults, cavities. J. Appl. Geophys. 33, 177–193.
Beres, M., Haeni, F.P., 1991. Application of ground-penetrating-radar methods in hydrogeologic studies. Groundwater 29, 375–386.
Beres, M., Green, A.G., Huggenberger, P., Horstmeyer, H., 1995. Mapping the architecture of glaciofluvial sediments with three-dimensional georadar. Geology 23, 1087–1090.
Beres, M., Huggenberger, P., Green, A.G., Horstmeyer, H., 1999. Using two- and three-dimensional georadar methods to characterize glaciofluvial architecture. Sediment. Geol. 129, 1–24.
Beres, M., Green, A.G., Pugin, A., 2000. Diapiric origin of the Chessel-Noville Hills of the Rhone Valley interpreted from georadar mapping. Environ. Eng. Geosci. 6, 141–153.
Berthling, I., Etzelmüller, B., Isaken, K., Sollid, J.L., 2000. Rock glaciers on Prins Karls Forland: II. GPR soundings and the development of internal structures. Permafr. Periglac. Process. 11, 357–369.
Best, J.L., Ashworth, P.J., Bristow, C.S., Roden, J., 2003. Three-dimensional sedimentary architecture of a large, mid-channel sand braid bar, Jamuna River, Bangladesh. J. Sediment. Res. 73, 516–530.
Binley, A., Winship, P., Middleton, R., Pokar, M., West, J., 2001. High-resolution characterization of vadose zone dynamics using cross-borehole radar. Water Resour. Res. 37, 2639–2652.
Birkhead, A.L., Heritage, G.L., White, H., van Niekerk, A.W., 1996. Ground-penetrating radar as a tool for mapping the phreatic surface, bedrock profile, and alluvial stratigraphy in the Sabie River, Kruger National Park. J. Soil Water Conserv. 51, 234–241.
Boggs, S., 1995. Principles of Sedimentology and Stratigraphy, 2nd edition. Prentice Hall, New Jersey.
Botha, G.A., Bristow, C.S., Porat, N., Duller, G., Armitage, S.J., Roberts, H.M., Clarke, B.M., Kota, M.W., Schoeman, P., 2003. Evidence for dune reactivation from GPR profiles on the Maputaland coastal plain, South Africa. In: Bristow, C.S., Jol, H.M. (Eds.), Ground Penetrating Radar in Sediments. Geol. Soc. London Spec. Publ. 211, 29–46.
Bridge, J.S., 1993. Description and interpretation of fluvial deposits: a critical perspective. Sedimentology 40, 801–810.
Bridge, J.S., Alexander, J., Collier, R.E.L.L., Gawthorpe, R.L., Jarvis, J., 1995. Ground-penetrating radar and coring used to study the large-scale structure of point-bar deposits in three dimensions. Sedimentology 42, 839–852.
Bridge, J.S., Collier, R., Alexander, J., 1998. Large-scale structure of Calamus River deposits (Nebraska, USA) revealed using ground-penetrating radar. Sedimentology 45, 977–986.
Bristow, C.S., 1995. Facies analysis in the Lower Greensand using ground-penetrating radar. J. Geol. Soc. 152, 591–598.
Bristow, C.S., Jol, H.M. (Eds.), 2003. Ground Penetrating Radar in Sediments. Geol. Soc. London Spec. Publ., vol. 211.
Bristow, C.S., Pugh, J., Goodall, T., 1996. Internal structure of aeolian dunes in Abu Dhabi determined using ground-penetrating radar. Sedimentology 43, 995–1003.
Bristow, C.S., Skelly, R.L., Etheridge, F.G., 1999. Crevasse splays from the rapidly aggrading, sand-bed, braided Niobrara River, Nebraska: effect of base-level rise. Sedimentology 46, 1029–1047.
Bristow, C.S., Bailey, S.D., Lancaster, N., 2000a. The sedimentary structure of linear sand dunes. Nature 406, 56–59.
Bristow, C.S., Best, J.L., Ashworth, P.J., 2000b. The use of GPR in developing a facies model for a large sandy braided river, Brahmaputra River, Bangladesh. In: Noon, D.A., Stickley, G.F., Longstaff, D. (Eds.), Proceedings of the Eighth International Conference on Ground Penetrating Radar. SPIE, Billingham, vol. 4084, pp. 95–100.
Bristow, C.S., Chroston, P.N., Bailey, S.D., 2000c. The structure and development of foredunes on a locally prograding coast: insights from ground penetrating radar surveys, Norfolk, UK. Sedimentology 47, 923–944.
Bruno, F., Marillier, F., 2000. Test of high-resolution seismic reflection and other geophysical techniques on the Boup Landslide in the Swiss Alps. Surv. Geophys. 21, 333–348.
Busby, J.P., 1997. Calibration and interpretation of ground penetrating radar data from around Sellafield, West Cumbria, UK. Eur. J. Environ. Eng. Geophys. 2, 137–152.
Busby, J.P., Merritt, J.W., 1999. Quaternary deformation mapping with ground-penetrating radar. J. Appl. Geophys. 41, 75–91.
Buynevich, I.V., FitzGerald, D.M., 2003. High-resolution subsurface (GPR) imaging and sedimentology of coastal ponds, Maine, USA: implications for Holocene back-barrier evolution. J. Sediment. Res. 3, 559–571.
Cagnoli, B., Russell, J.K., 2000. Imaging the subsurface stratigraphy in the Ubehebe hydrovolcanic field (Death Valley, California) using ground penetrating radar. J. Volcanol. Geotherm. Res. 96, 45–56.
Cagnoli, B., Ulrych, T.J., 2001a. Ground penetrating radar images of unexposed climbing dune-forms in the Ubehebe hydrovolcanic field (Death Valley, California). J. Volcanol. Geotherm. Res. 109, 279–298.

Cagnoli, B., Ulrych, T.J., 2001b. Singular value decomposition and wavy reflections in ground-penetrating radar images of base surge deposits. J. Appl. Geophys. 48, 175–182.
Cai, J., McMechan, G.A., Fisher, M.A., 1996. Application of ground-penetrating radar to investigation of near-surface fault properties in the San Francisco Bay region. Bull. Seismol. Soc. Am. 86, 1459–1470.
Campbell, C.V., 1967. Lamina, laminaset, bed and bedset. Sedimentology 8, 7–26.
Carcione, J.M., Cavallini, F., 1995. On the acoustic-electromagnetic analogy. Wave Motion 21, 149–162.
Cardenas, M.B., Zlotnik, V.A., 2003. Three-dimensional model of modern channel bend deposits. Water Resour. Res. 39 1141. (doi:10.1029/2002WR001383)
Carreón-Freyre, D., Cerca, M., Hernández-Marín, M., 2003. Correlation of near-surface stratigraphy and physical properties of clayey sediments from Chalco Basin, Mexico, using ground penetrating radar. J. Appl. Geophys. 53, 121–136.
Cassidy, N.J., Russell, A.J., Marren, P.M., Fay, H., Knudsen, Ó., Rushmer, E.L., van Dijk, T.A.G.P., 2003. GPR derived architecture of November 1996 jökulhlaup deposits, Skeidarársandur, Iceland. In: Bristow, C.S., Jol, H.M. (Eds.), Ground Penetrating Radar in Sediments. Geol. Soc. London Spec. Publ. 211, 153–166.
Clemmensen, L.B., Andreasen, F., Nielsen, S.T., Sten, E., 1996. The late Holocene coastal dunefield at Vejers, Denmark: characteristics, sand budget and depositional dynamics. Geomorphology 17, 79–98.
Clemmensen, L.B., Pye, K., Murray, A., Heinemeier, J., 2001. Sedimentology, stratigraphy and landscape evolution of a coastal dune system, Lodbjerg, NW Jutland, Denmark. Sedimentology 48, 3–27.
Clough, J.W., 1976. Electromagnetic lateral waves observed by earth-sounding radars. Geophysics 41, 1126–1132.
Collinson, J.D., Thompson, D.B., 1989. Sedimentary Structures, 2nd edition. Chapman & Hall, London.
Conyers, L.B., Goodman, D., 1997. Ground-Penetrating Radar: An Introduction for Archaeologists. Altamira Press, London.
Corbeanu, R.M., Soegaard, K., Szerbiak, R.B., Thurmond, J.B., McMechan, G.A., Wang, D., Snelgrove, S., Forster, C.B., Menitove, A., 2001. Detailed internal architecture of a fluvial sandstone determined from outcrop, cores, and 3-D ground-penetrating radar: example from the middle Cretaceous Ferron Sandstone, east–central Utah. AAPG Bull. 85, 1583–1608.
Corbeanu, R.M., McMechan, G.A., Szerbiak, R.B., Soegaard, K., 2002. Prediction of 3-D fluid permeability and mudstone distributions from ground-penetrating radar (GPR) attributes: examples from the Cretaceous Ferron Sandstone Member, east–central Utah. Geophysics 67, 1495–1504.
Dagallier, G., Laitinen, A.I., Malarte, F., van Campenhout, I.P.A.M., Veeken, P.C.H., 2000. Ground penetrating radar application in a shallow marine Oxfordian limestone sequence located on the eastern flank of the Paris Basin, NE France. Sediment. Geol. 130, 149–165.
Daly, J., McGeary, S., Krantz, D.E., 2002. Ground-penetrating radar investigation of a late Holocene spit complex: Cape Henlopen, Delaware. J. Coast. Res. 18, 274–286.
Daniels, D.J., 1996. Surface-Penetrating Radar. Institut. Electric. Engineers, London.
Davis, J.L., Annan, A.P., 1989. Ground-penetrating radar for high-resolution mapping of soil and rock stratigraphy. Geophys. Prospect. 3, 531–551.
Degenhardt Jr., J.J., Giardino, J.R., 2003. Subsurface investigation of a rock glacier using ground-penetrating radar: implications for locating stored water on Mars. J. Geophys. Res. Planets 108 8036. (doi:10.1029/2002JE001888)
Degenhardt Jr., J.J., Giardino, J.R., Junck, M.B., 2003. GPR survey of a lobate rock glacier in Yankee Boy Basin, Colorado, USA. In: Bristow, C.S., Jol, H.M. (Eds.), Ground Penetrating Radar in Sediments. Geol. Soc. Lond. Spec. Publ., vol. 211, pp. 167–179.
Dehls, J.F., Olesen, O., Olsen, L., Blikra, L.H., 2000. Neotectonic faulting in northern Norway; the Stuoragurra and Nordmannvikdalen postglacial faults. Quat. Sci. Rev. 19, 1447–1460.
Demanet, D., Evers, L.G., Teerlynck, H., Dost, B., Jongmans, D., 2001. Geophysical investigation across the Peel boundary fault (The Netherlands) for a paleoseismological study. Geol. Mijnb. 80, 119–127.
Dominic, D.F., Egan, K., Carney, C., Wolfe, P.J., Boardman, M.R., 1995. Delineation of shallow stratigraphy using ground penetrating radar. J. Appl. Geophys. 33, 167–175.
Doolittle, J.A., Collins, M.E., 1998. A comparison of EM induction and GPR methods in areas of karst. Geoderma 85, 83–102.
Dott, E.R., Mickleson, D., 1995. Lake Michigan water levels and the development of Holocene beach-ridge complexes at Two Rivers, Wisconsin: stratigraphic, geomorphic and radiocarbon evidence. Geol. Soc. Am. Bull. 107, 286–296.
Ékes, C., Hickin, E.J., 2001. Ground penetrating radar facies of the paraglacial Cheekye Fan, southwestern British Columbia, Canada. Sediment. Geol. 143, 199–217.
Ékes, C., Friele, P., 2003. Sedimentary architecture and post-glacial evolution of Cheekye fan, southwestern British Columbia, Canada. In: Bristow, C.S., Jol, H.M. (Eds.), Ground Penetrating Radar in Sediments. Geol. Soc. London Spec. Publ. 211, 87–98.
Emery, D., Myers, K.J. (Eds.), 1996. Sequence Stratigraphy. Blackwell, Oxford.
Engheta, N., Papas, C.H., Elachi, C., 1982. Radiation patterns of interfacial dipole antennas. Radio Sci. 17, 1557–1566.
Fisher, E., McMechan, G.A., Annan, A.P., Cosway, S.W., 1992a. Examples of reverse-time migration of single-channel, ground-penetrating radar profiles. Geophysics 57, 577–586.
Fisher, E., McMechan, G.A., Annan, A.P., 1992b. Acquisition and processing of wide-aperture ground-penetrating radar data. Geophysics 57, 495–504.
Fisher, T.G., Jol, H.M., Smith, D.G., 1995. Ground-penetrating radar used to assess aggregate in catastrophic flood deposits, northeast Alberta, Canada. Can. Geotech. J. 32, 871–879.
Fisher, S.C., Stewart, R.R., Jol, H.M., 1996. Ground penetrating radar (GPR) data enhancement using seismic techniques. J. Environ. Eng. Geophys. 1, 89–96.
FitzGerald, D.M., van Heteren, S., 1999. Classification of paraglacial barrier systems: coastal New England, USA. Sedimentology 46, 1083–1108.
FitzGerald, D.M., Baldwin, C.T., Ibrahim, N.A., Humphries, S.M.,

1992. Sedimentologic and morphologic evolution of a beach-ridge barrier along an indented coast: Buzzard Bay, Massachusetts. In: Fletcher, C.H., Wehmiller, J.F. (Eds.), Quaternary Coasts of the United States: Marine and Lacustrine Systems. SEPM Spec. Publ. 48, 64–75.

Fowler, J.C., Still, W.L., 1977. Surface and subsurface profiling using ground-probing radar. Geophysics 42, 1502–1503.

Freeland, R.S., Yoder, R.E., Ammons, J.T., Leonard, L.L., 2002. Integration of real-time global positioning with ground-penetrating radar surveys. Appl. Eng. Agric. 18, 647–650.

Friele, P.A., Ékes, C., Hickin, E.J., 1999. Evolution of Cheekye fan, Squamish, British Columbia: Holocene sedimentation and implications for hazard assessment. Can. J. Earth Sci. 36, 2023–2031.

Gawthorpe, R.L., Collier, R.E.L., Alexander, J., Leeder, M., Bridge, J.S., 1993. Ground penetrating radar: application to sandbody geometry and heterogeneity studies. In: North, C.P., Prosser, D.J. (Eds.), Characterization of Fluvial and Aeolian Reservoirs. Geol. Soc. Lond. Spec. Publ., vol. 73, pp. 421–432.

Geophysical Survey Systems, 1996. Radan for Windows Version 3.1 Manual MN43-116. Geophysical Survey Systems, North Salem.

Gilbert, R., 2000. A Pleistocene frost-heaved dome in Palaeozoic limestone in Kingston, Ontario, Canada. Permafr. Periglac. Process. 11, 259–265.

Goes, B.J.M., 2000. Ground penetrating radar as a tool to improve local flow models of the ice-pushed ridges in the Netherlands. In: Noon, D.A., Stickley, G.F., Longstaff, D. (Eds.), Proceedings of the Eighth International Conference on Ground Penetrating Radar. SPIE, Billingham, vol. 4084, pp. 572–578.

Grant, J.A., Koeberl, C., Reimold, W.U., Schultz, P.H., 1997. Gradation of the Roter Kamm impact crater, Namibia. J. Geophys. Res. 102, 16327–16338.

Grant, J.A., Brooks, M.J., Taylor, B.E., 1998. New constraints on the evolution of Carolina Bays from ground-penetrating radar. Geomorphology 22, 325–345.

Grasmück, M., Green, A.G., 1996. 3-D georadar mapping: looking into the subsurface. J. Environ. Eng. Geosci. 2, 195–200.

Greaves, R.J., Lesmes, D.P., Lee, J.M., Toksöz, M.N., 1996. Velocity variations and water content estimated from multi-offset, ground-penetrating radar. Geophysics 61, 683–695.

Green, A., Gross, R., Holliger, K., Horstmeyer, H., Baldwin, J., 2003. Results of 3-D georadar surveying and trenching the San Andreas fault near its northern landward limit. Tectonophysics 368, 7–23.

Hammon III, W.S., Zeng, X., Corbeanu, R.M., McMechan, G.A., 2002. Estimation of the spatial distribution of fluid permeability from surface and tomographic GPR data and core, with a 2-D example from the Ferron Sandstone, Utah. Geophysics 67, 1505–1515.

Hänninen, P., 1992. Application of ground penetrating radar and radio wave moisture probe techniques to peatland investigations. Geol. Surv., Finland 361.

Harari, Z., 1996. Ground-penetrating radar (GPR) for imaging stratigraphic features and groundwater in sand dunes. J. Appl. Geophys. 36, 43–52.

Hardage, R.A. (Ed.), 1987. Handbook of Geophysical Exploration. Section 1. Seismic Exploration. Seismic Stratigraphy, Geophysical Press, London, vol. 9.

Hatton, L., Worthington, M.H., Makin, J., 1986. Seismic Data Processing: Theory and Practice. Blackwell, Oxford.

Heinz, J., 2001. Sedimentary geology of glacial and periglacial gravel bodies (SW-Germany): dynamic stratigraphy and aquifer sedimentology. Unpubl. PhD Thesis, Univ Tübingen.

Heinz, J., Aigner, T., 2003. Three-dimensional GPR analysis of various Quaternary gravel-bed braided river deposits (southwestern Germany). In: Bristow, C.S., Jol, H.M. (Eds.), Ground Penetrating Radar in Sediments. Geol. Soc. London Spec. Publ. 211, 99–110.

Holden, J., Burt, T.P., Vilas, M., 2002. Application of ground-penetrating radar to the identification of subsurface piping in blanket peat. Earth Surf. Processes Landf. 27, 235–249.

Hornung, J., Aigner, T., 2002. Reservoir architecture in a terminal alluvial plain: an outcrop analogy study (Upper Triassic, southern Germany): Part 1. Sedimentology and petrophysics. J. Petrol. Geol. 25, 3–30.

Hruska, J., Hubatka, F., 2000. Landslides investigation and monitoring by a high-performance ground penetrating radar system. In: Noon, D.A., Stickley, G.F., Longstaff, D. (Eds.), Proceedings of the Eighth International Conference on Ground Penetrating Radar. SPIE, Billingham, vol. 4084, pp. 688–693.

Hubbard, S.S., Peterson, J.E., Majer, E.L., Zawislanski, P.T., Williams, K.H., Roberts, J., Wobber, F., 1997. Estimation of permeable pathways and water content using tomographic radar data. The Leading Edge 16, 1623–1628.

Huggenberger, P., 1993. Radar facies: recognition of facies patterns and heterogeneities within Pleistocene Rhine gravels, NE Switzerland. In: Best, J.L., Bristow, C.S. (Eds.), Braided Rivers. Geol. Soc. London Spec. Publ. 75, 163–176.

Huggenberger, P., Meier, E., Pugin, A., 1994. Ground-probing radar as a tool for heterogeneity estimation in gravel deposits: advances in data-processing and facies analysis. J. Appl. Geophys. 31, 171–184.

Huisink, M., 2000. Changing river styles in response to Weichselian climate changes in the Vecht Valley, eastern Netherlands. Sediment. Geol. 133, 115–134.

Jackobsen, P.R., Overgaard, T., 2002. Georadar facies and glaciotectonic structures in ice marginal deposits, northwest Zealand, Denmark. Quat. Sci. Rev. 21, 917–927.

Jol, H.M., 1995. Ground penetrating radar antennae frequencies and transmitter powers compared for penetration depth, resolution and reflection continuity. Geophys. Prospect. 43, 693–709.

Jol, H.M., Bristow, C.S., 2003. GPR in sediments: advice on data collection, basic processing and interpretation, a good practice guide. In: Bristow, C.S., Jol, H.M. (Eds.), Ground Penetrating Radar in Sediments. Geol. Soc. London Spec. Publ. 211, 9–27.

Jol, H.M., Smith, D.G., 1991. Ground penetrating radar of northern lacustrine deltas. Can. J. Earth Sci. 28, 1939–1947.

Jol, H.M., Smith, D.G., 1995. Ground penetrating radar surveys of peatlands for oilfield pipelines in Canada. J. Appl. Geophys. 34, 109–123.

Jol, H.M., Smith, D.G., Meyers, R.A., 1996a. Digital Ground Penetrating Radar (GPR): a new geophysical tool for coastal barrier

research (examples from the Atlantic, Gulf and Pacific coasts, USA). J. Coast. Res. 12, 960–968.
Jol, H.M., Smith, D.G., Meyers, R.A., 1996b. Three dimensional GPR imaging of a fan-foreset delta: an example from Brigham City, Utah, U.S.A. Proceedings of GPR '96: 6th International Conference on Ground Penetrating Radar, September 30–October 3. Tohuko University, Sendai, Japan, pp. 33–37.
Jol, H.M., Junck, M.B., Kaminsky, G.M., 2000. High resolution ground penetrating radar imaging (225–900 MHz) of geomorphic and geological settings: examples from Utah, Washington and Wisconsin. In: Noon, D.A., Stickley, G.F., Longstaff, D. (Eds.), Proceedings of the Eighth International Conference on Ground Penetrating Radar. SPIE, Billingham, vol. 4084, pp. 69–74.
Jol, H.M., Lawton, D.C., Smith, D.G., 2002. Ground penetrating radar: 2-D and 3-D subsurface imaging of a coastal barrier spit, Long Beach, WA, USA. Geomorphology 53, 165–181.
Junck, M.B., Jol, H.M., 2000. Three-dimensional investigation of geomorphic environments using ground penetrating radar. In: Noon, D.A., Stickley, G.F., Longstaff, D. (Eds.), Proceedings of the Eighth International Conference on Ground Penetrating Radar. SPIE, Billingham, vol. 4084, pp. 314–318.
Kearey, P., Brooks, M., 1991. An Introduction to Geophysical Exploration. Blackwell, Oxford.
Knapp, R.W., 1990. Vertical resolution of thick beds, thin beds and thin-bed cyclothems. Geophysics 55, 1183–1190.
Kruse, S.E., Schneider, J.C., Campagna, D.J., Inman, J.A., Hickey, T.D., 2000. Ground penetrating radar imaging of cap rock, caliche and carbonate strata. J. Appl. Geophys. 43, 239–249.
LaFlèche, P.T., Todoeschuck, J.P., Jensen, O.G., Judge, A.S., 1991. Analysis of ground-probing radar data: predictive deconvolution. Can. Geotech. J. 28, 134–139.
Lapen, D.R., Moorman, B.J., Price, J.S., 1996. Using ground-penetrating radar to delineate subsurface features along a wetland catena. Soil Sci. Soc. Am. J. 60, 923–931.
Leatherman, S.P., 1987. Coastal geomorphological applications of ground-penetrating radar. J. Coast. Res. 3, 397–399.
Leclerc, R.F., Hickin, E.J., 1997. The internal structure of scrolled floodplain deposits based on ground-penetrating radar, North Thompson River, British Columbia. Geomorphology 21, 17–38.
Lehmann, F., Green, A.G., 1999. Semiautomated georadar data acquisition in three dimensions. Geophysics 64, 719–731.
Lehmann, F., Green, A.G., 2000. Topographic migration of georadar data: implications for acquisition and processing. Geophysics 65, 836–848.
Lehmann, F., Boerner, D.E., Holliger, K., Green, A.G., 2000. Multicomponent georadar data: some important implications for data acquisition and processing. Geophysics 65, 1542–1552.
Lehmann, K., Klostermann, J., Pelzing, R., 2001. Palaeoseismological investigations at the Rurrand Fault, Lower Rhine Embayment. Geol. Mijnb. 80, 139–154.
Leopold, M., Völkel, J., 2003. GPR images of periglacial slope deposits beneath peat bogs in the Central European Highlands, Germany. In: Bristow, C.S., Jol, H.M. (Eds.), Ground Penetrating Radar in Sediments. Geol. Soc. London Spec. Publ. 211, 181–189.
Liberty, L.M., Hemphill-Haley, M.A., Madin, I.P., 2003. The Portland Hills Fault: uncovering a hidden fault in Portland. Oregon using high-resolution geophysical methods. Tectonophysics 368, 89–103.
Liner, C.L., Liner, J.L., 1995. Ground-penetrating radar: a near-face experience from Washington County, Arkansas. The Leading Edge 14, 17–21.
Liner, C.L., Liner, J.L., 1997. Application of GPR to a site investigation involving shallow faults. The Leading Edge 16, 1649–1651.
Lønne, I., Lauritsen, T., 1996. The architecture of a modern push-moraine at Svalbard as inferred from ground-penetrating radar measurements. Arct. Alp. Res. 28, 488–495.
Lønne, I., Nemec, W., Blikra, L.H., Lauritsen, T., 2001. Sedimentary architecture and dynamic stratigraphy of a marine ice-contact system. J. Sediment. Res. 71, 922–943.
Lutz, P., Garambois, S., Perroud, H., 2003. Influence of antenna configurations for GPR survey: information from polarization and amplitude versus offset measurements. In: Bristow, C.S., Jol, H.M. (Eds.), Ground Penetrating Radar in Sediments. Geol. Soc. London Spec. Publ. 211, 299–313.
Maijala, P., 1992. Application of some seismic data processing methods to ground penetrating radar data. In: Hänninen, P., Autio, S. (Eds.), Fourth International Conference on Ground Penetrating Radar. Geol. Surv. Finland Spec. Pap. 16, 103–110.
Mäkinen, J., Räsänen, M., 2003. Early Holocene regressive spit-platform and nearshore sedimentation on a glaciofluvial complex during the Yolida Sea and Ancylus Lake phases of the Baltic Basin, SW Finland. Sediment. Geol. 158, 25–56.
McCann, D.M., Jackson, P.D., Fenning, P.J., 1988. Comparison of the seismic and ground probing radar methods in geological surveying. Proc. Inst. Electr. Eng. 135, 380–390.
McGourty, J., Wilson, P., 2000. Investigating the internal structure of Holocene coastal sand dunes using ground-penetrating radar: example from the north coast of Northern Ireland. In: Noon, D.A., Stickley, G.F., Longstaff, D. (Eds.), Proceedings of the Eighth International Conference on Ground Penetrating Radar. SPIE, Billingham, vol. 4084, pp. 14–19.
McKee, E.D., Weir, G.W., 1953. Terminology for stratification and cross-stratification in sedimentary rocks. Bull. Geol. Soc. Am. 64, 381–390.
McMechan, G.A., Gaynor, G.C., Szerbiak, R.B., 1997. Use of ground-penetrating radar for 3-D sedimentological characterization of clastic reservoir analogs. Geophysics 62, 786–796.
McMechan, G.A., Loucks, R.G., Zeng, X., Mescher, P., 1998. Ground penetrating radar imaging of a collapsed paleocave system in the Ellenburger dolomite, central Texas. J. Appl. Geophys. 39, 1–10.
McMechan, G.A., Loucks, R.G., Mescher, P., Zeng, X., 2002. Characterization of a coalesced, collapsed paleocave reservoir analog using GPR and well-core data. Geophysics 67, 1148–1158.
McQuillin, R., Bacon, M., Barclay, W., 1979. An Introduction to Seismic Interpretation. Graham and Trotman, London.
Mellet, J.S., 1995. Profiling of ponds and bogs using ground-penetrating radar. J. Palaeolimnol. 14, 233–240.

Meschede, M., Asprion, U., Reicherter, K., 1997. Visualisation of tectonic structures in shallow-depth high-resolution ground-penetrating radar (GPR) profiles. Terra Nova 9, 167–170.

Meyers, R.A., Smith, D.G., Jol, H.M., Peterson, C.D., 1996. Evidence for eight great earthquake-subsidence events detected with ground-penetrating radar, Willapa barrier, Washington. Geology 24, 99–102.

Miall, A.D., 1991. Hierarchies of architectural units in terrigenous clastic rocks, and their relationship to sedimentation rate. In: Miall, A.D., Tyler, N. (Eds.), The Three-dimensional Facies Architecture of Terrigenous Clastic Sediments and its Implications for Hydrocarbon Discovery and Recovery. Concepts Sedim. Palaeont., vol. 3, SEPM, Tulsa, OK, pp. 6–12.

Miall, A.D., Miall, C.E., 2001. Sequence stratigraphy as a scientific enterprise: the evolution and persistence of conflicting paradigms. Earth-Sci. Rev. 54, 321–348.

Mills, H.H., Speece, M.A., 1997. Ground-penetrating radar exploration of alluvial fans in the southern Blue Ridge Province, North Carolina. Environ. Eng. Geosci. 3, 487–499.

Mitchum, R.M., Vail, P.R., Sangree, J.B., 1977. Stratigraphic interpretation of seismic reflection patterns in depositional sequences. In: Payton, C.E. (Ed.), Seismic Stratigraphy—Applications to Hydrocarbon Exploration. AAPG Mem. 16, 117–123.

Møller, I., Anthony, D., 2003. A GPR study of sedimentary structures within a transgressive coastal barrier along the Danish North Sea Coast. In: Bristow, C.S., Jol, H.M. (Eds.), Ground Penetrating Radar in Sediments. Geol. Soc. London Spec. Publ. 211, 55–65.

Moore, L.J., Kaminsky, G.M., Jol, H.M., 2003. Exploring linkages between coastal progradation rates and the El Nino Southern Oscillation, southwest Washington, USA. Geophys. Res. Lett. 30, 1448. (doi:10.1029/2002GL016147).

Moran, M.L., Arcone, S.A., Greenfield, R.J., 2000. GPR radiation pattern effects on 3-D Kirchoff array imaging. In: Noon, D.A., Stickley, G.F., Longstaff, D. (Eds.), Proceedings of the Eighth International Conference on Ground Penetrating Radar, SPIE, Billingham, vol. 4084, pp. 208–212.

Naegeli, M.W., Huggenberger, P., Uehlinger, U., 1996. Ground penetrating radar for assessing sediment structures in the hyporheic zone of a prealpine river. J. N. Am. Benthol. Soc. 15, 353–366.

Neal, A., Roberts, C.L., 2000. Applications of ground-penetrating radar (GPR) to sedimentological, geomorphological and geoarchaeological studies in coastal environments. In: Pye, K., Allen, J.R.L. (Eds.), Coastal and Estuarine Environments: Sedimentology, Geomorphology and Geoarchaeology. Geol. Soc. London Spec. Publ. 175, 139–171.

Neal, A., Roberts, C.L., 2001. Internal structure of a trough blowout, determined from migrated ground-penetrating radar profiles. Sedimentology 48, 791–810.

Neal, A., Dackombe, R.V., Roberts, C.L., 2001. Applications of ground-penetrating radar (GPR) to the study of coarse clastic (shingle) coastal structures. In: Packham, J.R., Randall, R.E., Barnes, R.S.K., Neal, A. (Eds.), Ecology and Geomorphology of Coastal Shingle. Westbury Academic and Scientific, Yorkshire, pp. 77–106.

Neal, A., Pontee, N.I., Pye, K., Richards, J., 2002a. Internal structure of mixed-sand-and-gravel beach deposits revealed using ground-penetrating radar. Sedimentology 49, 789–804.

Neal, A., Richards, J., Pye, K., 2002b. Structure and development of shell cheniers in Essex, southeast England, investigated using high-frequency ground-penetrating radar. Mar. Geol. 185, 435–469.

Neal, A., Richards, J., Pye, K., 2003. Sedimentology of coarse-clastic beach-ridge deposits, Essex, southeast England. Sediment. Geol. 162, 167–198.

Nichol, S.L., 2002. Morphology, stratigraphy and origin of last interglacial beach ridges at Bream Bay, New Zealand. J. Coast. Res. 18, 149–159.

Nitsche, F.O., Green, A.G., Horstmeyer, H., Büker, F., 2002. Quaternary depositional history of the Reuss delta, Switzerland: constraints from high-resolution seismic reflection and georadar surveys. J. Quat. Sci. 17, 131–143.

Nobes, D.C., Ferguson, R.J., Brierley, G.J., 2001. Ground-penetrating radar and sedimentological analysis of Holocene floodplains: insight from the Tuross valley, New South Wales. Aust. J. Earth Sci. 48, 347–355.

Olhoeft, G.R., 1981. Electrical properties of rocks. In: Touloukian, Y.S., Judd, W.R., Roy, R.F. (Eds.), Physical Properties of Rocks and Minerals. McGraw-Hill, New York, pp. 257–330.

Olhoeft, G.R., 1998. Electrical, magnetic, and geometric properties that determine ground penetrating radar performance. Proceedings of GPR'98, Seventh International Conference on Ground Penetrating Radar. University of Kansas, Lawrence, KS, pp. 177–182.

Olhoeft, G.R., 1999. Applications and frustrations in using ground penetrating radar. Proceedings Ultra Wideband Conference, Washington DC, 20–22 September 1999.

Olhoeft, G.R., 2000. Maximising the information return from ground penetrating radar. J. Appl. Geophys. 43, 175–187.

Olsen, H., Andreasen, F., 1995. Sedimentology and ground-penetrating radar characteristics of a Pleistocene sandur deposit. Sediment. Geol. 99, 1–15.

Olson, C.G., Doolittle, J.A., 1985. Geophysical techniques for reconnaissance investigations of soils and surficial deposits in mountainous terrain. Soil Sci. Soc. Am. J. 49, 1490–1498.

O'Neal, M.L., Dunn, R.K., 2003. GPR investigation of multiple stage-5 sea-level fluctuations on a siliciclastic estuarine shoreline, Delaware Bay, southern New Jersey, USA. In: Bristow, C.S., Jol, H.M. (Eds.), Ground Penetrating Radar in Sediments. Geol. Soc. London Spec. Publ. 211, 67–77.

O'Neal, M.L., McGeary, S., 2002. Late Quaternary stratigraphy and sea-level history of the northern Delaware Bay margin, southern New Jersey, USA: a ground penetrating radar analysis of composite Quaternary coastal terraces. Quat. Sci. Rev. 21, 929–946.

Orlando, L., 2000. Evaluation of the integrity of massive rock by ground penetrating radar. In: Noon, D.A., Stickley, G.F., Longstaff, D. (Eds.), Proceedings of the Eighth International Conference on Ground Penetrating Radar. SPIE, Billingham, vol. 4084, pp. 816–821.

Orlando, L., 2003. Semiquantitative evaluation of massive rock quality using ground penetrating radar. J. Appl. Geophys. 52, 1–9.

Overgaard, T., Jakobsen, P.R., 2001. Mapping of glaciotectonic

deformation in an ice marginal environment with ground penetrating radar. J. Appl. Geophys. 47, 191–197.
Papziner, U., Nick, K.-P., 1998. Automatic detection of hyperbolas in georadargrams by slant-stack processing and migration. First Break 16, 219–223.
Payan, I., Kunt, N., 1982. Subsurface radar signal deconvolution. Signal Process. 4, 249–262.
Pedley, H.M., Hill, I., 2003. The recognition of barrage and paludal tufa systems by GPR: case studies in the geometry and correlation of Quaternary freshwater carbonates. In: Bristow, C.S., Jol, H.M. (Eds.), Ground Penetrating Radar in Sediments. Geol. Soc. London Spec. Publ. 211, 207–223.
Pedley, H.M., Hill, I., Denton, P., Brasington, J., 2000. Three-dimensional modeling of a Holocene tufa system in the Lathkill Valley, north Derbyshire, using ground-penetrating radar. Sedimentology 47, 721–737.
Pelpola, C.P., Hickin, E.J., 2003. Long-term bed load transport rate based on aerial-photo and ground penetrating radar surveys of fan-delta growth, Coast Mountains, British Columbia. Geomorphology. 57, 169–181.
Pipan, M., Baradello, L., Forte, E., Prizzon, A., Finetti, I., 1999. 2-D and 3-D processing and interpretation of multi-fold ground penetrating radar data: a case history from an archaeological site. J. Appl. Geophys. 41, 271–292.
Pipan, M., Baradello, L., Forte, E., Prizzon, A., 2000a. GPR study of bedding planes, fractures and cavities in limestone. In: Noon, D.A., Stickley, G.F., Longstaff, D. (Eds.), Proceedings of the Eighth International Conference on Ground Penetrating Radar. SPIE, Bellingham, vol. 4084, pp. 682–687.
Pipan, M., Baradello, L., Forte, E., Gasperini, L., Bonatti, E., Longo, G., 2000b. Ground penetrating radar study of the Cheko Lake area (Siberia). In: Noon, D.A., Stickley, G.F., Longstaff, D. (Eds.), Proceedings of the Eighth International Conference on Ground Penetrating Radar. SPIE, Bellingham, vol. 4084, pp. 329–334.
Plewes, L.A., Hubbard, B., 2001. A review of the use of radio-echo sounding in glaciology. Prog. Phys. Geogr. 25, 203–236.
Poole, G.C., Naiman, R.J., Pastor, J., Stanford, J.A., 1997. Uses and limitations of ground penetrating radar in two riparian systems. In: Gibert, J., Mathieu, J., Fournier, F. (Eds.), Groundwater/Surface Water Ecotones: Biological and Hydrological Interactions and Management. Cambridge Univ. Press, Cambridge, pp. 140–148.
Powers, M.H., 1997. Modeling frequency-dependent GPR. The Leading Edge 16, 1657–1662.
Pratt, B.R., Miall, A.D., 1993. Anatomy of a bioclastic grainstone megashoal (Middle Silurian, southern Ontario) revealed by ground-penetrating radar. Geology 21, 223–236.
Rashed, M., Kawamura, D., Nemoto, H., Miyata, T., Nakagawa, K., 2003. Ground penetrating radar investigations across the Uemachi fault, Osaka, Japan. J. Appl. Geophys. 53, 63–75.
Reading, H.G., 1996. Introduction. In: Reading, H.G. (Ed.), Sedimentary Environments: Processes, Facies and Stratigraphy, 3rd edition. Blackwell, Oxford.
Rees, H.V., Glover, J.M., 1992. Digital enhancement of ground probing radar data. In: Pilon, J. (Ed.), Ground Penetrating Radar. Geol. Surv. Can. Pap. 90-4, 187–192.
Regli, C., Huggenberger, P., Rauber, M., 2002. Interpretation of drill core and georadar data of coarse gravel deposits. J. Hydrol. 255, 234–252.
Reicherter, K.R., 2001. Palaeoseismologic advances in the Granada basin (Betic Cordilleras, southern Spain). Acta Geol. Hisp. 36, 267–281.
Reicherter, K.R., Reiss, S., 2001. The Carboneras Fault Zone (southeastern Spain) revisited with ground penetrating radar—Quaternary structural styles from high-resolution images. Geol. Mijnb. 80, 129–138.
Reiss, S., Reicherter, K.R., Reuther, C.-D., 2003. Visualization and characterization of active normal faults and associated sediments by high-resolution GPR. In: Bristow, C.S., Jol, H.M. (Eds.), Ground Penetrating Radar in Sediments. Geol. Soc. London Spec. Publ. 211, 247–255.
Reynolds, J.M., 1997. An Introduction to Applied and Environmental Geophysics. Wiley, Chichester.
Roberts, R.L., Daniels, J.J., 1996. Analysis of GPR polarization phenomena. J. Environ. Eng. Geophys. 1, 139–157.
Roberts, M.C., Jol, H.M., 2000. The sedimentary architecture and geomorphology of a cuspate spit: Tsawwassen, British Columbia. Regensbg. Geogr. Schr. 33, 141–156.
Roberts, M.C., Bravard, J.P., Jol, H.M., 1997. Radar signatures and structure of an avulsed channel, Rhone River, Aoste, France. J. Quat. Sci. 12, 35–42.
Roberts, M.C., Niller, H.-P., Helmstetter, N., 2003. Sedimentary architecture and radar facies of a fan delta, Cypress Creek, West Vancouver, British Columbia. In: Bristow, C.S., Jol, H.M. (Eds.), Ground Penetrating Radar in Sediments. Geol. Soc. London Spec. Publ. 211, 111–126.
Robinson, E.S., Çoruh, C., 1988. Basic Exploration Geophysics. Wiley, Chichester.
Roksandic, M.M., 1978. Seismic facies analysis concepts. Geophys. Prospect. 26, 383–398.
Rossetti, D.F., 2003. Delineating shallow Neogene deformation structures in northeastern Para State using ground penetrating radar. An. Acad. Bras. Cienc. 75, 235–248.
Rossetti, D.F., Góes, A.M., 2001. Imaging Upper Tertiary to Quaternary deposits from northern Brazil applying ground penetrating radar. Rev. Bras. Geosciênc. 31, 195–202.
Russell, J.K., Stasiuk, M.V., 1997. Characterization of volcanic deposits with ground-penetrating radar. Bull. Volcanol. 58, 515–527.
Russell, A.J., Knudsen, Ó., Fay, H., Marren, P.M., Heinz, J., Tronicke, J., 2001. Morphology and sedimentology of a giant supraglacial, ice-walled, jökulhlaup channel, Skeidarárjökull, Iceland: implications for esker genesis. Global Planet. Chan. 28, 193–216.
Rust, A.C., Russell, J.K., 2000. Detection of welding in pyroclastic flows with ground penetrating radar: insights from field and forward modeling data. J. Volcanol. Geotherm. Res. 95, 23–34.
Sandberg, S.K., Slater, L.D., Versteeg, R., 2002. An integrated geophysical investigation of the hydrogeology of an anisotropic unconfined aquifer. J. Hydrol. 267, 227–243.
Sangree, J.B., Widmier, J.M., 1979. Interpretation of depositional facies from seismic data. Geophysics 44, 131–160.

Sass, O., Wollny, K., 2001. Investigations regarding alpine talus slopes using ground-penetrating radar (GPR) in the Bavarian Alps, Germany. Earth Surf. Proc. Landf. 26, 1071–1086.

Schenk, C.J., Gautier, D.L., Olhoeft, G.R., Lucius, J.E., 1993. Internal structure of an aeolian dune using ground-penetrating radar. In: Pye, K., Lancaster, N. (Eds.), Aeolian Sediments Ancient and Modern. Spec. Public. Int. Assoc. Sedimentologists, vol. 16, pp. 61–69.

Sénéchal, P., Perroud, H., Sénéchal, G., 2000. Interpretation of reflection attributes in a 3-D GPR survey at Vallée d'Ossau, western Pyrenees, France. Geophysics 65, 1435–1445.

Sensors and Software, 1996a. Technical Manual 21: PulseEKKO Basic Plotting and Editing. Sensors and Software, Ontario.

Sensors and Software, 1996b. Technical Manual 26: PulseEKKO 2D F-K Migration. User's Guide v1.1. Sensors and Software, Ontario.

Sensors and Software, 1998. Technical Manual 29: PulseEKKO Tools. User's Guide v2.0. Sensors and Software, Ontario.

Sensors and Software, 1999a. Technical Manual 25: PulseEKKO 100 Run. User's Guide v1.2. Sensors and Software, Ontario.

Sensors and Software, 1999b. Technical Manual 15: PulseEKKO Velocity Analysis. User's Guide v4.2. Sensors and Software, Ontario.

Sheriff, R.E., 1977. Limitations on resolution of seismic reflections and geologic detail derivable from them. In: Payton, C.E. (Ed.), Seismic Stratigraphy—Applications to Hydrocarbon Exploration. AAPG Mem. 16, 3–14.

Sheriff, R.E., Geldart, L.P., 1995. Exploration Seismology, 2nd edition. University Press, Cambridge.

Sigurdson, T., Overgaard, T., 1998. Application of GPR for 3-D visualisation of geological and structural variation in a limestone formation. J. Appl. Geophys. 40, 29–36.

Singh, K.K.K., Chauhan, R.K.S., 2002. Exploration of subsurface strata conditions for a limestone mining area in India with ground-penetrating radar. Environ. Geol. 41, 966–971.

Skelly, R.L., Bristow, C.S., Ethridge, F.G., 2003. Architecture of channel-belt deposits in an aggrading shallow sandbed braided river: the lower Niobrara River, northeast Nebraska. Sediment. Geol. 158, 249–270.

Slater, L., Niemi, T.M., 2003. Ground-penetrating radar investigation of active faults along the Dead Sea Transform and implications for seismic hazards within the city of Aqaba, Jordan. Tectonophysics 368, 33–50.

Slater, L.D., Reeve, A., 2002. Investigating peatland stratigraphy and hydrogeology using integrated electrical geophysics. Geophysics 67, 365–378.

Smith, D.G., Jol, H.M., 1992. Ground-penetrating radar investigation of a Lake Bonneville delta, Provo level, Bingham City, Utah. Geology 20, 1083–1086.

Smith, D.G., Jol, H.M., 1995a. Wasatch Fault (Utah), detected and displacement characterised by ground penetrating radar. Environ. Eng. Geosci. 1, 489–496.

Smith, D.G., Jol, H.M., 1995b. Ground-penetrating radar: antenna frequencies and maximum probable depths of penetration in Quaternary sediments. J. Appl. Geophys. 33, 93–100.

Smith, D.G., Jol, H.M., 1997. Radar structure of a Gilbert-type delta, Peyto Lake, Banff National Park, Canada. Sediment. Geol. 113, 195–209.

Smith, D.G., Meyers, R.A., Jol, H.M., 1999. Sedimentology of an upper-mesotidal (3.7 m) Holocene barrier, Willapa Bay, SW Washington, U.S.A. J. Sediment. Res. 69, 1290–1296.

Smith, D.G., Simpson, C.J., Jol, H.M., Meyers, R.A., Currey, D.R., 2003. GPR stratigraphy used to infer transgressive deposition of spits and a barrier, Lake Bonneville, Stockton, Utah, USA. In: Bristow, C.S., Jol, H.M. (Eds.), Ground Penetrating Radar in Sediments. Geol. Soc. London Spec. Publ. 211, 79–86.

Soldal, O., Mauring, E., Halvorsen, E., Rye, N., 1994. Seawater intrusion and fresh groundwater hydraulics in fjord delta aquifers inferred from ground penetrating radar and resistivity profiles—Sunndalsøra and Esebotn, western Norway. J. Appl. Geophys. 32, 305–319.

Stephens, M., 1994. Architectural element analysis within the Kayenta Formation (Lower Jurassic) using ground-probing radar and sedimentological profiling, southwestern Colorado. Sediment. Geol. 90, 179–211.

Stolt, R.H., 1978. Migration by Fourier transform. Geophysics 43, 23–48.

Strand Petersen, K., Andreasen, F., 1989. Holocene coastal development reflecting sea-level rise and isostatic movement in NW Jutland, Denmark. Geol. Fören. Stockh. Förh. 111, 287–303.

Sun, J., Young, R.A., 1995. Recognising surface scattering in ground-penetrating radar data. Geophysics 60, 1378–1385.

Sutinen, R., 1992. Glacial deposits, their electrical properties and surveying by image interpretation and ground penetrating radar. Geol. Sur. Finland, 359.

Szerbiak, R.B., McMechan, G.A., Corbeanu, R., Forster, C., Snelgrove, S.H., 2001. 3-D characterization of a clastic reservoir analogue: from 3-D GPR data to a 3-D fluid permeability model. Geophysics 66, 1026–1037.

Taylor, M.P., Macklin, M.G., 1997. Holocene alluvial sedimentation and valley floor development: the River Swale, Catterick, North Yorkshire, UK. Proc. Yorks. Geol. Soc. 51, 317–327.

Theimer, B.D., Nobes, D.C., Warner, B.G., 1994. A study of the geoelectrical properties of peatlands and their influence on ground-penetrating radar surveying. Geophys. Prospect. 42, 179–209.

Tillard, S., Dubois, J.-C., 1995. Analysis of GPR data: wave propagation velocity determination. J. Appl. Geophys. 33, 77–91.

Todoeschuck, J.P., LaFlèche, P.T., Jensen, O.G., Judge, A.S., Pilon, J.A., 1992. Deconvolution of ground probing radar. In: Pilon, J. (Ed.), Ground Penetrating Radar. Geol. Surv. Can. Pap. 90-4, 227–230.

Topp, G.C., Davis, J.L., Annan, A.P., 1980. Electromagnetic determination of soil water content: measurements in coaxial transmission lines. Water Resour. Res. 16, 574–582.

Tronicke, J., Blindow, N., Groß, R., Lange, M.A., 1999. Joint application of surface electrical resistivity- and GPR-measurements for groundwater exploration on the island of Spiekeroog-northern Germany. J. Hydrol. 223, 44–53.

Tronicke, J., Dietrich, P., Wahlig, U., Appel, E., 2002a. Integrated surface georadar and crosshole radar tomography: a validation experiment in braided stream deposits. Geophysics 67, 1516–1523.

Tronicke, J., Paasche, H., Holliger, K., Green, A.G., 2002b. Combining crosshole georadar and attenuation tomography for site characterisation: a case study in an unconsolidated aquifer. Proceedings of the 9th International Conference on Ground Penetrating Radar (GPR 2002), April 29–May 2, Santa Barbara, California.

Turner, G., 1992. Propagation deconvolution. In: Hänninen, P., Autio, S. (Eds.), Fourth International Conference on Ground Penetrating Radar. Geol. Surv. Finland Spec. Pap. 16, 85–93.

Turner, G., 1994. Subsurface radar propagation deconvolution. Geophysics 59, 215–223.

Ulriksen, C.P., 1982. The application of impulse radar to civil engineering. Unpubl. PhD thesis, Univ. Lund.

Urbini, S., Vittuari, L., Gandolfi, S., 2001. GPR and GPS data integration: examples of application in Antarctica. Annali di Geofisica 44, 687–702.

Ursin, B., 1983. Review of elastic and electromagnetic wave propagation in horizontally layered media. Geophysics 48, 1063–1081.

van Dam, R.L., 2001. Causes of ground-penetrating radar reflections in sediment. Unpubl. PhD Thesis, Univ. Amsterdam.

van Dam, R.L., 2002. Internal structure and development of an aeolian river dune in The Netherlands, using 3-D interpretation of ground-penetrating radar data. Geol. Mijnb. 81, 27–37.

van Dam, R.L., Schlager, W., 2000. Identifying causes of ground-penetrating radar reflections using time-domain reflectometry and sedimentological analyses. Sedimentology 47, 435–449.

van Dam, R.L., Schlager, W., Dekkers, M.J., Huisman, J.A., 2002a. Iron oxides as a cause of GPR reflections. Geophysics 67, 536–545.

van Dam, R.L., van den Berg, E.H., van Heteren, S., Kasse, C., Kenter, J.A.M., Groen, K., 2002b. Influence of organic matter in soils on radar-wave reflection: sedimentological implications. J. Sediment. Res. 72, 341–352.

van Dam, R.L., van den Berg, E.H., Schaap, M.G., Broekema, L.H., Schlager, W., 2003. Radar reflections from sedimentary structures in the vadose zone. In: Bristow, C.S., Jol, H.M. (Eds.), Ground Penetrating Radar in Sediments. Geol. Soc. London Spec. Publ. 211, 257–273.

Vandenberghe, J., van Overmeeren, R.A., 1999. Ground penetrating radar images of selected fluvial deposits in the Netherlands. Sediment. Geol. 128, 245–270.

Vanderburgh, S., Havlom, K.G., Jol, H.M., 1998. GPR studies of coastal aeolian (foredune and crescentic) environments: examples from Oregon and North Carolina, USA. Proceedings of the 7th International Conference on Ground Penetrating Radar (GPR '98), May 27–30. University of Lawrence, Lawrence, KS, pp. 681–685.

van der Kruk, J., Slob, E.C., 2000. The influence of soil on reflections from above surface objects in GPR data. In: Noon, D.A., Stickley, G.F., Longstaff, D. (Eds.), Proceedings of the Eighth International Conference on Ground Penetrating Radar. SPIE, Billingham, vol. 4084, pp. 453–458.

van Gestel, J.-P., Stoffa, P.L., 2001. Application of Alford rotation to ground-penetrating radar data. Geophysics 66, 1781–1792.

van Heteren, S., van de Plassche, O., 1997. Influence of relative sea-level change and tidal-inlet development on barrier-spit stratigraphy, Sandy Neck, Massachusetts. J. Sediment. Res. 67, 350–363.

van Heteren, S., Fitzgerald, D.M., Barber, D.C., Kelley, J.T., Belknap, D.F., 1996. Volumetric analysis of a New England barrier system using ground-penetrating radar and coring techniques. J. Geol. 104, 471–483.

van Heteren, S., Fitzgerald, D.M., McKinlay, P.A., Buynevich, I.V., 1998. Radar facies of paraglacial barrier systems: coastal New England, USA. Sedimentology 45, 181–200.

van Overmeeren, R.A., 1994. Georadar for hydrogeology. First Break 12, 401–408.

van Overmeeren, R.A., 1997. Imaging groundwater 'steps' in push moraines by georadar. In: McCann, D.M., Eddleston, M., Fenning, P.J., Reeves, G.M. (Eds.), Modern Geophysics in Engineering Geology. Geol. Soc. Eng. Geol. Spec. Publ. 12, 63–73.

van Overmeeren, R.A., 1998. Radar facies of unconsolidated sediments in The Netherlands: a radar stratigraphy interpretation method for hydrogeology. J. Appl. Geophys. 40, 1–18.

van Overmeeren, R.A., Sariowan, S.V., Gehrels, J.C., 1997. Ground penetrating radar for determining volumetric soil water content; results of comparative measurements at two test sites. J. Hydrol. 197, 316–338.

van Wagoner, J.C., Mitchum, R.M., Campion, K.M., Rahmanian, V.D., 1990. Siliciclastic Sequence Stratigraphy in Well Logs, Cores and Outcrops: Concepts for High-Resolution Correlation of Time and Facies. AAPG Methods Explor. 7.

Volkel, J., Leopold, M., Roberts, M.C., 2001. The radar signatures and age of periglacial slope deposits, Central Highlands of Germany. Permafr. Periglac. Process. 12, 379–387.

Walden, J., Oldfield, F., Smith, J., 1999. Environmental magnetism: a practical guide. QRA Technical Guide, vol. 6. QRA, London.

Warner, B.G., Nobes, D.C., Theimer, B.D., 1990. An application of ground penetrating radar to peat stratigraphy of Ellice Swamp, southwestern Ontario. Can. J. Earth Sci. 27, 932–938.

Woodward, J., Ashworth, P.J., Best, J.L., Sambrook Smith, G.H., Simpson, C.J., 2003. The use and application of GPR in sandy fluvial environments: methodological considerations. In: Bristow, C.S., Jol, H.M. (Eds.), Ground Penetrating Radar in Sediments. Geol. Soc. London Spec. Publ. 211, 127–142.

Worfield, R.D., Parashar, S.K., Perrott, T., 1986. Depth profiling of peat deposits with impulse radar. Can. Geotech. J. 23, 142–154.

Wyatt, D.E., Temples, T.J., 1996. Ground-penetrating radar detection of small-scale channels, joints and faults in the unconsolidated sediments of the Atlantic Coastal Plain. Environ. Geol. 27, 219–225.

Wyatt, D.E., Waddell, M.G., Sexton, G.B., 1996. Geophysics and shallow faults in unconsolidated sediments. Ground Water 34, 326–334.

Xia, J., Franseen, E.K., Miller, R.D., Weis, T.V., Byrnes, A.P., in press. Improving ground-penetrating radar data in sedimentary rocks using deterministic deconvolution. J. Appl. Geophysics.

Yetton, M.D., Nobes, D.C., 1998. Recent vertical offset and near-surface structure of the Alpine Fault in Westland, New Zealand,

from ground-penetrating radar profiling. New Zealand J. Geol. Geophys. 41, 485–492.
Yilmaz, Ö., 1987. Seismic Data Processing. Investigations in Geophysics, vol. 2. Soc. Explor. Geophys., Tulsa.
Yilmaz, Ö., 2001. Seismic Data Analysis. Soc. Explor. Geophys., Tulsa.
Young, R.A., Deng, Z., Sun, J., 1995. Interactive processing of GPR data. The Leading Edge 14, 275–280.
Zenero, R.R., Seng, D.L., Byrnes, M.R., McBride, R.A., 1995. Geophysical techniques for evaluating the internal structure of cheniers, southwestern Louisiana. Trans. Gulf Coast Assoc. Geol. Soc. 45, 611–620.